

PETROCHEMISTRY OF THE SHEWA-SHAHBAZGARHI COMPLEX

MARDAN

Thesis presented for the degree
of Master of Philosophy at the
University of Peshawar.



BY

Irshad Ahmad

National Centre of Excellence in Geology
University of Peshawar
September, 1986

The project reported in this thesis was started in October, 1984. No portion of this work has been submitted in support of an application for another degree or qualifications at this or any other University

ACKNOWLEDGEMENT

Assistant Professor, Dr. S. Hamidullah was kind enough in en^couraging me to embark on this project. He is highly acknowledged for suffering my persistent questioning during all this work. I express my gratitude to Dr. M. Qasim Jan whose personal interest made this work, a reality.

Dr. M. Majid is equally receiving my thanks for reading and suggesting corrections in the final manuscript. The work did really improved through the fruitful discussions with Mr. Munir Humayun. Similarly the discussions and guidance provided by Assistant Professor M. Rafique, are unforgettable. I am not forgetting the sincere help of Mr. Tahir Shah for not only wet chemical analyses but also making suggestions for the improvement of this work. For microprobe analysis Mr. M.U.K. Khattak's efforts are irreplaceable.

My sincere thanks are due, to Mr. Jamil Ahmad and Mr. Abid Ahmed (geologists from PAEC) for providing accomodation and necessary help in the field. In fact they were the most helpful people during all this work. Their staff was also very helpful in collection of samples. I am much indebted to Mr. Mohammad Riaz for drafting and arranging the figures and diagrams. Mr. Sabir Hussain's efforts are highly appreciated for typing the final manuscript.

Lastly, I heartedly recognize the apparent patience of my family during all this work.

<u>C O N T E N T S</u>	No.
ABSTRACT	1
CHAPTER - 1	3
INTRODUCTION	3
Previous work	5
Theories of origin	7
Scope of the present study	8
Analytical techniques	
CHAPTER - 2	12
REGIONAL GEOLOGICAL SETTING	17
FIELD RELATION AND LOCAL GEOLOGICAL SETTING	18
Microporphyry	19
Metagabbro	19
Porphyritic granite	21
Riebeckite gneiss	21
Aegirine riebeckite porphyry	22
Metadolerite and Quartz	23
Monzonite dykes and sills	
Biotite schist	
CHAPTER - 3	33
PETROGRAPHY	33
Microporphyry	40
Metagabbro	48
Porphyritic granite	59
Riebeckite gneiss	65
Aegirine riebeckite porphyry	70
Metadolerite	73
Quartz monzonite	
CHAPTER - 4	82
GEOCHEMISTRY	82
GENERAL FEATURES	87
MAJOR AND TRACE ELEMENT VARIATION	

MAJOR ELEMENT VARIATION	89
TRACE ELEMENT VARIATION	93
ELEMENT STABILITY AND ALTERATION	96
NON COMAGMATIC NATURE OF BASIC AND ACIDIC ROCKS	104
TECTONIC ENVIRONMENTS	104
FRACTIONAL CRYSTALLIZATION	109
CHEMISTRY OF ALKALI AMPHIBOLE	115
CHAPTER - 5	
SUMMARY AND DISCUSSION	119
Petrography	119
Chemistry and Petrogenesis	122

LIST OF PLATES AND FIGURES

<u>PLATES NO</u>		<u>PAGE NO</u>
1.	Banding in microporphyry at Machai	24
2.	The contact of microporphyry with porphyritic granite at Machai.	24
3.a,b.	Xenoliths of microporphyry in porphyritic granite at Machai.	25
3.c.	Xenolith of microporphyry in aegirine riebeckite porphyry at Machai.	26
4.a,b.	The peculiar "pillar type" structure (mural joints) of the porphyritic granite at Shewa.	27
5.a.	Contact relationship of riebeckite gneiss and metadolerite at Werana Gariala.	28
5.b.	Chilling effect in metadolerite contact against riebeckite gneiss.	28
6.	Acidic dykes in riebeckite gneiss.	29
7.	Photomicrograph showing elongated feldspar grain in microporphyry. Mortar texture can also be seen around the grain (Nicol crossed Magn. x 30).	37
8.	Photomicrograph showing bands of fine and coarse quartz and feldspar grains. (Nicol crossed, Magn. x 30).	37
9.	Photomicrograph showing spindle shape magnetite in microporphyry (Plane light, Magn. x 30).	38
10.	Photomicrograph showing kinking in magnetite and in the ground mass of quartz and feldspar in microporphyry, (Nicol crossed, Magn. x 30).	38
11.	Photomicrograph showing development of muscovite after K-feldspar, (Nicol crossed, Magn. x 30).	39

- | | | |
|---------|---|----|
| 12. | Photomicrograph showing flow or fluxion structure around feldspar porphyroclast. (Nicols crossed, Magni. x 30). | 39 |
| 13a,b. | Photomicrograph showing formation of amphibole at the expense of magnetite and plagioclase. An amphibole grain can also be seen in the core of magnetite. (Nicols crossed, Magni. x 30). | 42 |
| 14. | Photomicrograph showing rim of fine grained sphene around magnetite grains in metagabbro, (Nicols crossed, Magni. x 30). | 44 |
| 15. | Photomicrograph showing an orthoclase grain corroded at the margins and core with inclusions of biotite and epidote, (Nicols crossed, Magni. x 30). | 51 |
| 16. | Photomicrograph showing broken perthite grains filled up by recrystallized quartz and orthoclase along the fracture, (Nicols crossed, Magni. x 30). | 51 |
| 17. | Photomicrograph showing the development of muscovite after k-feldspar in porphyritic granite (Nicols crossed, Magni. x 30). | 52 |
| 18. | Photomicrograph showing alteration of plagioclase to epidote and myrmekitic intergrowth of quartz with orthoclase, (Nicols crossed, Magni. x 25). | 54 |
| 19. | Photomicrograph showing quartz grain with overgrowth of the second generation. Fluxion structure and mortar texture can also be seen around the grain, (Nicols crossed, Magni. x 25). | 54 |
| 20. | Photomicrograph showing perthite grain with myrmekitic intergrowth on margin, (Nicols crossed, Magni. x 25). | 55 |
| 21. | Photomicrograph showing the development of biotite at the expense of magnetite and feldspar in porphyritic granite, (Plane light, Magni. x 25). | 55 |
| 22.a,b. | Photomicrograph showing fluxion structure around feldspar grains in porphyritic granite. Fine flaky muscovite and epidote parallel to the fluxion structure can also be seen (Nicols crossed, Magni. x 30). | 58 |

- | | | |
|-----|--|----|
| 23. | Photomicrograph showing corroded and elongated porphyroclasts of quartz and feldspar in porphyritic granite, (Nicols crossed, Magni. x 30). | 57 |
| 24. | Photomicrograph showing a broken and elongated feldspar grain in the laminated groundmass. Overgrowth of second generation in the form of rims can also be seen around the broken grains. (Nicols crossed, Magni. x 25). | 61 |
| 25. | Photomicrograph showing fluxion structure around corroded feldspar grain in riebeckite gneiss. (Nicols crossed, Magni. x 25). | 61 |
| 26. | Photomicrograph showing fluxion structure around the plagioclase grain. A fine grained crushed mass can also be seen in the lower left corner, of the lower photomicrograph, (Nicols crossed, Magni. x 25). | 62 |
| 27. | Photomicrograph showing a rotated plagioclase grain. Mortar texture can also be seen around the grain in riebeckite gneiss. (Nicols crossed, Magni. x 25). | 64 |
| 28. | Photomicrograph showing the development of sillimanite after feldspar in riebeckite gneiss. Epidote grains can also be seen in upper left corner (Nicols crossed, Magni. x 25). | 64 |
| 29. | Photomicrograph showing a broken and corroded perthite grain in aegirine riebeckite porphyry. Epidote inclusion can be seen in its core, (Nicols crossed, Magni. x 25). | 67 |
| 30. | Photomicrograph showing rotated perthite porphyroclasts surrounded by matrix indicating fluxion structure, (Nicols crossed, Magni. x 25). | 67 |
| 31. | Photomicrograph showing a kinked plagioclase grain indicating deformation, (Nicols crossed Magni. x 25). | 68 |

PLATES NO

PAGE NO

32. Photomicrograph showing kinked and corroded plagioclase grain indicating deformation, (Nicols crossed, Magni. x 25). 68
- 33a,b,c,d. Photomicrographs showing plagioclase crystals with partial alteration to epidote. Note zoning in c and d, (Nicols crossed, Magni. x 30). 75
- 34a,b. Photomicrograph showing myrmekitic and graphic intergrowth between quartz and feldspar in quartz monzonite, (Nicols crossed, Magni.x30). 77

FIGURES

1. Speculative tectonic model. 15
- 2a. An index map of the Shewa-Shahbazgarhi complex. 9
- 2b. Geological sketch map of north Pakistan and Kashmir after Bard et al., 1983. 13
3. Q vs P diagram for the Shewa-Shahbazgarhi complex. 88
5. Major element variation of basic rocks against FeO^*/MgO ratios. 90
6. Major element variation of basic and acidic rocks against solidification index (S.I.). 91
7. Major element variation of acidic rocks against differentiation index (D.I.). 94
8. Trace element variation of basic rocks against FeO^*/MgO ratio. 95
9. Trace element variation of basic and acidic rocks against MgO . 97

FIGURES NOPAGE NO

10.	Sr vs CaO plot for basic and acidic rocks.	97
11.	Rb, K/Rb vs K_2O for basic and acidic rocks.	97
12.	Trace element variation in acidic rocks against differentiation index (D.I.)	98
13.	Trace elements against Zr.	101
14.a	SiO_2 vs Nb/Y plot for the basic rocks of the Shewa-Shahbazgarhi complex.	102
14.b	SiO_2 vs $Al_2O_3 + CaO + \text{Total alk.} / Al_2O_3 + CaO - \text{Total alk.}$ alkalinity ratio Shabazgarhi complex.	103
15.	Zr vs SiO_2 plot for basic and acidic rocks.	105
16.	Cr-Y plot for the basic rocks.	107
17.	Ti-Zr plot for the basic rocks.	107
18.	Y, Nb, Ta vs SiO_2 plots for the acidic rocks.	108
19.	Nb-Y plot for the acidic rocks.	108
20.	Ca/Zr, Al/Zr, (Fe+Mg)/Zr vs. Si/Zr plot for the basic rocks.	111
21.	Projection from Ky into plag-En-Qtz plane for the rocks of Shewa-Shahbagarhi complex.	113
22.	Projection from Qtz into En-Ky-Wol plane for the Shewa-Shahbazgarhi rocks.	114
23.	$100 Fe^{+2} / Fe^{+2} + (MgO - MnO)$ vs $100 Fe^{+3} / Fe^{+3} + (Al^6) + Ti$ plot for alkali amphiboles.	118
24.	Ca vs. Na+K plot for alkali amphiboles.	118
25.	ORG vs. K_2O , Rb, Ba, Th, Ta, Nb, Ce, Hf, Zr, Sm, Y, Yb plot of Pearce <u>et al.</u> , 1984.	125

LIST OF TABLES

<u>TABLES NO</u>		<u>PAGE NO</u>
1.	Modal composition of microporphyry.	34
2.	Modal composition of metagabbro.	41
3.	Modal composition of metagabbro after Noorjehan (1985).	46
4.	Modal composition of basic dykes after Noorjehan (1985).	47
5.	Modal composition porphyritic granite.	49
6.	Modal composition of gneissose micro-granite after Noorjehan (1985).	58
7.	Modal composition of riebeckite gneiss.	60
8.	Modal composition of aegirine riebeckite porphyry.	66
9.	Modal composition of metadolerite.	71
10.	Modal composition of quartz monzonite.	74
11.	Classification of acidic rocks of the Shewa Shahbazgarhi complex on the basis textural classification of Higgins, 1971.	78
12.	Comparison of Shewa-Shahbazgarhi rocks with within plate granite of other place of the world.	83
13.	Chemical analyses of metagabbro, metadolerite quartz monzonite and basic dykes.	84
14.a	Chemical analyses of microporphyry and porphyritic granite from Shewa-Shahbazgarhi complex.	86
14.b	Chemical analyses of riebeckite gneiss and aegirine riebeckite porphyry.	110
15.	Probe analysis of alkali amphiboles from Shewa-Shahbazgarhi complex.	116

LIST OF MAPS

MAPS NO

PAGE NO

- | | | |
|----|---|----|
| 1. | Geological map of Shahbazgarhi section
(Shewa-Shahbazgarhi complex). | 30 |
| 2. | Geological map of Machai section (Shewa-
Shahbazgarhi complex) | 31 |
| 3. | Geological map of Shewa section (Shewa-
Shahbazgarhi complex). | 32 |

ABSTRACT

The Shewa-Shahbazgarhi complex is an isolated triangular outcrop, occurring about 12 km north-east of Mardan. The complex consists of acidic rocks, intruded by basic rocks such as metagabbro, metadolerite and local quartz monzonite dykes and sills. The acidic rocks, in order of decreasing relative ages, are microporphyry, porphyritic granite, riebeckite gneiss and aegirine riebeckite porphyry.

The common minerals in basic rocks include hastingsite, clinopyroxene, orthopyroxene (in metadolerite), magnetite, biotite, epidote, apatite and leucoxene. The acidic rocks contain perthitized orthoclase, orthoclase, perthite, plagioclase, with riebeckite and aegirine as the common ferromagnesian minerals. (Specially in riebeckite porphyry) and the presence of the alkali amphibole and alkali pyroxene is indicative of their alkaline character. Chemical analyses of the amphibole grains obtained with electron probe closely correspond to riebeckite composition. The rocks show considerable degree of deformation and alteration (cataclasis and/or mylonitization). Two types of metamorphism (a) an amphibolite facies metamorphism and (b) retrogressive epidote amphibolite facies metamorphism has been noticed.

Assessment of the chemical data on conventional two dimension plots and CMAS model, suggest the control of fractional

crystallization over the major and trace element distribution in both the rock types. Fractional control of olivine, clinopyroxene and plagioclase is conspicuous in the basic rocks and plagioclase fractionation in the acidic rocks.

Major and trace element data suggest that the basic and the acidic rocks are not comagmatic. These are derivative from two different parent liquids. A magma of subalkaline character is proposed for the basic rocks and alkaline to peralkaline for the acidic rocks, both, however, being emplaced in continental rift environments.

A rift valley origin is proposed for the complex with the generation of felsic magma, probably as the result of partial melting in the lower crust. The rock so formed were later intruded by basic dykes of continental flood basalt type.

CHAPTER-1

INTRODUCTION

The Shewa-Shahbazgarhi complex is an isolated, triangular outcrop consisting of acidic and basic meta-igneous rocks intruding into a metasedimentary sequence. The metasediments, known as the Swabi-Chamla group, are mainly phyllitic shales, quartzites and schists of possible Precambrian age. The complex is located about 12 km north-east of Mardan (Longitudes $72^{\circ}10'$ to $72^{\circ}20'$ E, Latitudes $34^{\circ}10'$ to $34^{\circ}30'$ N). It has a low to moderate relief, ranging from 314m at Shahbazgarhi to 1035m at Karamar Ziarat, above sea level. The climate is arid and extreme or continental type, i.e. it is dry and cool in winter and hot and humid in summer.

Previous work

The Shewa-Shahbazgarhi complex has been frequently investigated by workers since Coulson (1936) described the petrography and chemistry of some of the rocks for the first time. He described these rocks as porphyries of Mesozoic age and correlated these with the soda granite at Warsak. Martin et al. (1962) called these rocks as albite porphyries. They also pointed out cataclasis in certain types near Taja, east of Machai. Several other workers (Siddiqui, 1965; Chaudhry and Shakoor, 1968; Kempe and Jan, 1970, 1980; Kempe, 1973, 1983; Ahmad and Ahmad, 1974; and

Chaudhry et al, (1976) correlated these rocks with Koga alkaline complex, Naranji-Kandao carbonatite, and with various alkaline and acidic rocks of the Peshawar plain alkaline igneous province. These workers have assigned a probable Early Tertiary age to these rocks.

Bakhtiar and Waleed (1980) classified the rocks of the Shewa-Shahbazgarhi complex in the following ascending order:

6. Alluvium	Quarternary
5. Quartz, feldspar and epidote veins	Early Tertiary to Late Cretaceous
4. Dolerite and quartz diorite dykes and sills.	
3. Riebeckite-aegirine-porphyrific microgranite	
2. Porphyritic microgranite	
1. Microporphyry	

On the basis of field relationships and petrography, Chaudhry et al. (1984) classified the rocks at Shewa into acid black porphyries riebeckite porphyries, acid grey porphyries and riebeckite gneisses. Noorjehan (1985) classified the rocks of a small outcrop south of Shahbazgarhi into the following types:

5. Acidic dykes
4. Lamprophyric dykes

- | | | |
|--------------------------------|-------|----------------|
| 3. Gneissose microgranite | ----- | Age decreasing |
| 2. Metagabbros | | |
| 1. Cataclasite (Microporphyry) | | |

On the basis of mineralogy and texture Noorjehan, (1985) following Higgins, (1971) further classified the cataclasite and gneissose microgranite into mylonite and ultramylonite.

Theories of origin

Complexes of alkaline rocks are distributed in a semi-circular/ fashion around the northern half of Peshawar Plain, NW Pakistan. Stretching from west to East over 200 km., they occur in eastern Afghanistan, Mohmand agency, Khyber agency, Warsak, Malakand, Shewa-Shahbazgarhi, Koga-Ambe-la-Utla area, Tarbela and possibly in Mansehra. The rocks include alkali granites and microgranites, syenites, albitites and carbonatites, intruded generally along fault zones mainly into Early Paleozoic metasediments. The following theories have been suggested about the origin of the Shewa Shahbazgarhi complex as well as the rest of the alkaline rocks of the region.

(a) Kempe (1973) presented a hypothetical differentiation scheme suggesting that the Himalayan tholeiitic magma derived from the upper mantle gave rise to the upper Swat basic and intermediate rocks. These rocks remelted to quartz trachitic magma which by further differentiation

gave rise to rocks like Warsak alkaline porphyritic microgranite and Tarbela albitites. Further differentiation of this liquid yielded the Warsak alkaline granites ^{and} Shewa-Shahbazgarhi complex.

(b) Powell and Conaghan (1973) have suggested that a fundamental crustal fracture developed within the Indian block and that the Indian subcontinent was underthrust along this fracture. The down buckling of the underthrust portion of the leading edge produced a large scale monocline type of structure where tensional fracture developed at the crest of the structure. This fracture zone provided the sites of intrusion of highly alkaline magma.

(c) Generation along a fault called the "Vale-rift zone" Kempe & Jan (1980). Alkaline rocks are commonly associated with rifting and Peshawar plain is considered to be an irregular rift valley modified greatly by Pleistocene glacial deposits and Swat river alluvial remains. The rifting resulted in the release of compression, produced by the plate collision and the generation of alkaline magma.

(d) The tectonic environments of the Shewa Shahbazgarhi outcrops is known to be fault-bounded (Martin et al., 1962) and, therefore, of pulsating

compressional and extensional nature. Considering nearness to MMT and the fact that subduction phenomenon in a collisional mountain system under the influence of bouyance constraints would have created discontinous drift with increasing tectonic stresses. Chaudry et.al., (1984) regarded such an environment to be related to subduction at Indo-Pak plate margin, folowed by release of stress on subduction and resulting in the generation of rifting of the continental crust.

(e) The occurence of metagabbro south of MMT at Warsak and Shahbazgarhi, their emplacement into continental metasediments and their intrusion by younger granites, led Noorjehan (1985) to consider that these basic rocks are as older as Precambrian age. She also suggested that the development of these basic rocks and of the associated cataclasite (micro-porphyry) may be related to an older subduction of corresponding age.

Scope of the present study

Apart from the general and pertographic studies performed by Bakhtiar and Waleed (1980), Chaudry et.al. (1984) and Noorjehan (1985), detail investigation, leading to important petrogenetic conclusions are lacking. The present study was carried out to map and perform detailed petrographic and geochemical studies of the complex in order to (a) determine magmatic affinities of the various rock types (b) to elucidate the

metamorphic and igneous crystallization history of various rock types and if possible, (c) to investigate geotectonic environment responsible for the evolution of this complex.

Field and laboratory Procedures

Field work was carried out in February, March, and September, 1984 for about 28 days. The area has been geologically investigated on 1cm = $\frac{1}{2}$ scale map, using toposheets No. $43\frac{B}{3}$, $43\frac{B}{4}$, $43\frac{B}{7}$, $43\frac{B}{8}$ of the survey of Pakistan. Geology has been plotted on separate maps in portions (see map 1,2,3). An index map of the Shewa Shahbazgahi complex is also presented Fig. 1.

During field work, different rock units were mapped. One hundred and fifty rock samples were collected. About seventy six samples were cut into thin sections and sixty one were analysed for major and trace elements.

Analytical Techniques

Samples have been analysed for major and trace elements by wet chemical and x-ray fluorescence (XRF) methods. A total of 23 samples which were analysed by wet chemical method, include 12 porphyritic granites, 8 metagabbros, 2 microporphyries,

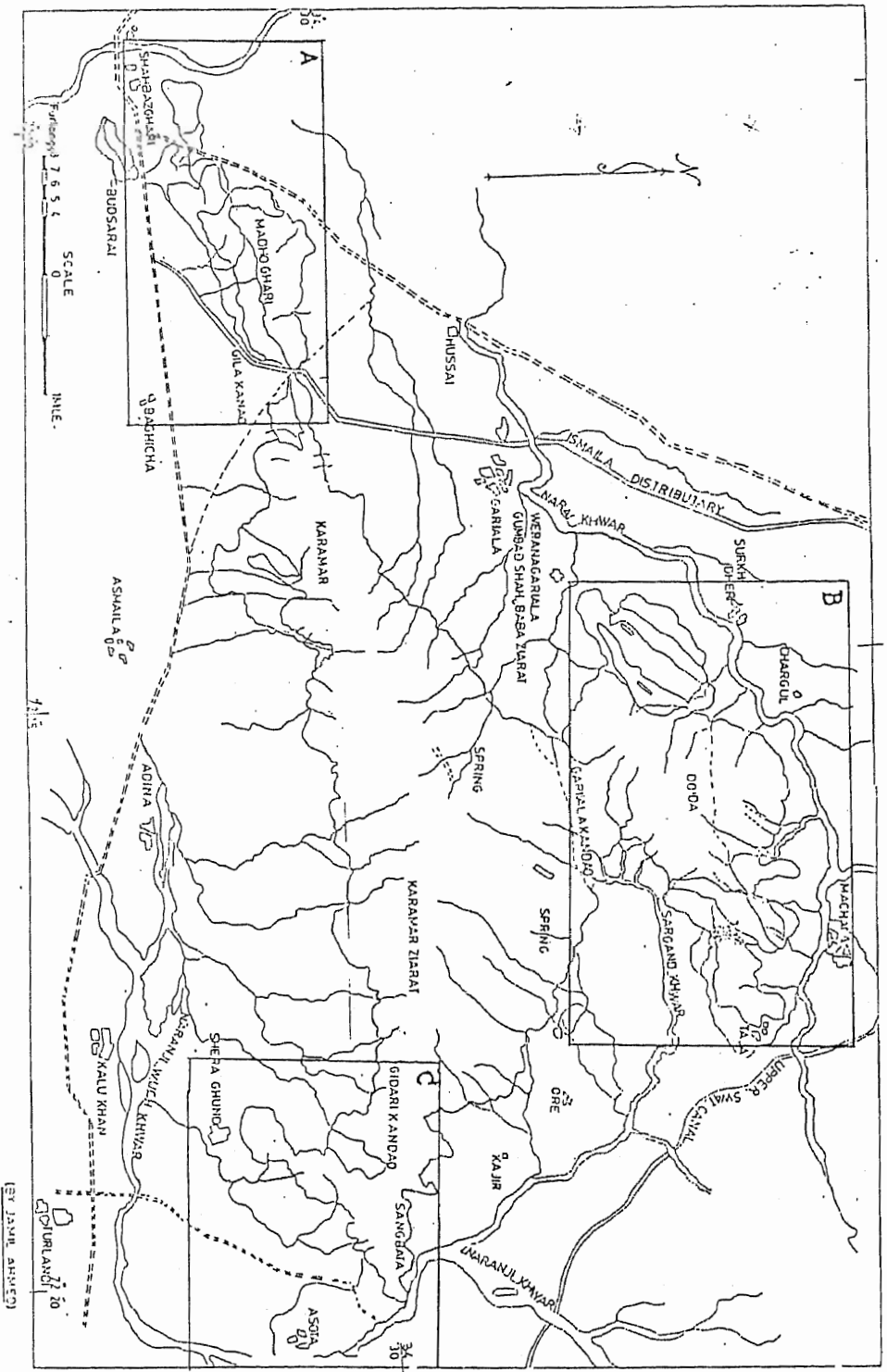


Fig. 1 . An index map of the Shewa-Shahbazgarhi complex. The area mapped are boxed in.
 A= Map 1; B= Map 2; C= Map 3.

and 1 basic dyke. These samples were analysed by atomic absorption for total iron as Fe_2O_3 , MnO , MgO , CaO , K_2O , Na_2O (the latter two by emission mode), and ^{by}UV/Visible spectrometer for Al_2O_3 , P_2O_5 and TiO_2 using suitable standards for comparison. SiO_2 was determined by the gravimetric method. The SN series were selected from those of Noorjehan (1985).

Rest of the samples were analysed by XRF using pellets of rock powder crushed to 300 BSM and pressed at 22 tonnes. Readings on the pellets were determined on a working curve calibrated with USGS standard (G-2, DNC-1, BCR-1, W-2 and STM-1) through a minicomputer. All these samples were analysed for major and trace elements. Total iron was determined as Fe_2O_3 in XRF analyses. The weight percent FeO was determined by the ammonium meta-vanadate (AMV) method (Wilson, 1955). Ignition loss was determined by heating the rock powder to 1000°C for two hours. CIPW norms were calculated on an IBM personal computer Xt.

Two samples were selected for electron probe microanalyses of alkali amphibole using computer automated Jeol Superprobe model JCXA-733. Accelerating voltage was kept on 15 KV and x-rays were generated at 1700 volts, keeping a

probe current of 150×10^{-7} A. For SiO_2 , Al_2O_3 , MgO , and Na_2O , a regular gas-flow ($\text{CH}_4 + \text{Ar}$) proportional counter channel was used. A thirteen element program was run to analyse proportions of different oxides, using Japanese and Museum of Natural History silicate and synthetic standards. Total iron was determined as Fe_2O_3 .

CHAPTER - 2

REGIONAL GEOLOGICAL SETTING

The geological and tectonic features developed in the northern part of Pakistan are the product of collision of Eurasian plate with Indian plate, 55 m.y. ago (Powell, 1979). This collision occurred due to northwards subduction of Tethys ocean floor under the Eurasian plate. The Kohistan island arc formed in response to this subduction during the Cretaceous and was sandwiched between the two mighty continents, (Eurasia and Indo-Pakistan) during Early Tertiary. The northern and southern limits of Kohistan island arc ^{are} marked by two branches of the Indus suture zone which marks the collisional line of India and Eurasia in Tibet (Desio, 1964). The northern one, the Hini-Chalt-Yasin-Drosh fault is called Main Karakoram Thrust (Tahirkheli et al., 1979). It separates the Kohistan arc from Eurasia. The southern one is traced along Babu Sar Ulla-Jijal-Shangla-Mingora and Khar, and has been named as Main Mantle Thrust (Tahirkheli et al., 1979) along which the Kohistan island arc is wedged with Indo-Pakistan plate. (See Fig. 2a.

The tectonic settings of the Kohistan and the adjoining areas have been variously interpreted by Tahirkheli (1979), Klootwijk (1979). Considering recent radiometric ages and previous tectonic models of the Indo-Eurasian suture

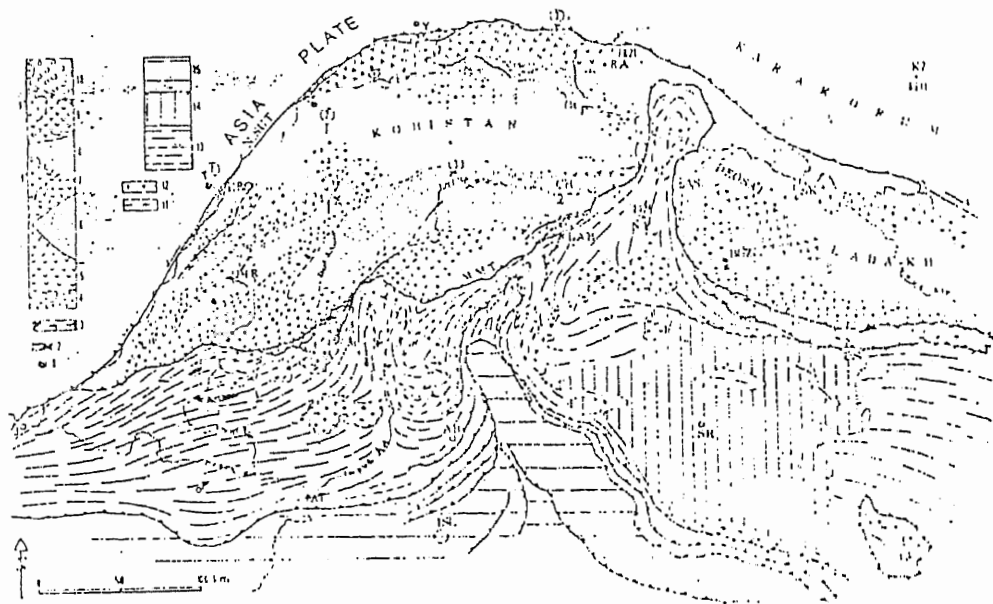


Fig. 2a. Geological sketch map of northern Pakistan and Kashmir with special reference to Kohistan area (slightly modified after Bard *et al.*, 1980). 1 : fossils (Mid Cretaceous to Lower Eocene); 2 : serpentines and allochthonous ultrabasic; 3 : Blueschist belt and associated "tectonic melange" under the Main Mantle Thrust (M.M.T.) paleosuture; 4 : Jijal-Patan mafic-ultramafic complex and western equivalents near Mingora (Swat Valley); 5 : Southern amphibolitic series; 6 : Kohistan "granulitic belt" (metamorphic calc-alkaline layered gneiss); 7 : Northern amphibolitic series; 8 : Kalam metasedimentary and volcanosedimentary series; 9 : Utror volcanics (mainly andesitic to dacitic lavas and tuffs); 9 : late dioritic granitic intrusives; 10 : Yasin-group (Mid-Cretaceous); 11 : Indian plate (I.P.) orthogneissic rocks; 12 : late kinematic I.P. granitoids; 13 : (I.P.) metasediments (Upper Precambrian to Paleozoic); 14 : Upper Paleozoic to Triassic Series of Srinagar and Panjal Traps; 15 : Foreland Cenozoic deposits (Murree formation, etc., ...). AB : Abbottabad; AS : Astor; AT : Attock; DAB : Dabusar Pass; BUZ : Buz Pass; CH : Chilas; DRO : Drosh; DS : Drosh; GI : Gilgit; ISL : Islamabad; J : Jallalabad; K : Kalam; M : Mingora; NP : Nanga Parbat; P : Peshawar; R : Rakaposhi Mountain; S : Srinagar; SE : Shardu; Y : Yasin.

zone (Coward et al., 1982, Andrews-Speed and Brookfield, 1982), Jan and Agif, (1983) present a recent tectonic model of north Pakistan (Fig.2b).

Rocks of the Indo-Pak plate occur to the south of MMT include Precambrian to Pleozoic metasediments overlain by Mesozoic rocks (see Calkin et al., 1975). Granitic rocks of variable lithology and age also occur in this region.

Being part of the Peshawar plain alkaline igneous province, the Shewa-Shahbazgarhi complex is considered Cret-Tertiary in age and is generally related with major episodes of the Himalayan orogeny which is ⁿtrun are considered to be the product of collision between the Eurasia and Indo-Pak plate (Jan et al., 1981). These rocks occur as isolated outcrops about 55 km south of MMT in the north-eastern extension of "Peshawar vale". On the basis of field relationship, texture and tectonic environments, (Tahirkheli, 1979) classified the granites of Himalayas into (a) coarse grained granite gneisses belonging to precollisional environments, (b) medium to fine-grained foliated granites belonging to somewhat later orogenic episodes and (c) homogenous

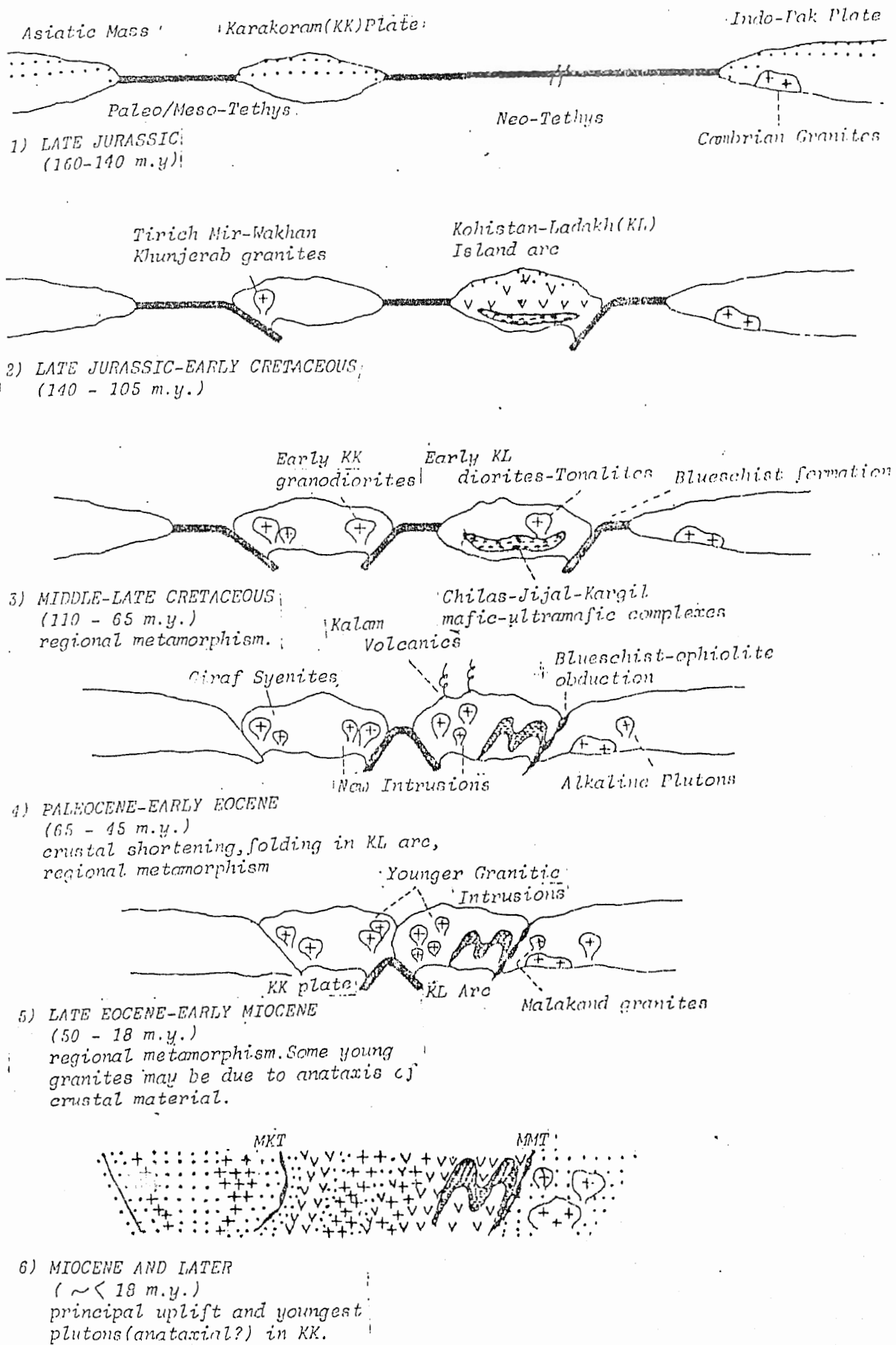


Fig.2b. Tentative model for the tectonic and magmatic evolution of North Pakistan (After Jan and Asif, 1981).

(nonschistose) granites related to post tectonic environments of the Himalayan orogeny during late Pliocene-Pleistocene period. On the basis of petrography and field relation, rocks of the thesis area can be related to the type
e.g.
(b)/fine grained foliated granites.

Jan et al. (1981) divided the granitic rocks from north Pakistan into two major age groups as (a) Late Precambrian (?) and Cambrian granites of Indo-Pakistan subcontinent exposed at Mansehra, Kaghan, Nanseri, and Nanga Parbat area and (b) Cret-Tertiary (Alpine) granites related to subduction of the Indian plate under Eurasian plate. The later type is further subdivided on the basis of age, chemistry and location into: ,

(i) Calc-alkaline types including Khunjerab-Tirichmir-Karakoram and Ladakh-Kohistan granites.

(ii) Per-alkaline to alkaline granites found as small intrusions around the Peshawar plain, including Ambela, Shewa Shahbazgarhi, Malakand proper, Warsak and Tarbela (rift related 30-40 m.y. old).

Considering all these criteria and also the work of Siddiqui (1967) and Kempe (1973), rocks of the area under present investigation can be classified as part of the alkaline province of extensional environment.

Field relation and local geological setting

The field relationships of the Shewa Shahbazgarhi complex have been described by Martin et al. (1962), Bakhtiar and Waleed (1980), ^{and} Chaudhry et al. (1984). They have not described the detailed contact relationship of the various rock units with each other. However, Bakhtiar and Waleed have reported xenoliths of microporphyry in the porphyritic microgranite. Noorjehan (1985) described the contact relationship of cataclasite (microporphyry) with gneissose porphyritic microgranite as sharp and reported the xenoliths of the former in the latter. She also reported the intrusive relationship of metagabbro with, and chilling effects against, the cataclasite (microporphyry). In addition, Noorjehan (1985) also reported xenoliths of metagabbro in the gneissose porphyritic microgranite and intrusive relationship of the latter with metagabbro and the country rocks (Swabi-Chamla sedimentary group) with which a sharp contact has been also noticed.

On the basis of present field and petrographic observations and the previous studies, the following rock types can be distinguished:

7. Basaltic breccia
6. Metadolerite and quartz monzonite
dykes and sills

- | | |
|---------------------------------|----------------|
| 5. Aegirine-riebeckite porphyry | Age decreasing |
| 4. Riebeckite gneiss | |
| 3. Porphyritic granite | |
| 2. Metagabbro | |
| 1. Microporphyry | |

Microporphyry

an

It is extremely fine grained rock, varying in colour from earthy white through greyish green to slaty black. It is splintery and well jointed, with a slaty appearance on the surface. It is generally hard and less susceptible to weathering but at certain places iron leaching can be noticed on its surface. Near Shewa and Garijala Kandao the microporphyry is highly sheared. Layering has also been noticed in microporphyry at Machai (Plate 1), where it has sharp contact with the porphyritic granite (Plate 2) and gradational contact with the aegirine-riebeckite porphyry. Fragments and small lenses of microporphyry are present as xenolith in the porphyritic granite (see also Noorjehan, 1985) and aegirine-riebeckite porphyry (Plate 3 a-c) indicating that the former type is older than the latter varieties.

Metagabbro

Metagabbro is the dominant basic igneous rock at Shahbazgarhi (Map 1). It is a medium to coarse-grained rock of dark-green to yellowish green and reddish brown colours. It is hard, compact, and fresh, except locally where substantial weathering and iron leaching can be observed. The metagabbro is intruded by a small body of porphyritic granite along Shahbazgarhi-Rustam road. At the contact with granite, the metagabbro is of lighter colour (? due to hybridization) and it gets dark-green away from the contact.

Based on the intrusive relationship of metagabbro with microporphyry, the metagabbro is considered to be representing the second phase of igneous emplacement in the area. On the other hand, the porphyritic granite has intrusive relationship with metagabbro and xenoliths of metagabbro have been noticed in porphyritic granite near Shahbazgarhi (Noorjehan, 1985, plate 3).

Porphyritic granite

The porphyritic granite occurs as the major rock unit at Shahbazgarhi and Shewa and is locally present at Machai (see Map 2,3). It is a fine to coarse-grained rock of light

grey to grey and greyish green colour. On the basis of grain size, the porphyritic granite can be divided into (a) coarse-grained (b) medium-grained, and (c) fine-grained varieties.

(a) Coarse-grained variety: The coarse-grained variety is hard, compact and light grey in colour. It contains large porphyroclasts of felsic minerals up to 3mm in diameter. In majority of the sections, augen structure and foliation are the characteristic features and consist of alternate spots of feldspars and brownish black ferromagnesian minerals (biotite). It is relatively more weathered and show iron leaching on the surface at different places. At Sherghund near Kidara Kandao, it occurs in the form of large pillar type structure (mural joints) of 3.04m to 6m in length and 0.30m to 0.60m in width (Plate 4a,b).

(b) Medium-grained variety: The medium-grained variety varies from grey to greyish green in colour. It is harder than the previous variety and contains ferromagnesian minerals ^{which} range from 2-3mm in length. Foliation is almost absent in this variety.

(c) Fine-grained variety: The fine-grained variety can be divided into (i) light grey and (ii) and greyish varieties, on the basis of its colour and texture. The light - grey variety can easily be distinguished from the greyish variety due to the absence of foliation. It is devoid of any deformation structures except a very weak alignment of the ^{constituent} minerals at places. The porphyritic granite has sharp contact with microporphyry and aegirine riebeckite porphyry. Porphyritic granite has intrusive relation

with metagabbro and the former type contains xenolith of the latter, thus the porphyritic granite represents a later phase of emplacement than the metagabbro. However, xenoliths of the porphyritic granite in aegirine riebeckite porphyry indicate that the former type is earlier in age than the latter types.

Riebeckite gneiss

The prominent occurrences of riebeckite gneiss are noticed at Sherghund, at Shewa section and from Grialala Kandao to Taja at Machai section (see Map 2,3). It is a fine-grained rock, highly sheared and foliated, containing large porphyroclast of fine glassy black material. The porphyroclast are stretched parallel to the direction of shearing. The rocks at Sherghund and Grialala Kandao are hard and compact, grey in colour, while at Taja these are whitish in colour, slightly weathered. Porphyroclast of quartz and feldspar showing augen structure are common. The riebeckite gneiss has a sharp contact with porphyritic granite and the former shows chilled margins against the latter which indicates that riebeckite gneiss is later than porphyritic granite and represents the fourth phase of emplacement in the area.

Aegirine riebeckite porphyry

The aegirine riebeckite porphyry covers mostly in the Machai section (see Map 2). It occurs along the Machai-Charghul section below Doda top and near Taja. It is a bluish colour rock with porphyroclast of feldspar and quartz. The rock is very fine grained.

and massive. Near Taja village, the aegirine riebeckite porphyry shows a peculiar out look. It contains large porphyroclast of feldspars varying from 1cm to 5cm in length. The rock has well developed fabric with porphyroclast lying parallel to it, generally in N-S direction. Some apatite veins, cross cutting these rocks have been noticed.

The contact of aegirine riebeckite porphyry with the microporphyry is clear and sharp at Machai. Xenoliths of porphyritic granite and microporphyry have been found in the aegirine riebeckite porphyry as discussed earlier.

Metadolerite and quartz monzonite dykes and sills

Dolerite and quartz monzonite have been intruded ⁱⁿ the riebeckite gneiss and aegirine riebeckite porphyry throughout the Machai section in the form of dykes and sills. Comparatively large bodies of meta dolerite are exposed near Werana Gariala and Taja below Doda top (see Map 2). The only locality where a large dyke near Werana Gariala shows an abrupt change in its composition either due to differentiation or it may have resulted as a consequence of hybridization close to the granitic contact. (Engle)

The metadolerite are mostly weathered, soft and massive with peculiar surficial appearance different from the acid igneous rocks. Spheroidal weathering is a characteristic feature in

the central parts of the big bodies/near village Taja and below Doda top. The colour of these rocks on weathered surface varies from greenish grey to dark brownish grey. Smaller dykes and sills are fine grained while the larger ones are fine grained at the margin, getting coarser towards the centre.

Quartz monzonite is comparatively fresh, hard and massive. The colour is greenish grey but lighter than metadolerite. It is probably the product of differentiation or hybridization of the metadolerite.

Both the metadolerite and quartz monzonite show intrusive relationship with chilling effect against aegirine riebeckite porphyry and riebeckite gneiss which indicate that the former are younger than the latter two varieties. (see Plate 5a,b).

In addition to these dykes and sills, a small fine-grained backed body of whitish colour and a basaltic breccia of dark-green colour have been found intruding the porphyritic granite at Shewa (see Map 3). An acidic dyke is also found intruding riebeckite gneiss (Plate 6a,b).

Biotite schist

Biotite schist represents the only country rock unit of the Swabi Chamla group in the complex. It is occurring near Shewa (Map 3). It is a fine-grained, light green rock and has a sharp contact with porphyritic granite.

Plate-1. Banding in microporphyry at Machai.

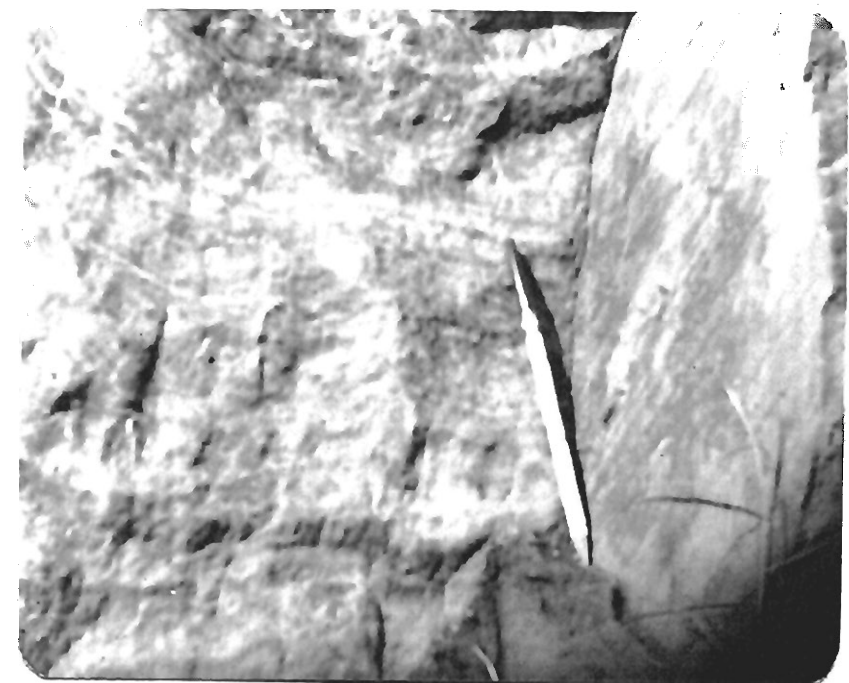


Plate-2a,b. The contact of microporphyry with porphyritic granite at Machai.

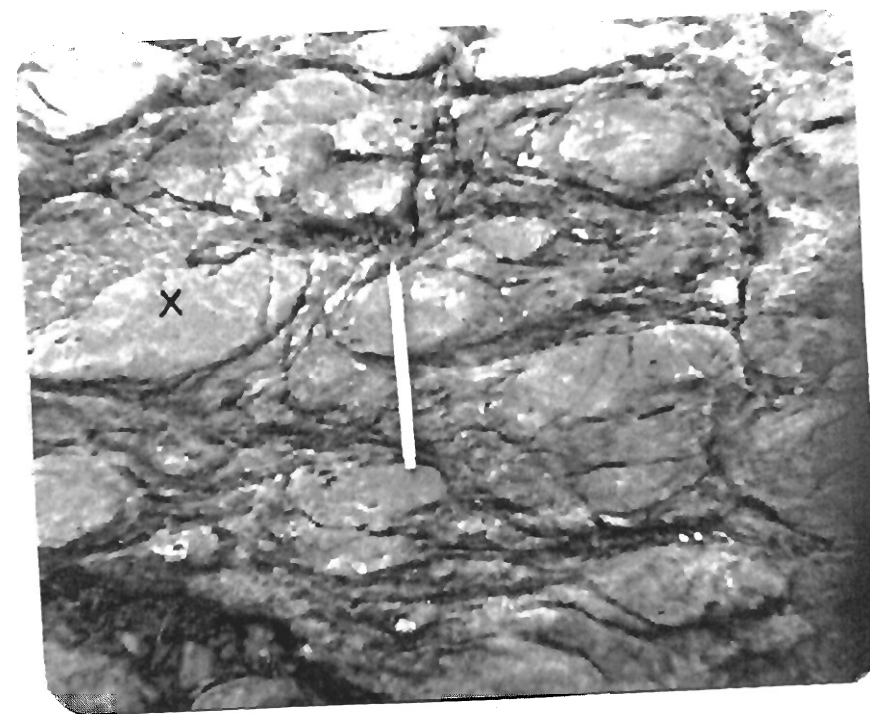




Plate-3a,b. Xenoliths of microporphyry in
porphyritic granite at Machai.



Plate-3c. Xenoliths of microporphyry in aegirine
riebeckite porphyry at Taja.





a

Plate-4a,b. The peculiar "pillar type" structure (mural joint) of the porphyritic granite at Shewa.



b

Plate-5a. Contact relationship of riebeckite gneiss and metadolerite at Werana Gariala.



a

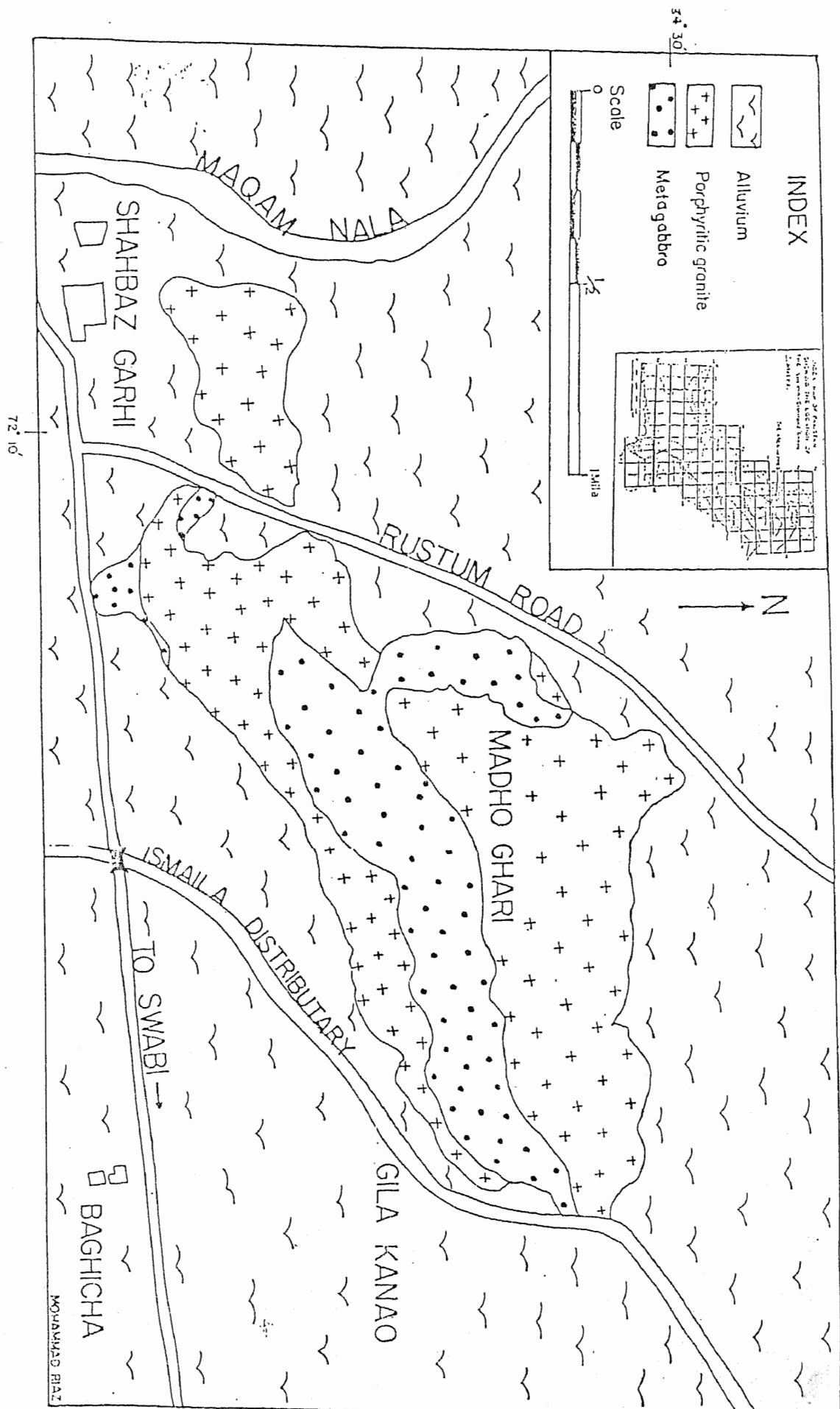
Plate-5b. Chilling effect in metadolerite contact against riebeckite gneiss.



b

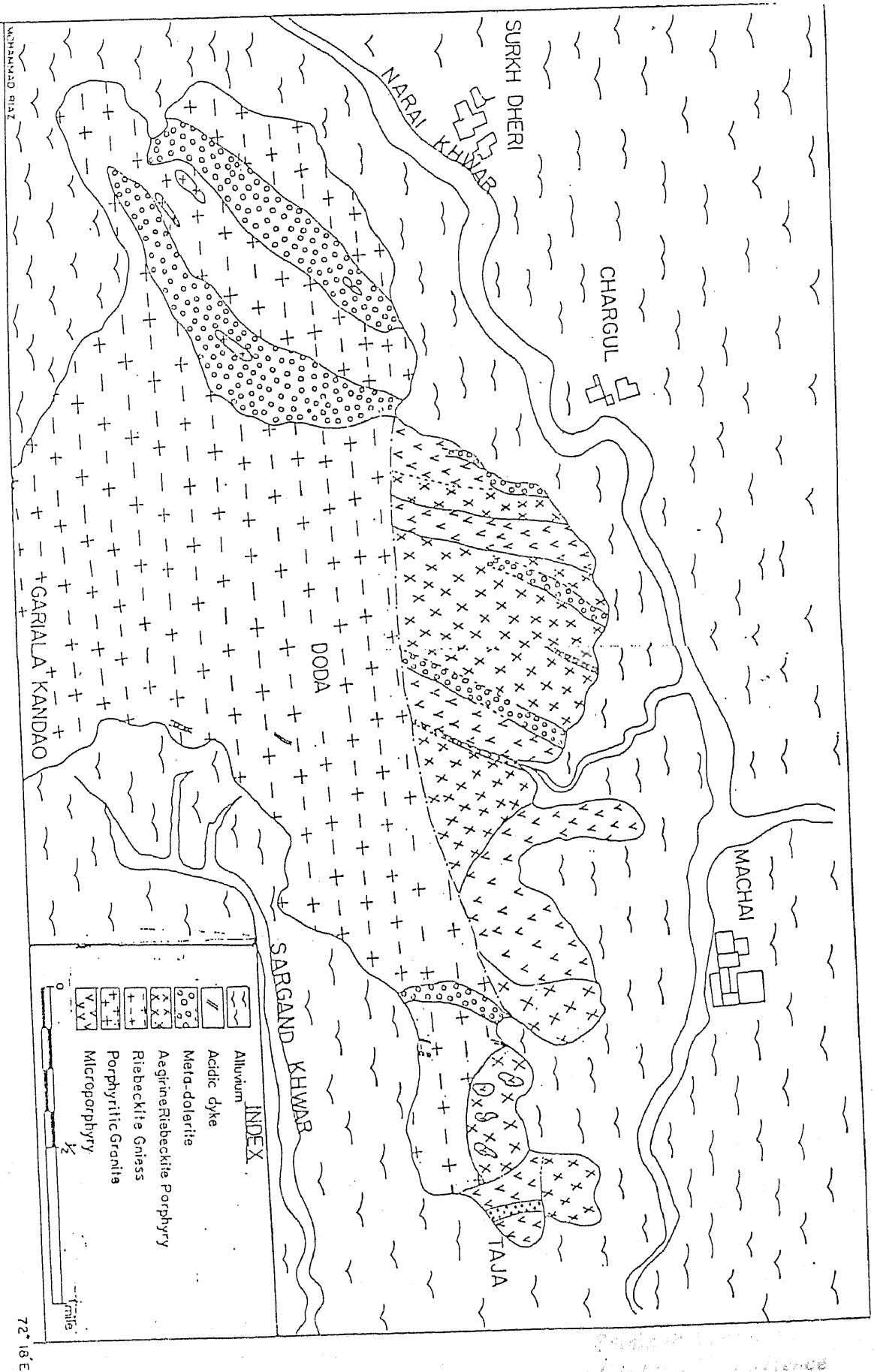
Plate-7 Acidic dyke in riebeckite gneiss
at Werana Gariala.





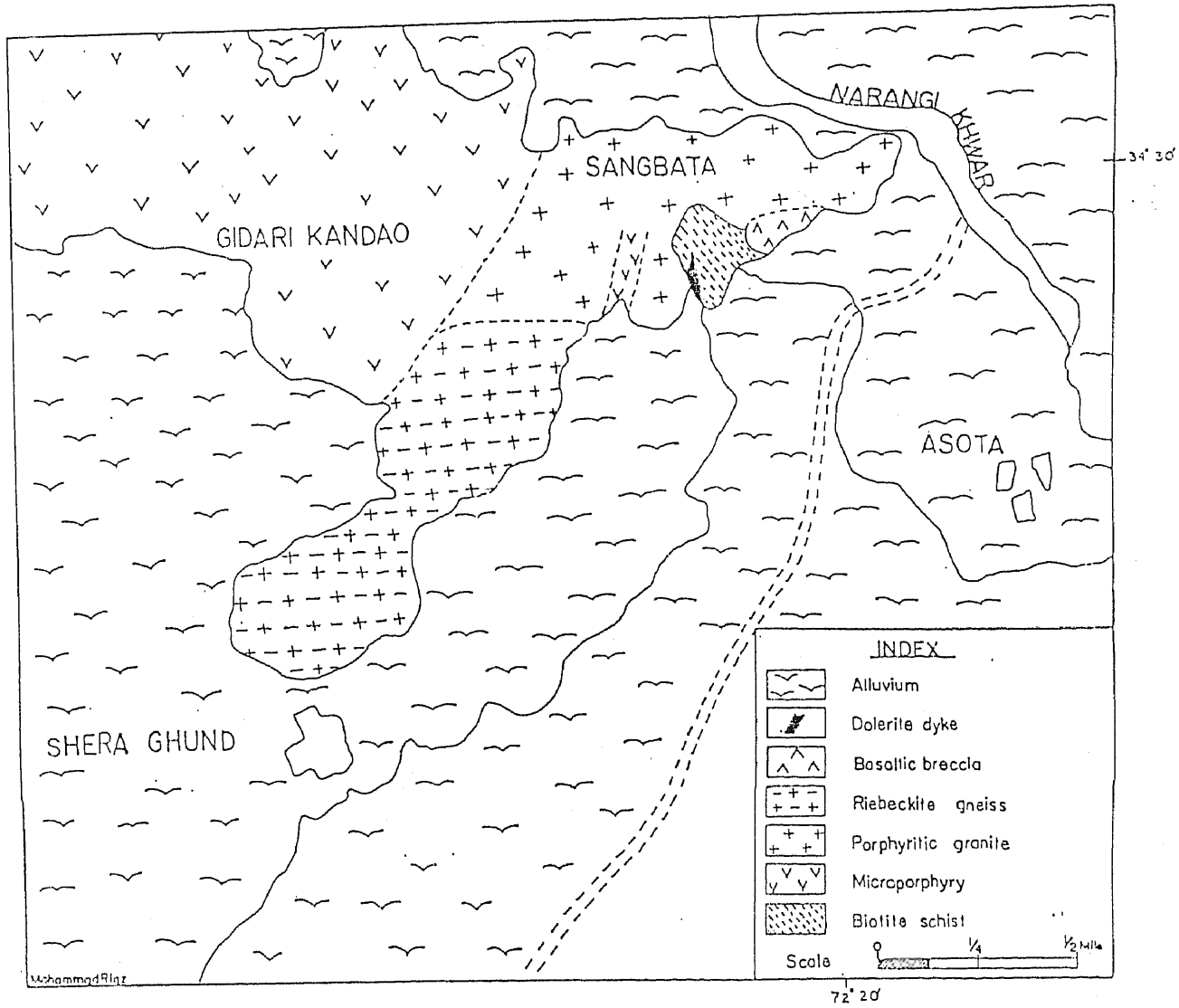
Map-1 Geology of the Shahbaz Garhi area (Shewa-Shahbaz Garhi complex).

72° 14' E



72° 18' E

Map-2 Geology of Machai area (Shewa-Shahbaz Garhi complex).



Map-3 Geology of the Shewa area (Shewa-Shahbaz Garhi complex).

CHAPTER - 3

PETROGRAPHY

Petrography of the various rocks of the Shewa Shah-bazgarhi complex has been described by Bakhtiar and Waleed (1980), Chaudhry et al. (1984), and Noorjehan (1985). During the present investigation, more samples were collected for detailed investigation specially from the cataclasized rocks.

Microporphyry

The microscopic study reveals that the microporphyry are very fine-grained rocks with orthoclase, plagioclase, perthite, quartz, biotite, magnetite and epidote as major constituents while amphibole, sphene and muscovite occur as accessories. In the earthy white variety the felsic constituents, found as microporphyroclast (C. 1-2 % Table 1) are quartz and feldspar ranging in size from 0.5mm to 1mm in diameter.

Feldspars (perthite and orthoclase) and quartz make upto about 84 - 90 % of the total mineral constituents of these rocks. These are mostly stretched and elongated along the foliation planes (Plate 7). In addition, the earthy white variety of microporphyry shows involvement of quartz

34

Felsic content																	Mafic content																
Sample No.	SH4	SH7	SH14	SHM21	SHM24	SHM29	SHM30	SH32	SHM34	SHM50	SHM52	SHM59	SHM65	SHM72	SHM73	SH	Biotite	Ore	Epidote	Muscovite	Sphene	Amphibole	Rutile										
Orthoclase																	2	2	Tr	Tr	Tr	-	-										
Plagioclase	96	94	94	10	85	80	85	85	86	86	90	90	75	84	65		1	2	Tr	-	-	-	-										
Quartz																	5	5	-	-	-	-	-										
Pertnite																	8	2	Tr	-	-	-	Tr										

and feldspar along the plane of foliation to depict layers. Feldspar and quartz grain are generally corroded at margins and their size varies from layer to layer (Plate 8).

Biotite, ranging in amount from 2 to 8 %, occurs as small grains and thin flakes in the interstices between the quartz and feldspar grains. It has altered to epidote.

Magnetite occurs as spindle shape porphyroclasts as well as fine grains and dust, scattered throughout the groundmass (Plate 9). Alteration to limonite is commonly noted in magnetite. In sections SHM21 and SHM24, magnetite concentrations in the form of thin layers is common. In section SHM24 microfolds in magnetite has also been noticed (Plate 10).

Riebeckite occurs in the form of fine needles and has apparently developed at the expense of primary amphibole.

Other characteristic accessory and minor minerals, studied in micrpporphyry , incorporate in various topocrystalline texture of the feldspars are quartz

muscovite, which shows a clear myrmekitic intergrowth within the grains of feldspars (orthoclase, Plate 11). In addition, fluxion structure also occurs around feldspar microporphyroclasts (Plate 12).

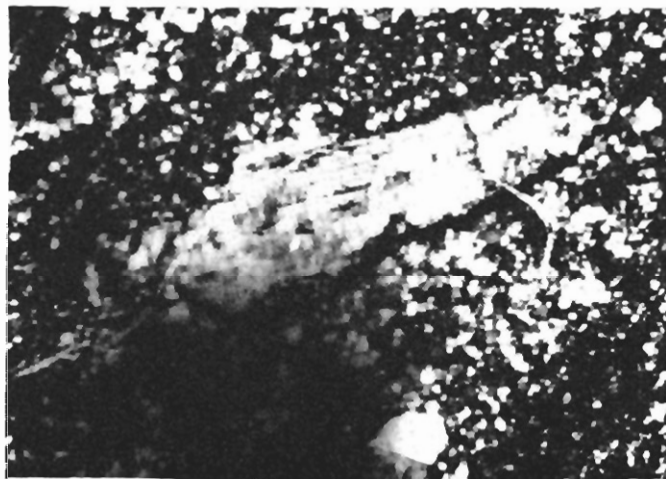


Plate-7. Photomicrograph showing elongated feldspar grain in microporphyry. Mortar texture can also be seen around the grain, (Nicols crossed, Magni. x 30).

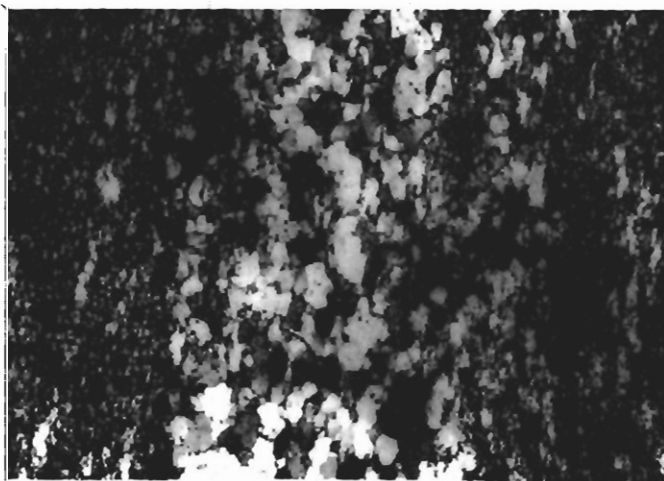


Plate-8. Photomicrograph showing bands of fine and coarse quartz and feldspar grains, (nicols crossed, Magni. x 30)

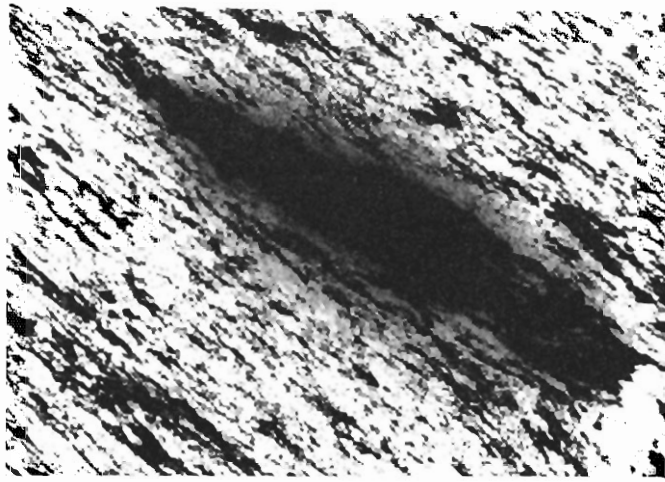


Plate-9. Photomicrograph showing spindle shape crystal of magnetite in microporphyry (Plane light, Magni. x 30).

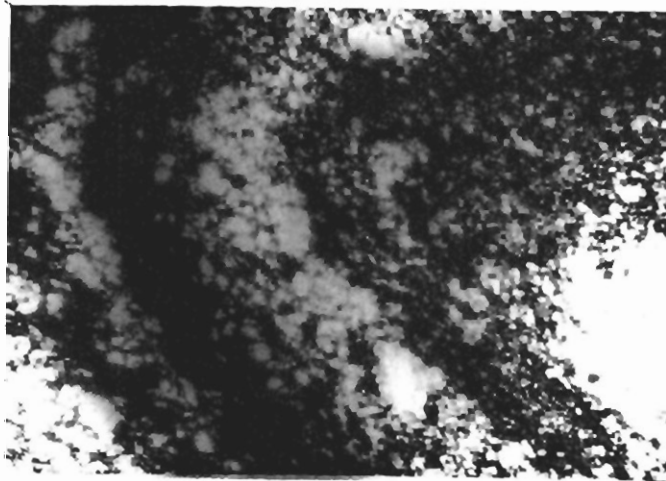


Plate-10. Photomicrograph showing kinking in magnetite and in the ground-mass of quartz and feldspar in microporphyry, (nicols crossed, Magni. x 30).

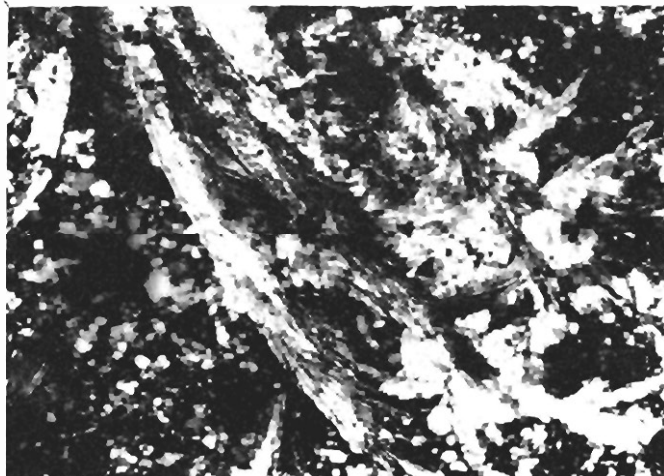


Plate-11. Photomicrograph showing development of muscovite after k-feldspar, (Nicols crossed, Magni. x 30).

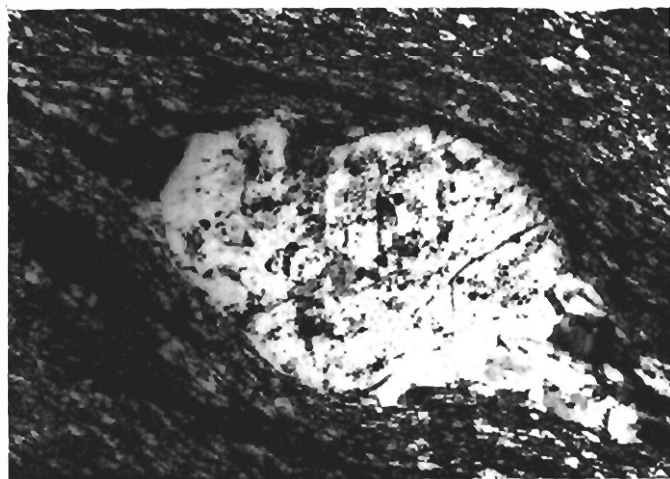


Plate-12. Photomicrograph showing flow or fluxion structure around feldspar porphyroclast, (Nicols crossed, Magni. x 30).

Metagabbro

The dominant constituents of metagabbro are amphibole, plagioclase, magnetite, biotite, epidote, orthoclase, whereas quartz, sphene, apatite and chlorite occur as minor constituents (see Table 2). Nearly all the major constituents^s are subhedral to euhedral and their grain size ranges from 1mm to 2mm. The overall texture is inequigranular to subophitic.

Amphibole occur as primary as well as secondary mineral. The primary amphibole is present as irregular masses disseminated throughout the groundmass. It is pleochroic from pale green to light blue with an extinction angle in the range of $5-10^{\circ}$; thus it seems to be hastingsite. The larger amphibole grains are fractured, corroded at the margins and have inclusions of biotite and magnetite. The secondary amphibole is associated with primary amphibole, plagioclase and magnetite and seems to have been developed at the expense of the plagioclase and magnetite. (Plate-13a,b) its light bluish colouration is thought to be the product of secondary processes, probably metasomatism.

Plagioclase (oligoclase) ranges from 20-45 % and occurs as prismatic crystals and subhedral to euhedral crystals in these rocks. Most of the plagioclase grains are cloudy and show alteration to epidote. Some fresh grains of plagioclase can be noticed which show good albite twinning.

TABLE 2. MODAL COMPOSITION OF METAGABBROS

	1	2	3	4	5	6
Sample No.	SH1	SH9	SH11	SHM116	SHM117	SHM119
Amphibole	50	45	35	45	55	50
Plagioclase	15	22	40	10	10	15
Biotite	10	10	5	5	5	6
Magnetite	12	10	10	12	12	10
Epidote	5	6	5	10	10	6
Orthoclase	5	4	3	5	2	5
Quartz	2	2	1	8	5	3
Apatite	Trace	1	Trace	2	1	2
Sphene	Trace	Trace	Trace	1	Trace	1
Chlorite	Trace	Trace	-	-	-	-
Pyroxene	-	-	-	-	-	-
Rutile	-	-	-	-	-	-

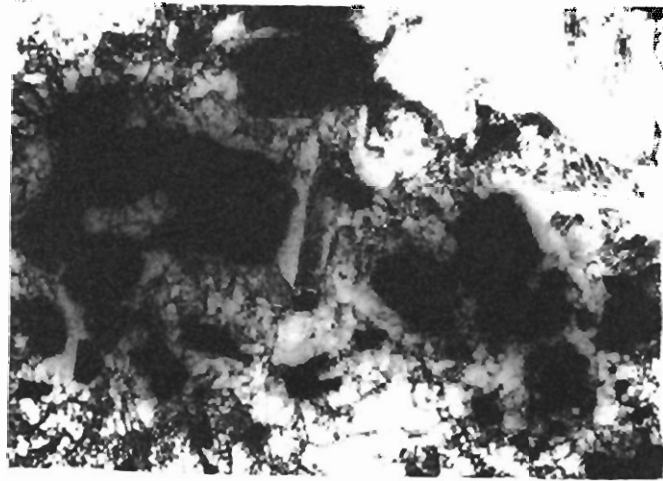


Plate-13a.

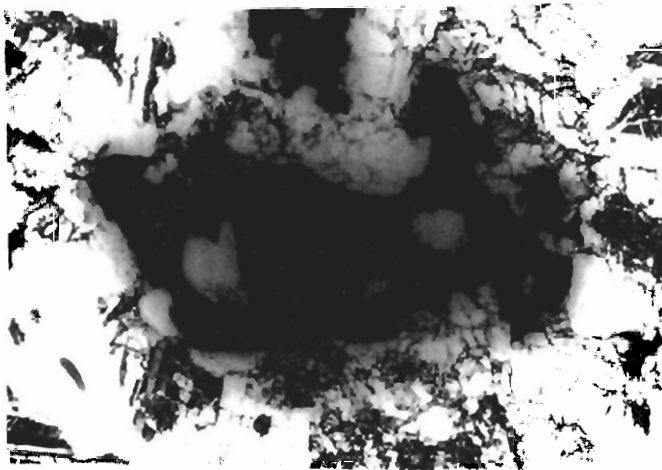


Plate-13a,b. Photomicrographs showing formation of amphibole at the expenses of magnetite and plagioclase, an amphibole grain can also be seen in the core of magnetite, (Nicols crossed, Magni. x 30).

In the fractured grains, biotite, amphibole and apatite are common along fractures.

Magnetite occurs as small rounded to large irregular grains mostly surrounded by amphibole, biotite and epidote. Magnetite contains inclusion of other minerals and in some cases it is surrounded by coronas of sphene, suggesting their development from ilmenite which also occurs as fibrous aggregates. It is also surrounded by shells of sphene or leucoxene (Plate- 14).

Biotite and epidote occur in close association, generally along the margins and cleavages of the amphibole, indicating that these have developed after amphibole. Biotite is pleochroic from pale green to dark-brown and is occasionally replaced by chlorite.

Felsic constituents such as orthoclase and quartz make up some 10-15% of the total mineral constituents. These occur as subhedral to euhedral grains in the interstices of the amphibole crystals and also as inclusion in amphibole and magnetite grains.

Apatite (C. 2-3%) is commonly associated with amphibole and magnetite and occasionally occurs as inclusion in these minerals.

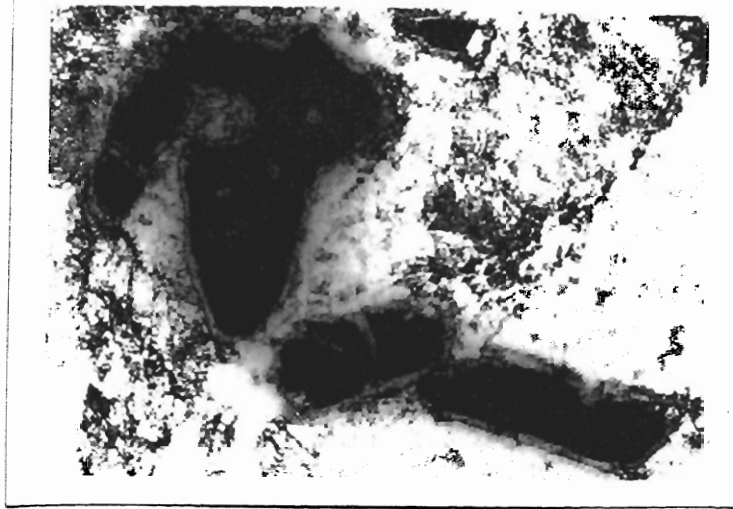


Plate-14. Photomicrograph showing rim of fine grained sphene around magnetite grains in metagabbro, (Nicols crossed, Magni. x 30).

Lamprophyric dykes intruding in to metagabbro at Shahbazgarhi are reported ^{by} Noorjehan (1985). The mineralogy of these dykes is similar to those of metagabbro, studied during the present work. Model compositions of these lamprophyric dykes are given in table 4.

TABLE 3. MODAL COMPOSITION OF META-GABBRO BASED ON VISUAL ESTIMATE (AFTER NOORJEMIAN, 1985)

S.No.	1	2	3	4	5	6	7
Sample No.	SN1	SN3	SN5	SN7	SN10	SN12	SN49
Amphibole (Hastingsite)	60%	55%	15%	50%	60%	60%	50%
Quartz	5%	5%	6%	5%	5%	71%	10%
Orthoclase	5%	5%	5%	10%	5%	10%	10%
Plagioclase	5%	10%	45%	-	10%	-	1%
Epidote	10%	8%	6%	10%	10%	-	15%
Opaque Ore	5%	6%	6%	10%	5%	10%	6%
Biotite	5%	6%	15%	15%	31%	10%	-
Apatite	3%	2%	-	-	-	1%	6%
Perthite	1%	2%	1%	-	1%	1%	1%
Sphene	1%	1%	1%	-	1%	1%	1%
Calcite	-	-	-	-	-	-	-

TABLE 4 . MODAL COMPOSITION OF LAMPROPHYRIC DYKES, BASED ON
VISUAL ESTIMATE (AFTER NOORJEHAN, 1985)

S.No.	1	2	3
Sample No.	SN4	SN27	SN30
Amphibole (Hastingsite)	75%	50%	50%
Orthoclase	5%	20%	10%
Quartz	3%	10%	10%
Plagioclase	-	-	-
Biotite	10%	8%	15%
Epidote	5%	2%	4%
Perthite	-	1%	-
Ore Mineral	2%	8%	10%
Apatite	-	-	-
Sphene	-	1%	1%

Porphyritic granite

In thin section the porphyritic granites are generally foliated and show augen structures but in some sections, foliation is not distinct. The ratio of porphyroclast to groundmass varies between 40 % and 60 % in coarse-grained variety, 70 % and 30 % in medium-grained, and 20 % and 80 % in the fine-grained variety (see Table 5)). The length of the porphyroclasts are generally 1mm to 2.5mm in diameter with some exception in the white grey variety where the diameter of porphyroclast is 3-4 mm in diameter.

The important mineral constituents are orthoclase, perthite, plagioclase, microcline, biotite, epidote, opaques, minerals and amphibole. Apatite, sphene and muscovite occur as the minor constituents.

Alkali feldspar porphyroclast and phenocryst comprise orthoclase, microcline and their perthesized equivalents. The phenocrysts are euhedral to subhedral while the porphyroclasts are rounded in shape. Grains of orthoclase and microcline are failured by stresses. In such ^{cases} /the corners and edges are corroded, strained and show wavy extinction. Stretching and elongation is

is it possible
to have two
solutions

Orthoclase	25	30	35	40	25	35	30	15	15	25	35	20	35	30	40	20
Quartz	20	35	42	25	10	20	30	25	20	10	20	25	20	15	20	25
Plagioclase	15	10	10	6	20	30	15	10	20	15	10	10	15	25	5	Tr
Microcline	12	2	-	-	10	7	15	5	5	-	-	7	-	4	-	Tr
Perthite	6	8	-	7	15	-	-	25	15	20	20	20	17	15	25	45
Biotite	8	2	4	6	10	3	5	10	12	15	10	10	2	3	2	5
Muscovite	2	Tr	1	1	-	Tr	-	-	-	-	-	Tr	1	-	-	-
Aegirine	5	5	-	-	-	-	-	-	-	-	-	-	1	2	-	-
Amphibole	Tr	Tr	-	Tr	-	-	-	-	-	-	-	-	-	-	-	-
Epidote	4	6	6	-	Tr	-	1	Tr	3	2	Tr	Tr	Tr	1	Tr	Tr
Sphene	Tr	Tr	-	-	-	-	-	-	-	Tr	-	-	-	1	-	-
Zircon	-	-	-	-	-	-	-	Tr	-	Tr	-	-	-	-	-	-
Apatite	-	-	-	-	-	-	-	-	-	Tr	-	-	-	-	-	Tr
Rutile	Tr	-	-	-	Tr	-	-	-	-	Tr	-	-	-	-	-	-
Ore	3	2	2	15	10	5	4	10	10	13	10	8	9	4	8	5

Ratio 35/65 30/70 30/70 40/60 20/80 20/80 40/60 5/95 15/85 10/90 20/80 20/80 40/60 70/30 50/50 60/40 40/60
 Porphyroblast/
 Groundmass

commonly observed in these grains, however, the corrosion and brittleness is dominant over the clastic deformation (Plate- 15,16). In addition, the more deformed grains show sericitization and kaolinization. Some grains are so intensely sericitized that the original grains of orthoclase or microcline^{are} left in relics. Presence of muscovite over these grains show advancement in alteration (Plate - 17.).

Porphyroclast of plagioclases (C. 7-20%) occurs as euhedral to subhedral crystals and ranges in size from 1mm to 2.5mm, displaying good albite twinning. The crystals are broken, curved and corroded at margins (Plate-18).

Quartz (C. 20-30%) commonly occurs as porphyroclasts. It is an abundant felsic constituent in the fine grained groundmass. The porphyroclasts of quartz are highly fractured, corroded at margins and show wavy extinction. Certain quartz grains show overgrowth of a second generation (Plate-19). The fractured grains of quartz commonly contain biotite and epidote along the fractures. Myrmekitic intergrowth of quartz feldspar with alkali is a common feature in these rocks (Plate-20).

^{minerals}
Opaque / (C. 5-10%) occurs as rounded as well as irregular grains scattered throughout the groundmass. Sphene is generally associated with magnetite.

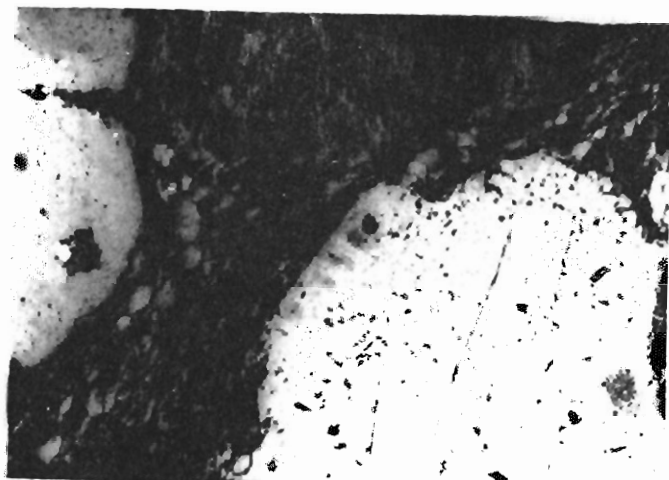


Plate-15. Photomicrograph showing an orthoclase grain corroded at the margins and core with inclusions of biotite and epidote, (Nicols crossed, Magni. x 30).



Plate-16. Photomicrograph showing broken perthite grains filled up by recrystallized quartz and orthoclase along the fracture, (Nicols crossed, Magni. x 30).

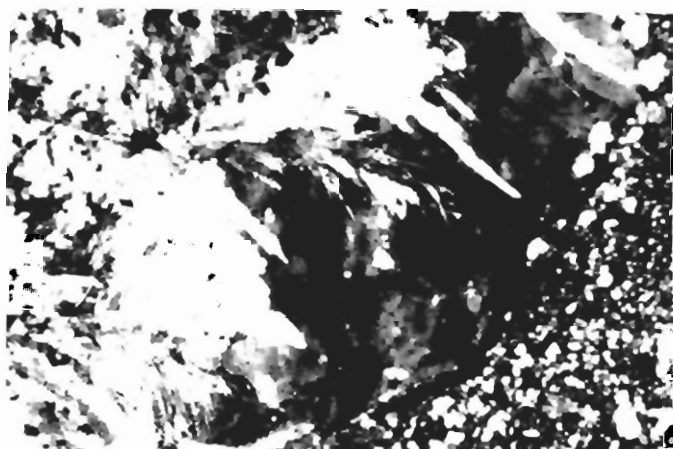


Plate-17. Photomicrograph showing the development of muscovite after k-feldspar in porphyritic granite (Nicols crossed, Magni. x 30).

Biotite, epidote, amphibole and apatite occur in close association and constitute up to 20 % of the total rock. Biotite is pleochroic from pale brown to greenish brown. It has developed at the expense of magnetite and K-feldspar (Plate-21),

Amphibole is mostly riebeckite and is restricted only to the light grey variety. Apatite mostly occurs as thin tabular crystals, however, a few crystal of 1mm in length have also been noticed.

The most peculiar feature of the fine-grained matrix is the development of fluxion structure and mortar texture around the quartz and feldspar porphyrocrysts. In some sections of the light grey variety, the comparatively coarse-grained matrix of angular fragments also show similar features. Fluxion structure and mortar texture reflect cataclasis and mylonitization (Plates 22a,b and 23), see also Noorjehan (1985, p. 30,34).

Garnet and chlorite are reported in the porphyritic granite by Kempe (1973) and Bakhtiar and Waleed (1980).

The gneissose microgranite reported by Noorjehan (1985) is renamed as porphyritic granite. The modal composition of the gneissose microgranite of Noorjehan is presented in table 6.



Plate-18. Photomicrograph showing alteration of plagioclase to epidote and myrmekitic intergrowth of quartz with orthoclase, (Nicols crossed, Magni. x 25).

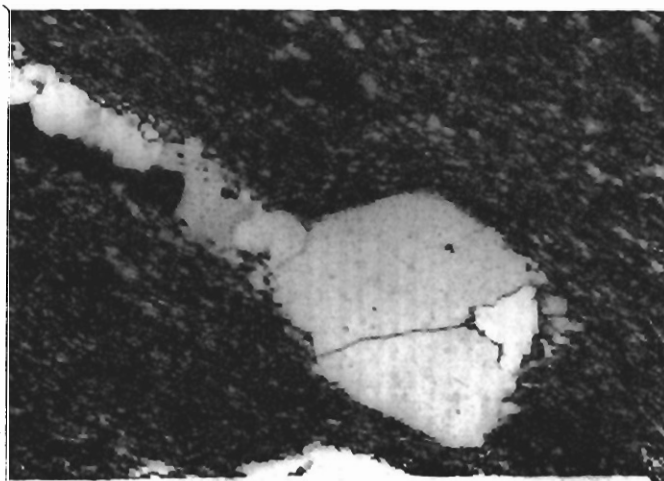


Plate-19. Photomicrograph showing quartz grain with overgrowth of the second generation. Fluxion structure and mortar texture can also be seen around the grain, (Nicols crossed, Magni. x 25).

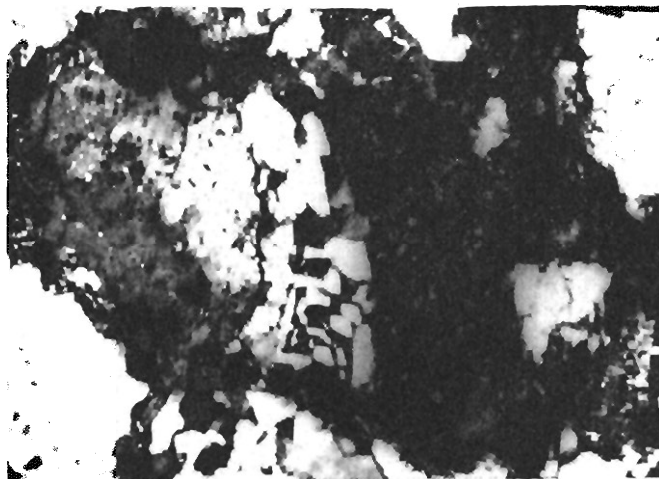


Plate-20. Photomicrograph showing perthite grain with myrmekitic intergrowth on margin, (Nicolis crossed, Magni. x 25).

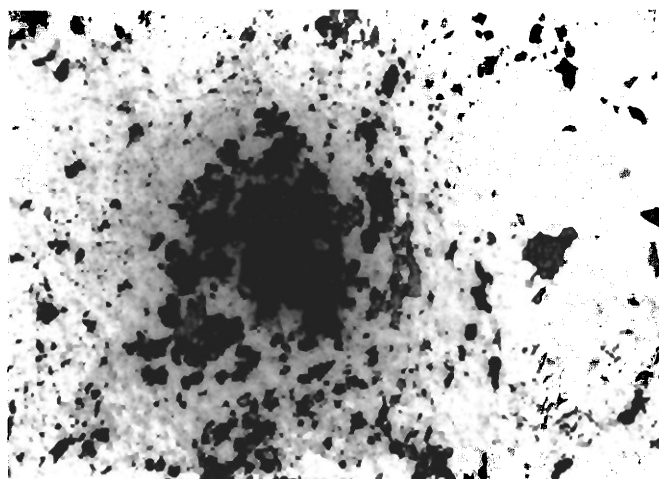


Plate-21. Photomicrograph showing the development of biotite at the expense of magnetite and feldspar in porphyritic granite, (Plane light, Magni. x 25).

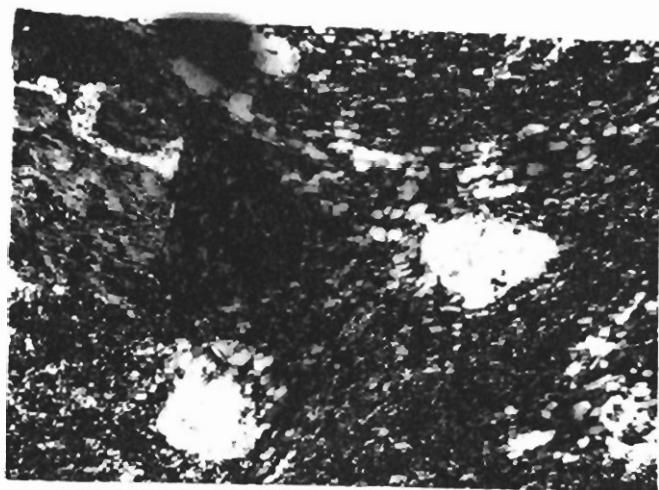


Plate-22a.

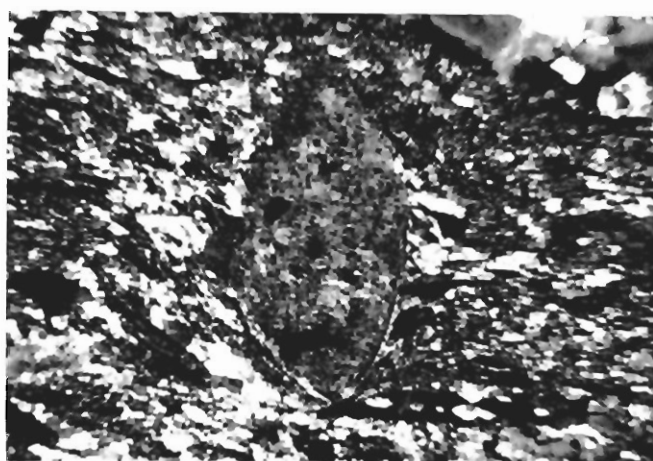


Plate-22a,b. Photomicrograph showing fluxion structure around feldspar grains in porphyritic granite. Fine flaky muscovite and epidote parallel to the fluxion structure can also be seen. (Nicols crossed, Magni.x 30).

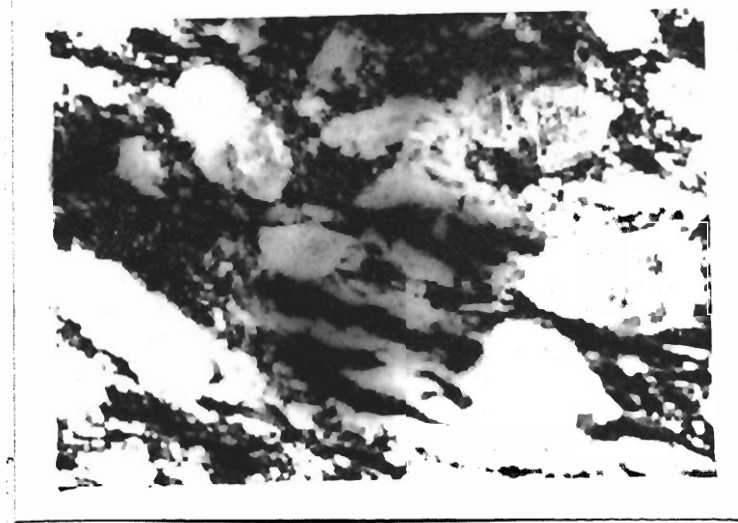


Plate-23. Photomicrograph showing corroded and elongated porphyroclasts of quartz and feldspar in porphyritic granite, (Nicols crossed, Magni. x 30).

TABLE 6. MODAL COMPOSITION OF GNEISSOSE MICROGRANITE BASED ON
VISUAL ESTIMATE (AFTER NOORJEHAN, 1985)

S.No.	1	2	3	4	5
Sample No.	SN11	SN16	SN20	SN21	SN25
Orthoclase	50%	35%	50%	60%	60%
Quartz	30%	25%	40%	20%	25%
Perthite	10%	15%	2%	10%	5%
Biotite	5%	5%	2%	3%	5%
Plagioclase	-	5%	1%	-	-
Ore mineral	3%	10%	5%	2%	3%
Epidote	-	5%	-	5%	4%
Apatite	2%	-	-	-	-
Sphene	-	-	-	-	1%

Riebeckite gneiss

*one fine (100
2000*

The major constituents of riebeckite gneiss are perthesized orthoclase, orthoclase, plagioclase, quartz, riebeckite, biotite, epidote and ore. Sphene, Zircon, apatite and sericite are found as accessories. Sillimanite needles have been studied in few sections. (SHM44, SHM45). (Table 7)

The porphyroclasts of perthesized orthoclase, and in orthoclase these rocks are fine to medium-grained. These also constitute the background or matrix in some sections. The orthoclase and perthesized orthoclase characteristically show all the features observed in the cataclasized rocks. However, the porphyroclasts are in cases tensely deformed and rotated in some / (Plate- 24,25) much more than the rocks earlier described. The porphyroclasts show a high degree of alteration. The alteration product of these porphyroclast are sericite, muscovite, kaoline and opaque dust.

Porphyroclasts of plagioclase are also highly deformed and have altered to epidote and sericite at the margin and along the fractures. (Plates-26,27).

Riebeckite, biotite and epidote occur in close association with each other. Riebeckite and biotite are



Plate-24. Photomicrograph showing a broken and elongated feldspar grain in the laminated groundmass. Overgrowth of second generation in the form of rims can also be seen around the broken grains. (Nicols crossed, Magni. x 25).



Plate-25. Photomicrograph showing fluxion structure around corroded feldspar grain in riebeckite gneiss. (Nicols crossed, Magni. x 25).

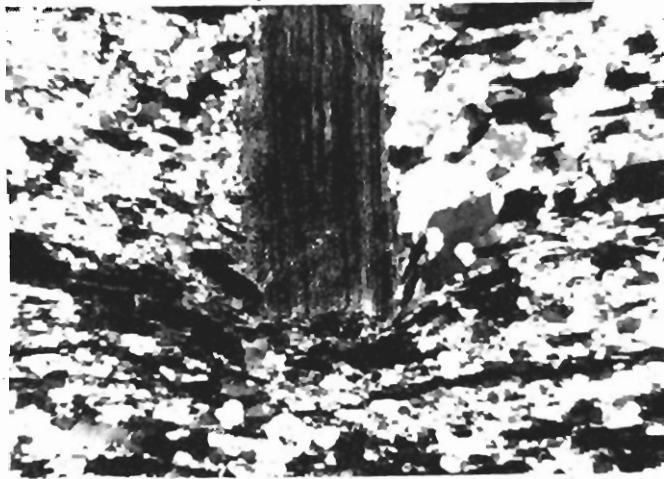
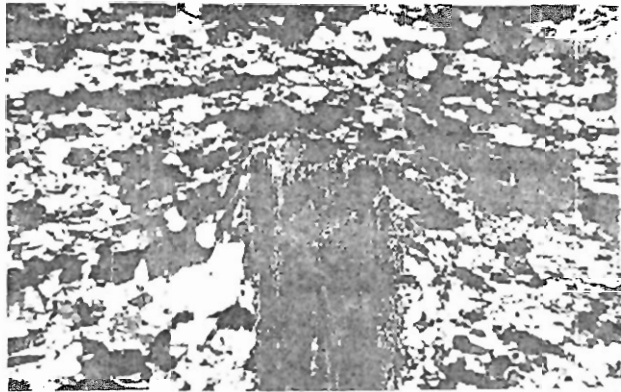


Plate-26. Photomicrograph showing fluxion structure around the plagioclase grain. A fine grained crushed mass can also be seen in the lower left corner, of the lower photomicrograph, (Nicols crossed, Magni. x 25).

found as thin, elongated, tabular grains while epidote occurs
/as aggregate of small rounded grains. Riebeckite is pleochroic from light green to deep blue. The textural relationship of riebeckite with biotite, and at places with K-feldspar and magnetite, is such that riebeckite appears to have developed at the expenses of these - minerals.

Opaque ore, possibly magnetite, occurs as irregular grains and is commonly associated with biotite. Iron leaching is common along the fractures and in most cases it seems that it has been released during the deformation of biotite.

Sillimanite occurs as thin prismatic needles and have seems to / developed at the expense of feldspar (Plate-28).

The groundmass of this particular unit is very fine, glassy and highly laminated and foliated (Plate-24).



Plate-27. Photomicrograph showing a rotated plagioclase grain. Mortar texture can also be seen around the grain in riebeckite gneiss. (Nicols crossed, Magni. x 25).

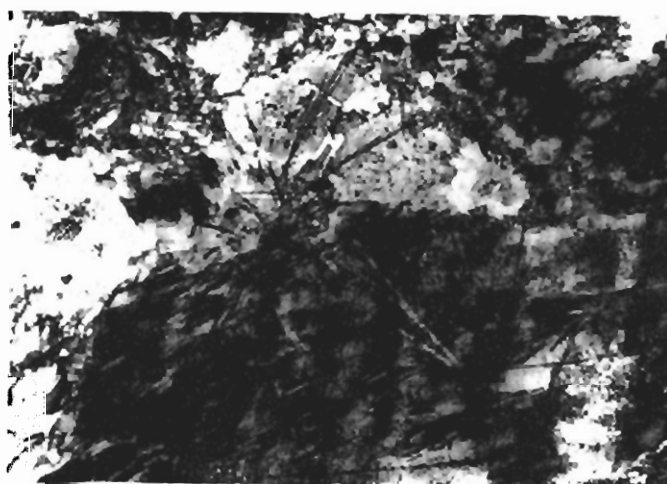


Plate-28. Photomicrograph showing the development of sillimanite after feldspar in riebeckite gneiss. Epidote grains can also be seen in upper left corner. (Nicols crossed, Magni. x 25).

Aegirine riebeckite porphyry

The important mineral constituents of this rock type are orthoclase, perthesized orthoclase, plagioclase, quartz, riebeckite, epidote, opaque ore and aegirine. Sphene, muscovite, zircon, sillimanite and apatite occur as minor constituents. ^{Table 8.} All the feldspars, riebeckite, quartz, opaque ore and aegirine occur as porphyroclast (10-70%) as well as fine-grained groundmass. The grain size of the porphyroclast ranges from 1mm to 3mm in diameter.

Orthoclase and perthesized orthoclase occur as porphyroclast which are broken, curved, corroded at margins and commonly altered to muscovite. (Plate- 29,30). The fractured grains contain biotite, riebeckite and quartz. Zoned orthoclase has also been noticed in some sections.

Plagioclase occurs as subhedral to euhedral grains similar in size to the potash feldspar. The plagioclase grains are also broken, fractured (Plate-31,32) occasionally zoned, cloudy and contain inclusion of biotite and riebeckite.

Riebeckite is present as fine needles to crystallites or globules, spread over the rock section along

TABLE 8. MODAL COMPOSITION OF AEGIRINE RIEBECKITE PORPHYRY.

S.No.	1	2	3	4	5	6	7	8	9	10	11
Sample No.	SHM25	SHM39	SHM69	SHM72	SHM85	SHM88	SHM89	SHM95	SHM98	SHM101	SHM127
Orthoclase	20	15	30	20	50	25	40	20	25	30	45
Quartz	25	20	25	15	35	20	18	25	20	15	20
Plagioclase	5	10	-	15	-	25	10	28	25	-	10
Microcline	-	20	5	5	-	-	-	-	-	20	-
Perthite	30	13	30	25	-	3	-	-	-	-	-
Bioltite	7	2	1	6	4	2	6	1	2	6	12
Muscovite	-	-	Tr	-	-	Tr	-	1	Tr	-	-
Ore	6	1	Tr	-	1	4	3	3	6	2	3
Riebeckite	4	6	5	7	1	15	20	16	15	20	7
Aegirine	3	3	2	5	1	2	2	2	2	3	2
Epidote	Tr	2	Tr	1	Tr	2	Tr	2	2	2	Tr
Apatite	Tr	-	Tr	Tr	-	Tr	1	Tr	Tr	1	1
Heamatite	-	4	Tr	Tr	7	2	-	2	2	1	-
Sillimanite	Tr	-	Tr	Tr	Tr	Tr	-	Tr	Tr	-	-
Zircon	Tr	Tr	Tr	Tr	1	-	Tr	Tr	Tr	-	-

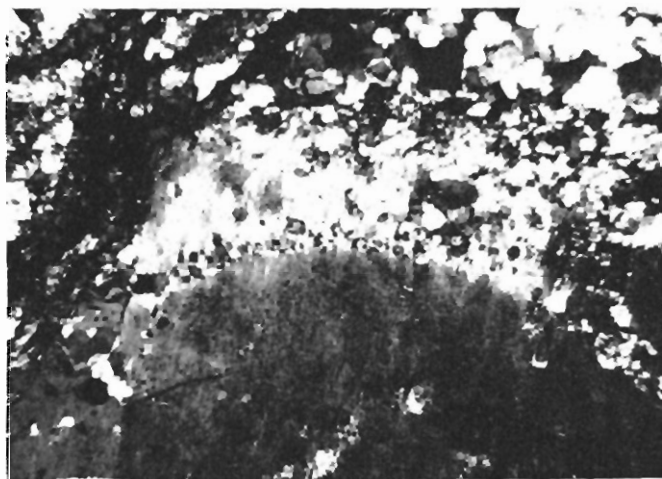


Plate-29. Photomicrograph showing a broken and corroded perthite grain in aegirine riebeckite porphyry. Epidote inclusion can be seen in its core, (Nicols crossed, Magni. x 25).

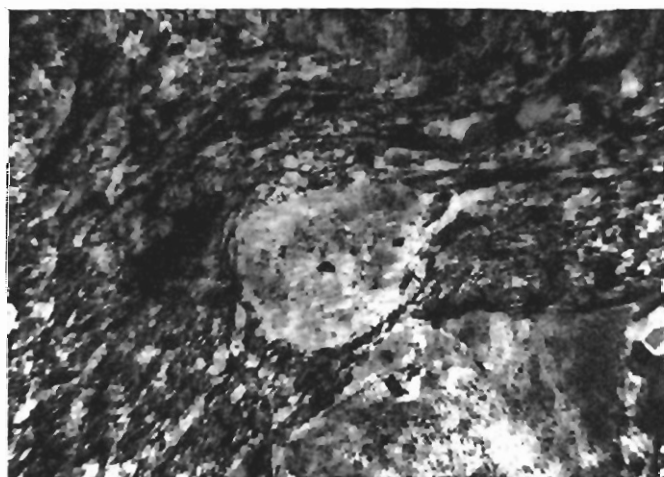


Plate-30. Photomicrograph showing rotated perthite porphyroclasts surrounded by matrix indicating fluxion structure, (Nicols crossed, Magni. x 25).



Plate-31. Photomicrograph showing a kinked plagioclase grain indicating deformation, (Nicols crossed Magni. x 25).



Plate-32. Photomicrograph showing kinked and corroded plagioclase grain indicating deformation, (Nicols crossed, Magni. x 25).

the planes of weakness. Na-bearing solutions probably migrated along these planes, causing metasomatic development of riebeckite. It is pleochroic from light brown to deep blue and has altered to epidote and sphene.

Biotite is pleochroic from light brown to reddish brown. It occurs as thin tabular as well as large elongated grains and has developed at the expense of magnetite and feldspar.

Aegirine occurs as subhedral to euhedral grains. It is pleochroic from light green to dark-green with a small extinction angle. The grains are broken and some show alteration to epidote. Apatite occurs in traces.

Metadolerite

The main constituents of the metadolerite are amphibole, plagioclase, biotite, epidote, opaque ore and apatite. Chlorite, leucoxene, clinopyroxene, and sphene occur as minor components. In two sections (SHM42, SHM97; see Table 9) orthopyroxene is the major constituent instead of amphibole.

Amphibole ranges from 46 to 65 %. It occurs as prismatic crystals as well as thin needles disseminated throughout the groundmass. It shows distinct pale green to light blue pleochroism, has low extinction angle $\underline{C}.5^{\circ}$, and can be classed as hastingsite. Epidote and chlorite are abundant within and close to amphibole grains, suggesting that they formed secondarily after the amphibole. Quartz and ore inclusions are also found in the amphibole.

Orthopyroxene (hypersthene) occurs in close association with magnetite as subhedral to euhedral grains, commonly altered to amphibole and epidote. Clinopyroxene also occur in traces in two of the sections.

Plagioclase ranges from 10 to 50 %. Most of the plagioclase grains are altered to epidote, clay and

TABLE 9. MODAL COMPOSITION OF METADOLERITE

S.No.	1	2	3	4	5	6	7	8	9
Sample No.	SHM40	SHM42	SHM46	SHM46	SHM97	SHM108	SHM111	SHM138	SHM139
Amphibole	50	5	50	48	15	65	65	48	50
Pyroxene	5	30	-	-	28	-	-	Trace	Trace
Plagioclase	25	50	15	22	15	10	15	20	15
Biotite	5	Trace	10	6	15	12	10	12	10
Magnetite	8	12	8	10	10	8	7	5	10
Epidote	1	1	5	2	8	2	1	5	5
Orthoclase	2	Trace	5	5	5	1	1	5	4
Quartz	1	Trace	5	4	2	Trace	1	3	5
Apatite	2	2	1	1	2	Trace	Trace	1	1
Sphene	Trace	Trace	1	1	Trace	Trace	Trace	1	Trace
Chlorite	Trace	Trace	Trace	Trace	Trace	Trace	Trace	Trace	Trace
Rutile	-	-	-	-	-	Trace	-	-	-

sericite. Quartz grains are also found in plagioclase as a byproduct of epidotization. At places secondary epidote and quartz follow the outlines of completely observed plagioclase with weak albite twinning. Some plagioclase grains are dirty, others are fractured and corroded. Some fresh crystals are subhedral to euhedral, having good albite twinning.

Biotite generally occurs along the margins and within cleavages / amphibole and/or pyroxene crystals, indicating its formation after the latter minerals. It is pleochroic from pale green to dark-brown and is some time altered to chlorite.

Quartz ranges in amount from 4 to 6 % as primary as well as secondary mineral. The primary quartz crystals have well-developed outline but are generally rounded in shape. The secondary quartz is in the form of small grains formed after the silica released during the alteration of plagioclase to epidote and amphibole.

Ore is presumably magnetite and ilmenite altered to leucoxene and sphene. Apatite is a constant accessory mineral. The mineral assemblage of metadol-
to
erite, thus more or less resembles those of the metagabbro.

Quartz monzonite

The quartz monzonite consists of orthoclase, orthoclase perthite, quartz, biotite, epidote and opaque ore as major minerals. Sphene and apatite occur as accessories. (see Table 10). The texture is inequigranular hypidiomorphic.

Plagioclase occur as subhedral to euhedral grains. The grains are mostly fractured and corroded and contain inclusions of biotite, quartz and feldspar (Plates-33a-d).

Orthoclase and orthoclase-perthite occur in close association/ They ore also fractured and occasionally altered to epidote. Myrmekitic and graphic intergrowth of quartz with the feldspar are common feature. (Plate-34a,b).

Quartz occurs as large rounded grain as well as in the form of fine graphic intergrowth in the intersticies of the plagioclase, and perthite. The larger grains at places, are broken and corroded at margins, and exhibit wavy extinction.

Biotite and opaque grains occur in close association, surrounding feldspar grains. Biotite is found as thin tabular laths as well as lamellar aggregates and has developed at the expense of magnetite and feldspar.

TABLE 10. MODAL COMPOSITION OF QUARTZ MONZONITE

S.No.	1	2
Sample No.	SHM110	SHM113
Plagioclase	60	60
Orthoclase perthite	15	15
Quartz	6	5
Biotite	16	15
Ore	2	2
Epidote	Trace	2
Sphene	1	1
Chlorite	Trace	Trace
Muscovite	-	Trace
Allanite	Trace	Trace
Zircon	Trace	Trace

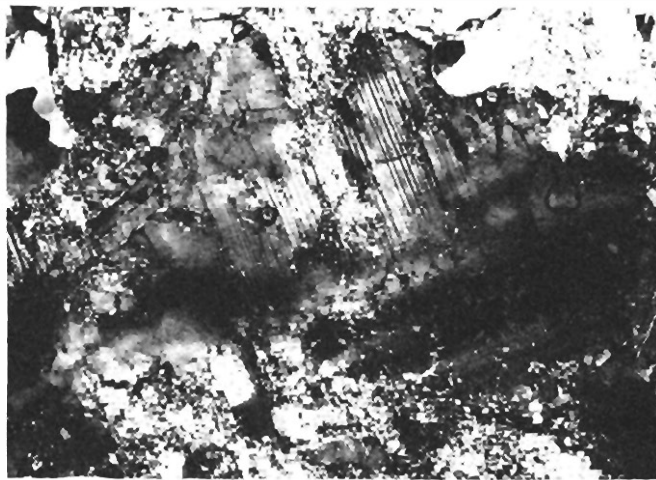


Plate-33a.



Plate-33b.

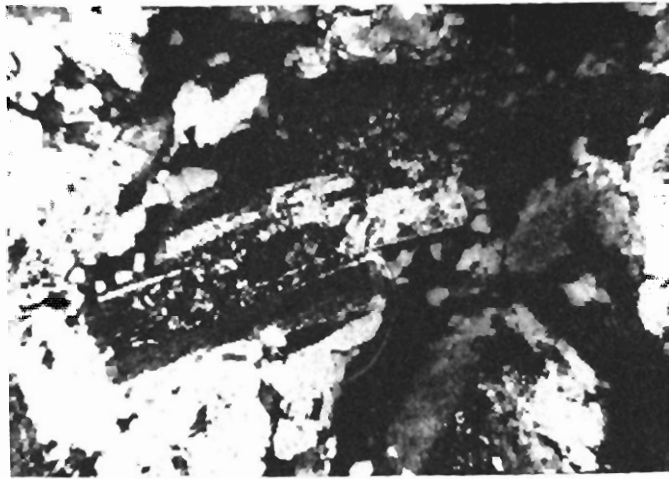


Plate-33c.

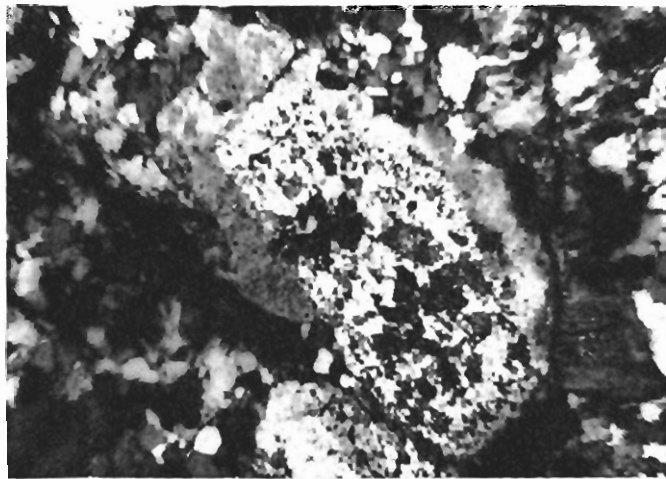


Plate-33d.

(a-d) Photomicrographs showing plagioclase crystals with partial alteration to epidote. Note zoning in c and d, (Nicols crossed, Magni.x 30).



Plate-34a.

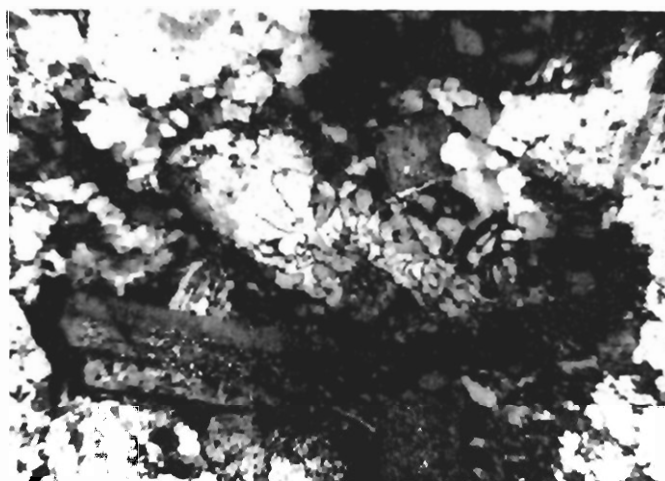


Plate-34a,b. Photomicrograph showing myrmekitic and graphic intergrowth between quartz and feldspar in quartz monzonite, (Nicols crossed, Magni. x 30).

TABLE 11. CLASSIFICATION OF ACIDIC ROCK OF THE SHEWA-SHAHAZGARHI COMPLEX
ON THE BASIS OF TEXTURAL CLASSIFICATION OF HIGGINS, 1971.

Sample No.	Cataclasis dominant over neomineralization-recrys- tallization	Neomineralization- recrystallization dominant over cata- clasis	Grain size of porphyro- clast	Name of the rock	Name of the rock on the basis of classification of Higgins, 1971.
	Rocks with- out fluxtion structure	Rocks with Fluxtion structure	Rocks with flux- tion structure		
SH4	N	N	P	0.2mm	Microporphyry Pseudotachylite
SH7	N	P	N	0.5mm	-do- Mylonite
SH14	N	N	P	0.2mm	-do- Pseudotachylite
SHM21	N	N	P	0.2mm	-do- -do-
SHM24	N	P	N	0.2mm	-do- Mylonite
SHM29	N	P	N	0.2mm	-do- Protomylonite
SHM30	N	P	N	0.2mm	-do- Ultramylonite
SHM32	N	P	N	0.2mm	-do- -do-
SHM34	N	P	N	0.5mm	-do- -do-
SHM50	N	P	N	0.2mm	-do- -do-
SHM52	N	N	P	0.2mm	-do- Pseudotachylite
SHM59	N	N	P	0.2mm	-do- -do-

N= not present
P= present

TABLE 11. CONTD.

Sample No.	Rocks without fluxtion structure	Rock with fluxtion structure	Rocks with fluxtion structure	Grain size of porphyroclast	Name of the rock	Name of the rock classification of Higgin 1971.
SHM65	N	P	N	0.2mm	Microporphyry	Ultramyylonite
SHM66	N	P	N	0.2mm	-do-	-do-
SHM73	N	P	N	0.2mm	-do-	-do-
SHM75	N	P	N	0.2mm	-do-	-do-
SHM109	N	N	P	0.2mm	-do-	Pseudotachylite
SH3	N	P	N	0.2mm	Porphyritic granites	Mylonite
SH8	P	N	N	2.5mm	-do-	Cataclasite
SH10	N	P	N	1.5mm	-do-	Mylonite
SH15	N	P	N	1mm	-do-	Mylonite
SH18	N	P	N	1mm	-do-	-do-
SH19	N	P	N	0.3mm	-do-	-do-
SH20	N	P	N	2mm	-do-	-do-
SHM41	N	P	N	1mm	-do-	Ultramyylonite

N= Not present

P= Present

TABLE 11. CONTD.

Sample No.	Rocks without Fluxtion Structure	Rocks with Fluxtion structure	Rocks with fluxtion structure	Grain size of porphyroclast	Name of the rock	Name of the rock on the basis of classification of Higgins, 1971.
SHM48	N	P	N	.5mm	Porphyritic granite	Mylonite
SHM49	N	P	N	1mm	-do-	-do-
SHM82	N	P	N	.5mm	-do-	-do-
SHM86	N	P	N	.5mm	-do-	-do-
SHM90	N	P	N	1mm - 4mm	-do-	Mylonite
SHM112	N	P	N	2mm	-do-	Ultramylonite
SHM119	N	P	N	1mm - 3mm	-do-	-do-
SHM124	N	P	N	2mm	-do-	-do-
SHM135	N	P	N	1mm - 2.5mm	-do-	Mylonite
SHM137	N	P	N	1mm - 4mm	-do-	-do-
SHM44	N	P	N	1mm - 3mm	Reibeckite gneiss	Ultramylonite
SHM45	N	P	N	1mm - 3mm	-do-	-do-
SHM115	N	P	N	0.2mm	-do-	-do-

N = Not present
PP Present

TABLE 11. CONTD.

Sample No.	Cataclasis dominant over Neomineralization-recrystallization.	Neomineralization-recrystallization dominant over cataclasis	Grain size of porphyroclast	Name of the rock	Name of the rock on the basis of classification of Higgins, 1971.
	Rocks without Fluxtion structure.	Rocks with Fluxtion structure			
SHM132	N	P	0.2mm	Reibekite gneiss	Ultramylonite
SHM136	N	P	0.2mm	-do-	-do-
SHM25	N	P	1mm - 3mm	Aegirine reibekite porphyry	Mylonite
SHM39	N	P	0.5mm	-do-	Mylonite
SHM64	N	P	1mm - 3mm	-do-	Ultramylonite
SHM72	N	P	1mm - 3mm	-do-	Mylonite
SHM85	N	P	1mm - 2mm	-do-	Protomylonite
SHM88	N	P	2mm	-do-	Mylonite
SHM89	N	P	2mm	-do-	-do-
SHM95	N	P	1mm - 3mm	-do-	-do-
SHM98	N	P	1mm - 3mm	-do-	-do-
SHM101	N	P	2mm	-do-	-do-
SHM127	N	P	2mm	-do-	Protomylonite

N = Not present
P = Present

Cataclasis dominant over recrystallization

CHAPTER - 4

GEOCHEMISTRY

Chemical analyses of 61 rock samples from the Shewa-Shahbazgarhi complex are presented in Tables (13, 14a & 14b). Also given are CIPW norms, Thornton and Tuttle's (1960) differentiation index ($D.I. = \text{normative Qtz} + \text{Or} + \text{Ab} + \text{Ne} + \text{Ks}$), and solidification index ($S.I. = 100 \text{ MgO} / (\text{MgO} + \text{FeO} + \text{Fe}_2\text{O}_3 + \text{Na}_2\text{O} + \text{K}_2\text{O})$) values, and $\text{FeO}^* / \text{MgO}$ ratios. The overall variation from mafic to felsic rocks is from 42 Wt.% to 78 Wt.% SiO_2 . On the basis of SiO_2 content, two major groups of rocks can be distinguished: (a) basic rocks with $\text{SiO}_2 < 55$ Wt.%, and (b) acidic rocks with $\text{SiO}_2 > 66$ Wt.%. Rocks with SiO_2 content between 55 Wt.% and 65 Wt.% probably represent hybrids, formed as the result of mixing ^{of} basic and acidic materials. The Al_2O_3 content of basic rocks ranges between 10 to 15%.

In all but two analyses, Na_2O exceeds K_2O (see Table 13). Majority of the samples are quartz-normative with the exception of two which show olivine in their norms.

The acidic rocks contain 68 to 78 Wt.% SiO_2 . Na_2O is higher than K_2O in the aegirine riebeckite porphyry and riebeckite gneiss. In the other varieties of the acidic rocks, K_2O exceeds Na_2O . P_2O_5 is higher in those acidic rocks which are in close contact with the basic rocks. The acidic rocks

TABLE 13. CHEMICAL ANALYSES AND CIPW NORMS OF THE METAGABBRO, METADOLERITE AND BASIC DYKES FROM SHEWA SHAHBAZGARHI COMPLEX

Sample No.	SHM60	SN49	SH1	SHM46	SN30	SH11	SHM97	SH9	SN4	SN10	SHM108	SHM47	SH12
SiO ₂	42.64	43.64	45.06	46.08	46.50	46.81	47.15	47.32	48.17	48.21	48.80	48.90	49.00
TiO ₂	6.05	3.77	5.00	4.03	3.96	4.29	4.13	4.75	4.11	3.42	1.73	3.71	4.21
Al ₂ O ₃	11.86	10.60	13.25	12.53	12.80	12.73	13.13	13.25	10.55	12.05	12.07	11.25	13.00
Fe ₂ O ₃	16.82	8.42	12.52	8.16	10.60	12.73	11.44	6.94	7.98	6.81	8.82	10.90	8.84
FeO	0.51	5.98	2.03	6.52	3.34	1.63	3.51	5.31	6.54	8.61	5.20	3.57	5.47
MnO	0.13	0.18	0.20	0.17	0.17	0.14	0.17	0.20	0.18	0.17	0.17	0.17	0.14
MgO	8.22	10.29	5.84	5.80	6.37	4.97	4.42	5.34	4.54	5.77	8.06	6.08	5.14
CaO	1.49	10.27	8.37	6.87	7.54	8.82	8.46	8.64	9.21	9.52	10.54	9.79	9.00
Na ₂ O	1.61	2.37	3.10	1.74	2.74	2.72	2.57	3.53	2.85	2.92	2.95	2.54	3.29
K ₂ O	6.22	0.86	1.18	3.59	1.90	1.20	0.59	1.47	1.71	0.71	0.57	0.61	1.07
P ₂ O ₅	0.65	1.20	1.38	0.64	0.61	0.56	1.11	1.33	0.66	0.59	0.22	0.42	0.57
Ig. loss	3.60	2.40	1.25	3.14	3.00	3.02	3.57	1.83	2.82	0.40	1.72	2.50	1.60
TOTAL	100.41	99.98	99.20	99.21	99.44	99.54	100.30	99.91	99.32	99.20	100.25	100.05	100.26
TRACE ELEMENTS													
Ni	81	60	NA	ND	72	41	34	NA	48	61	88	59	67
Cr	55	220	NA	75	102	29	11	NA	31	42	149	73	13
Co	75	60	NA	74	57	77	43	NA	145	201	50	45	321
V	814	421	NA	ND	507	663	451	NA	510	579	402	412	ND
Zr	145	290	NA	ND	148	122	221	NA	126	102	75	135	815
Rb	217	263	NA	106	70	17	7	NA	35	11	15	10	120
Sr	63	491	NA	264	170	275	497	NA	145	179	162	248	26
Ba	522	263	NA	450	285	419	353	NA	382	250	184	248	548
Y	49	27	NA	29	29	18	24	NA	26	20	17	20	93
Zn	75	ND	NA	178	225	58	75	NA	168	60	51	63	166
Cu	ND	ND	NA	ND	139	ND	ND	NA	ND	ND	174	ND	ND
Mn	7	17	32	17	13	ND	36	23	4	ND	7	12	145
Ta	7	ND	6	6	6	6	ND	6	6	7	6	6	7
Ce	61	ND	NA	131	2	49	58	NA	64	49	19	39	120
La	73	NA	NA	117	NA	NA	39	NA	NA	NA	NA	NA	NA
C.I.P.W. NORMS													
Q	0.00	0.00	2.72	3.70	2.81	5.93	10.97	2.36	6.97	4.48	2.56	9.04	5.47
Or	36.75	5.00	6.97	21.21	11.93	7.09	3.79	8.69	10.10	4.20	3.37	3.60	6.32
Ab	13.62	20.05	26.23	14.70	23.18	23.52	21.75	29.87	24.11	24.71	24.96	21.49	27.84
An	3.15	15.80	18.82	15.84	17.08	18.78	21.62	16.04	11.00	17.74	18.07	17.55	17.61
C	1.35	-	-	-	-	-	-	-	-	-	-	-	-
Ac	-	-	-	-	-	-	-	-	-	-	-	-	-
Cpx	-	21.26	3.83	10.94	12.57	10.31	9.42	14.12	23.65	20.55	25.51	22.01	18.15
Wo	-	-	-	-	-	-	-	-	-	-	-	-	-
Hy	6.54	10.27	12.77	9.37	10.04	7.60	6.64	6.71	0.34	9.41	8.25	4.94	4.39
Ol	9.69	3.50	-	-	-	-	-	-	-	-	-	-	-
Mt	-	8.93	-	4.81	-	-	0.09	4.00	9.75	4.87	12.30	2.47	5.88
Hm	15.52	2.26	12.52	1.34	10.60	12.73	-	4.18	1.25	-	0.34	9.20	4.78
Il	1.36	7.16	4.72	7.65	7.42	3.74	0.08	9.02	7.81	6.50	3.29	6.29	8.00
Ap	1.42	2.60	3.02	1.40	1.33	1.22	-	2.91	1.44	1.29	0.48	0.92	1.25
Tt	-	-	6.18	-	0.13	5.96	-	-	-	-	-	-	-
S.I.	24.62	36.85	23.67	22.47	25.53	21.32	19.56	23.63	19.22	21.58	31.48	25.65	21.56
D.I.	50.37	25.13	35.92	39.63	37.30	36.53	36.20	40.91	41.19	33.38	30.89	34.13	39.62
FeO/MgO	1.90	1.32	2.28	2.39	2.02	2.63	3.12	2.16	3.02	2.55	1.63	2.20	2.61

SHM46, SHM47, SHM60, SHM97, SHM108 = Metadolerite 1

SH1, SH9, SH11, SN10, SN12, SN49 = Metagabbro 0

SN4, SN30 = Basic dykes 3

TABLE 12. CONTD.

Sample No.	SH44	SN9	SHM111	SN1	SHM40	SN3	SHM42	SHM138	SHM139	SN5	SN27	SHM110	SHM113
SiO ₂	49.21	49.41	49.88	50.02	50.99	51.34	52.17	53.77	54.26	59.41	60.00	63.95	65.35
TiO ₂	3.91	3.86	1.63	3.46	3.34	2.39	3.53	2.29	2.47	1.39	3.05	1.05	1.08
Al ₂ O ₃	11.34	10.91	11.40	11.44	12.80	12.13	10.00	14.25	13.06	12.34	10.26	15.00	14.00
Fe ₂ O ₃	8.93	14.71	8.47	8.20	6.35	8.26	5.49	6.47	5.90	10.41	9.11	7.51	5.93
FeO	6.79	0.00	4.81	5.25	9.20	4.20	7.50	8.96	7.01	2.48	1.60	0.00	0.43
MnO	0.18	0.18	0.17	0.17	0.18	0.21	0.14	0.19	0.20	0.17	0.20	0.61	0.14
MgO	4.67	5.02	8.39	4.42	3.49	2.74	4.34	5.66	5.56	1.57	0.49	1.06	0.90
CaO	8.51	8.22	11.67	7.72	8.12	7.15	9.23	8.71	8.70	4.52	8.34	1.91	0.86
Na ₂ O	2.83	2.89	2.72	2.87	3.25	2.79	3.43	3.76	3.57	3.84	3.58	5.61	5.91
K ₂ O	1.28	1.53	0.50	1.83	1.25	1.91	0.49	0.99	1.30	2.14	2.18	2.99	3.98
P ₂ O ₅	1.42	0.95	0.21	1.04	0.96	1.30	1.24	0.65	0.69	0.65	0.72	0.21	0.15
Ig. loss	0.80	2.60	0.30	3.00	ND	3.00	2.34	ND	ND	1.40	ND	0.30	0.80
TOTAL	99.88	100.28	100.15	99.99	99.87	99.33	99.90	99.23		100.32	99.54	99.70	99.53

TRACE ELEMENTS

Ni	43	NA	82	ND	41	33	43	72	45	40	NA	46	52
Cr	27	NA	167	22	27	17	25	34	35	16	NA	37	15
Co	58	NA	68	9	60	57	44	47	47	43	NA	29	6
V	493	NA	373	ND	344	124	435	429	423	37	NA	ND	ND
Zr	26	NA	73	ND	155	203	8	337	335	397	NA	688	612
Rb	226	31	12	27	18	48	265	26	32	48	NA	62	111
Sr	568	233	151	234	217	267	238	235	228	311	NA	633	488
Ba	32	336	184	160	374	443	29	265	381	582	NA	871	841
Y	52	47	15	27	30	37	44	28	31	51	NA	62	72
Zn	ND	ND	99	311	72	90	ND	ND	ND	114	NA	126	148
Cu	ND	ND	49	60	ND	151	ND	ND	ND	ND	NA	ND	ND
Nb	25	232	7	31	15	ND	31	ND	ND	82	NA	95	102
Ta	ND	6	6	6	6	6	6	ND	ND	5	NA	4	ND
Ce	ND	ND	79	135	61	58	ND	ND	ND	77	NA	105	104
La	NA	NA	NA	NA	NA	10	ND	ND	ND	19	NA	43	84

C.I.P.W. NORMS

Q	10.64	9.13	3.63	10.20	8.12	14.65	11.80	3.53	4.70	20.42	20.99	19.54	13.70
Or	7.56	9.04	2.95	10.81	7.48	11.29	2.90	5.52	7.20	12.65	12.88	17.67	23.52
Ab	23.94	24.45	23.01	24.28	27.50	23.61	29.02	30.52	28.30	32.59	30.29	47.47	49.99
An	14.52	12.34	17.64	12.99	16.71	15.00	10.50	18.01	14.78	10.18	5.52	7.00	0.00
C	-	-	-	-	-	-	-	-	-	-	-	-	-
Ac	-	-	-	-	-	-	-	-	-	-	-	-	0.01
Cpx	14.34	7.40	30.26	14.42	14.50	9.33	21.80	15.22	17.56	6.23	2.63	-	1.36
Wo	-	-	-	-	-	-	-	-	-	-	10.08	-	-
Hy	4.98	9.07	6.87	4.32	8.05	2.50	4.03	12.96	13.39	1.02	-	2.64	1.61
Ol	-	-	-	-	-	-	-	-	-	-	-	-	-
Mt	11.14	-	11.33	7.45	9.21	7.29	7.96	9.82	8.02	4.52	-	-	-
Hm	1.25	14.71	0.65	3.56	-	3.23	-	-	-	7.29	9.11	7.51	5.93
Il	7.43	0.39	3.10	7.57	6.34	4.54	6.70	4.10	4.40	2.64	3.81	1.30	1.21
Ap	3.10	2.08	0.46	2.23	1.97	2.84	2.71	1.34	1.41	1.42	1.57	0.46	0.33
Tt	-	8.97	-	-	-	-	-	-	-	-	2.25	0.78	1.09
S.I.	19.06	20.78	33.70	19.15	14.82	13.76	20.42	21.67	21.10	7.88	2.88	6.17	5.24
D.I.	42.14	42.62	29.59	45.29	43.00	49.54	43.71	39.07	40.20	65.55	64.18	30.89	87.20
FeO/MgO	3.17	2.64	1.48	2.96	2.84	4.25	2.86	2.65	2.76	7.55	20.00	6.38	6.41

SHM40, SHM42, SHM111, SHM138, SHM139 = Metadolerite

SHM110, SHM113 = Quartz monzonite

SN1, SN3, SN5, SN9, SN44 = Metagabbro

SN27 = Basic dyke

SHM40, SHM42, SHM110, SHM111, SHM138, SHM139 = Metadolerite

SHM113 = Quartz monzonite

TABLE 10. CHEMICAL ANALYSES OF RIEBECKITE GNEISS AND AEGIRINE RIEBECKITE PORPHYRY FROM SHEWA SHAHBAZGARHI COMPLEX.

Sample No.	SHM140	SHM45	SHM136	SHM44	SHM98	SHM88	SHM89	SHM96	SHM25	SHM62	SHM68	SHM39	SHM64
SiO ₂	68.39	70.25	70.52	71.00	70.48	70.72	71.00	71.31	72.00	72.49	72.98	73.00	75.79
TiO ₂	0.46	0.69	0.42	1.02	0.54	1.05	1.12	0.54	1.12	0.60	0.62	1.22	0.89
Al ₂ O ₃	17.75	13.50	13.21	13.27	13.32	12.88	12.00	13.45	12.16	11.94	12.42	12.40	11.06
Fe ₂ O ₃	2.94	2.61	3.90	2.23	3.10	2.37	1.33	3.00	2.66	1.64	2.80	1.42	1.31
FeO	0.64	0.65	0.53	0.65	0.80	0.00	2.63	0.80	0.00	1.75	1.02	1.71	1.02
MnO	0.20	0.17	0.17	0.16	0.25	0.12	0.19	0.24	0.16	0.16	0.17	0.13	0.11
HgO	1.00	0.57	0.63	0.44	0.03	1.32	0.57	0.80	0.50	0.41	0.50	0.63	0.27
CaO	0.46	0.62	0.23	0.54	0.66	0.24	0.74	0.63	0.26	0.71	0.59	0.31	0.12
Na ₂ O	5.53	6.00	5.00	6.35	6.29	3.40	6.13	5.59	4.90	5.27	5.36	5.70	2.86
K ₂ O	3.03	4.02	3.71	3.63	3.54	6.50	4.13	4.03	3.93	4.80	3.34	3.04	6.20
P ₂ O ₅	0.00	0.09	0.00	0.08	0.09	0.05	0.13	0.01	0.11	0.05	0.13	0.06	0.04
Ig. loss	ND	1.30	ND	0.90	0.10	0.20	0.00	0.00	1.10	0.40	0.50	0.40	0.30
TOTAL	100.40	100.18	98.32	99.99	100.00	99.85	99.99	100.50	99.96	99.98	100.35	100.02	99.97
TRACE ELEMENTS													
Ni	38	62	48	57	32	63	60	35	60	64	60	68	59
Cr	4	31	46	26	29	27	17	18	61	41	24	53	71
Co	ND	71	10	45	44	49	69	64	75	60	26	38	46
Zr	NA	790	1035	124	1625	1024	92	1668	1045	1163	1035	1345	899
Rb	NA	123	168	57	116	111	52	112	116	119	182	122	142
Sr	NA	55	23	121	200	128	492	80	50	15	92	52	11
Ba	NA	1306	562	78	592	706	87	635	699	307	634	227	342
Y	NA	86	164	ND	151	89	ND	149	92	101	99	98	81
Zn	NA	NA	NA	NA	NA	202	NA	NA	198	158	199	150	139
Nb	NA	157	249	139	163	163	163	160	164	212	179	225	150
Ta	NA	3	ND	2	3	3	3	3	3	2	3	3	3
Ce	NA	NA	NA	NA	NA	137	NA	NA	195	168	121	142	120
La	NA	NA	NA	NA	NA	115	NA	NA	51	114	65	98	48
Th	NA	NA	24	NA	NA	NA	NA	NA	NA	NA	NA	NA	NA
U	NA	NA	4	NA	NA	NA	NA	NA	NA	NA	NA	NA	NA
C. I. P. W. NORMS													
Q	22.07	19.40	51.99	20.33	19.56	23.77	22.12	21.10	29.77	25.11	28.08	27.08	35.35
Or	17.83	23.75	23.23	21.49	2.94	16.41	24.40	23.70	23.22	26.36	19.25	17.96	36.34
Ab	46.60	47.19	8.97	48.18	46.85	26.77	38.65	46.51	40.79	34.81	45.35	46.98	22.48
An	2.27	-	1.14	-	-	0.75	-	-	-	-	0.27	-	-
C	4.52	-	7.58	-	-	-	-	-	-	-	-	-	-
Ac	-	3.15	-	4.80	3.90	-	7.61	1.23	0.59	5.35	-	1.10	1.51
Cpx	-	1.94	-	1.36	2.09	-	2.31	2.37	-	0.44	1.41	0.92	0.26
Wo	-	-	-	-	-	-	-	-	-	-	-	-	-
Hy	2.48	0.52	1.74	0.40	1.10	3.29	1.27	0.88	1.25	3.32	0.59	1.64	0.55
Mt	1.38	0.71	1.08	-	1.23	-	-	1.71	-	-	2.05	1.51	1.07
Hm	1.98	1.03	3.39	0.54	0.49	3.37	-	1.33	3.46	-	1.39	2.32	0.05
Il	0.87	1.27	0.87	1.72	1.03	0.26	2.13	1.02	0.34	1.14	1.18	0.13	1.69
Ap	-	0.20	0.02	0.17	0.20	0.13	0.28	0.02	0.24	0.11	0.28	-	0.09
Tt	-	-	-	0.29	-	0.03	-	-	0.40	-	-	-	-
Rt	-	-	-	-	-	0.90	-	-	0.83	-	-	-	-
Ks	-	-	-	-	-	-	-	-	-	-	-	-	-
Ns	-	-	-	-	-	-	1.02	-	-	0.06	-	-	-
S.I.	7.60	4.12	6.70	7.31	5.70	9.05	7.85	5.58	3.85	2.91	3.86	5.04	2.31
D.I.	86.50	90.35	84.18	89.95	98.35	90.95	85.38	91.36	91.76	88.29	92.67	92.03	94.47

Riebeckite gneiss

Aegirine Riebeckite Porphyry

TABLE 1. CHEMICAL ANALYSES OF MICROPORPHYRY AND PORPHYRITIC GRANITE FROM SHEMA SHABAZGANI COMPLEX

Sample No.	SHM109	SHM29	SHM21	SHM66	SHM65	SHM19	SHM32	SHM25	SHM124	SHM127	SHM112	SH10	SH2	SH8	SH3	SH16	SH11	SH7	SH20	SH20	SH21
SiO ₂	71.22	72.00	72.08	72.16	74.07	75.00	78.11	68.39	69.52	70.08	70.26	71.12	71.34	71.92	72.28	72.34	72.83	74.36	74.45	75.00	76.79
TiO ₂	1.03	0.65	0.68	0.42	0.45	0.12	0.37	3.05	0.47	0.37	1.08	0.86	0.04	0.44	0.42	0.45	0.45	0.51	0.00	0.41	0.50
Al ₂ O ₃	11.65	12.25	15.22	12.30	11.79	10.25	10.59	10.25	13.73	13.08	13.45	12.22	11.60	12.26	12.44	12.00	11.95	12.39	12.00	11.36	12.00
Fe ₂ O ₃	3.25	2.03	1.98	4.27	1.76	1.04	1.55	3.10	2.59	2.85	1.88	2.99	3.84	3.58	3.00	2.95	2.71	3.05	2.37	2.70	1.61
FeO	0.00	1.21	0.00	0.52	1.05	3.84	0.43	0.00	1.13	1.12	1.15	1.09	0.00	0.60	0.69	1.06	1.03	0.00	0.54	0.00	1.85
MnO	0.13	0.31	0.04	0.16	0.13	0.14	0.11	0.20	0.17	0.19	0.18	0.14	0.17	0.13	0.14	0.13	0.14	0.07	0.14	0.13	0.09
MgO	0.99	0.42	1.00	0.44	0.55	0.35	0.31	0.49	1.21	1.14	0.98	0.28	0.13	0.33	0.31	0.36	0.41	0.46	0.05	0.26	0.17
CaO	0.44	0.15	0.23	0.21	0.40	0.33	0.10	8.34	0.24	0.55	0.62	0.28	0.36	0.27	0.25	0.29	0.21	0.26	0.17	0.10	0.16
Na ₂ O	0.84	5.35	4.98	4.28	0.73	1.36	1.52	2.10	2.58	2.63	5.23	4.81	5.14	4.94	4.80	4.51	3.70	2.56	4.82	4.36	4.76
K ₂ O	8.00	4.56	3.92	4.52	8.20	7.30	6.04	3.30	3.77	3.95	4.50	4.68	5.98	4.50	4.63	5.34	5.50	6.27	5.46	5.00	1.26
P ₂ O ₅	0.07	0.04	0.16	0.06	0.05	0.05	0.03	0.72	0.01	0.02	0.15	0.04	0.00	0.04	0.05	0.05	0.85	0.06	0.00	0.04	0.00
Ig. loss	2.30	1.20	0.09	0.60	0.80	0.62	0.80	0.06	ND	ND	0.60	0.70	1.07	0.16	0.09	0.50	0.25	0.00	0.01	0.64	0.82
TOTAL	99.93	99.99	100.32	100.00	99.92	100.45	99.96	100.00	100.00	95.98	100.08	99.21	99.86	99.17	99.10	99.97	100.01	99.99	99.98	100.00	100.01

	T R A C E				E L E M E N T S				C I P W				N O R M S								
NI	68	61	66	68	64	NA	60	NA	40	38	64	60	NA	60	58	NA	NA	39	65	NA	NA
Cr	39	55	28	37	26	NA	73	NA	3	1	69	2	NA	17	17	NA	NA	ND	20	NA	NA
Co	27	50	15	50	42	NA	40	NA	83	91	1	161	NA	254	535	NA	NA	287	247	NA	NA
Zr	1012	1083	977	1238	858	NA	763	NA	1641	1375	139	771	NA	792	733	NA	NA	1501	924	NA	NA
Rs	208	114	109	122	200	NA	155	NA	159	172	89	132	NA	139	123	NA	NA	219	162	NA	NA
Sr	48	24	325	61	38	NA	17	NA	37	31	733	26	NA	24	23	NA	NA	11	12	NA	NA
Ba	701	692	740	534	415	NA	468	NA	849	821	93	620	NA	551	547	NA	NA	667	74	NA	NA
X	106	91	91	110	94	NA	82	NA	144	135	ND	81	NA	88	79	NA	NA	134	107	NA	NA
Zn	180	138	55	194	164	NA	113	NA	ND	ND	ND	183	NA	106	188	NA	NA	ND	191	NA	NA
Mb	182	188	129	172	148	NA	138	NA	221	283	174	126	NA	141	121	NA	NA	153	172	NA	NA
Ta	3	2	2	3	3	NA	2	NA	ND	ND	3	3	NA	3	2	NA	NA	3	2	NA	NA
Ce	101	181	126	161	94	NA	85	NA	486	637	ND	126	NA	128	209	NA	NA	ND	128	NA	NA
La	57	59	109	124	50	NA	31	NA	ND	ND	ND	65	NA	51	38	NA	NA	ND	46	NA	NA
Th	NA	NA	NA	NA	NA	NA	NA	NA	22	20	NA	NA	NA	NA	NA	NA	NA	NA	NA	NA	NA
U	NA	NA	NA	NA	NA	NA	NA	NA	4	3	NA	NA	NA	NA	NA	NA	NA	NA	NA	NA	NA

3

9

Cpx	-	0.40	-	-	-	0.74	-	-	2.63	-	-	1.63	0.88	1.43	0.84	0.71	0.56	0.81	-	0.74	-	-
Wo	-	-	-	-	-	-	-	6.10	-	-	-	-	-	-	-	-	-	-	-	-	-	
Hy	2.47	2.23	2.49	1.10	1.39	0.53	0.77	-	3.16	2.96	1.69	0.29	0.36	0.43	0.44	1.00	0.65	1.15	0.93	0.65	1.83	
Hc	-	-	-	1.17	2.46	4.36	0.66	-	2.97	3.29	1.16	1.46	-	1.08	1.46	1.61	0.41	-	-	-	2.33	
Hm	3.26	-	1.98	3.46	-	9.45	1.09	-	0.67	0.70	1.08	0.82	-	1.72	1.30	-	0.95	3.05	-	0.80	-	
Il	0.28	1.28	0.09	0.80	0.85	0.23	0.70	0.43	0.94	0.73	2.05	1.63	0.08	0.84	0.80	0.86	0.86	0.15	-	0.28	0.95	
Ap	0.15	0.09	0.22	0.13	0.11	0.11	0.07	1.57	0.02	0.05	0.33	0.90	-	0.09	0.11	0.11	-	0.13	-	0.09	-	
Tc	-	-	-	-	-	-	-	6.93	-	-	-	-	-	-	-	-	-	-	-	-	-	
Rt	0.88	-	0.63	-	-	-	-	-	-	-	-	-	-	-	-	-	-	-	0.43	-	-	
Ns	-	0.20	-	-	-	-	-	-	-	-	-	-	-	1.02	-	-	-	-	-	0.36	-	
S.I.	7.56	3.10	8.42	3.12	4.50	2.52	3.15	5.45	10.72	9.70	7.13	2.02	2.09	2.39	2.31	2.53	3.07	3.73	0.38	2.11	1.76	
D.I.	87.88	88.78	91.71	91.96	91.53	92.92	94.12	70.25	85.83	85.89	91.55	90.02	84.82	90.80	92.20	89.72	92.93	93.11	91.10	91.70	97.70	
Microphyry																						
Porphyritic granite																						

Microperiphyty

Porphyritic granite

range from peraluminous to alkaline as is indicated by the presence of corundum and acmite in their norms Table 14a, 14b. The rock analyses were plotted on a great number of variation diagrams but only a few are presented here.

On P vs Q plot of Debon and Le Fort (1982, Fig.3) majority of the basic rocks fall in the fields of gabbro and monzogabbro, while certain analyses plot in the fields of quartz monzodiorite, quartz diorite and quartz monzonite. The majority of the acidic rocks plot in the fields of granodiorite, adamellite and granite while three plot in the field of perquartzose granitoid.

The information obtained from the above chemical classification shows that the basic rocks range from metagabbro to ^{meta-}monzogabbro (due to excess Na_2O) while the acidic rocks range from granodiorite to granites.

The interpretation based on chemical classification above is more or less consistent with the petrographic observations.

Major and Trace Element Variation

Variation in major and trace element chemistry of basic rock types is represented by plots of oxides against FeO^*/MgO (FeO^* : total iron calculated as FeO).

INDEX

- * Metadolerite
- x Metagabbro
- o Basic dykes
- o Porphyritic granite
- Δ Aegirine riebeckite porphyry
- Δ Riebeckite gneiss
- Δ Microporphyry
- + Quartz monzonite

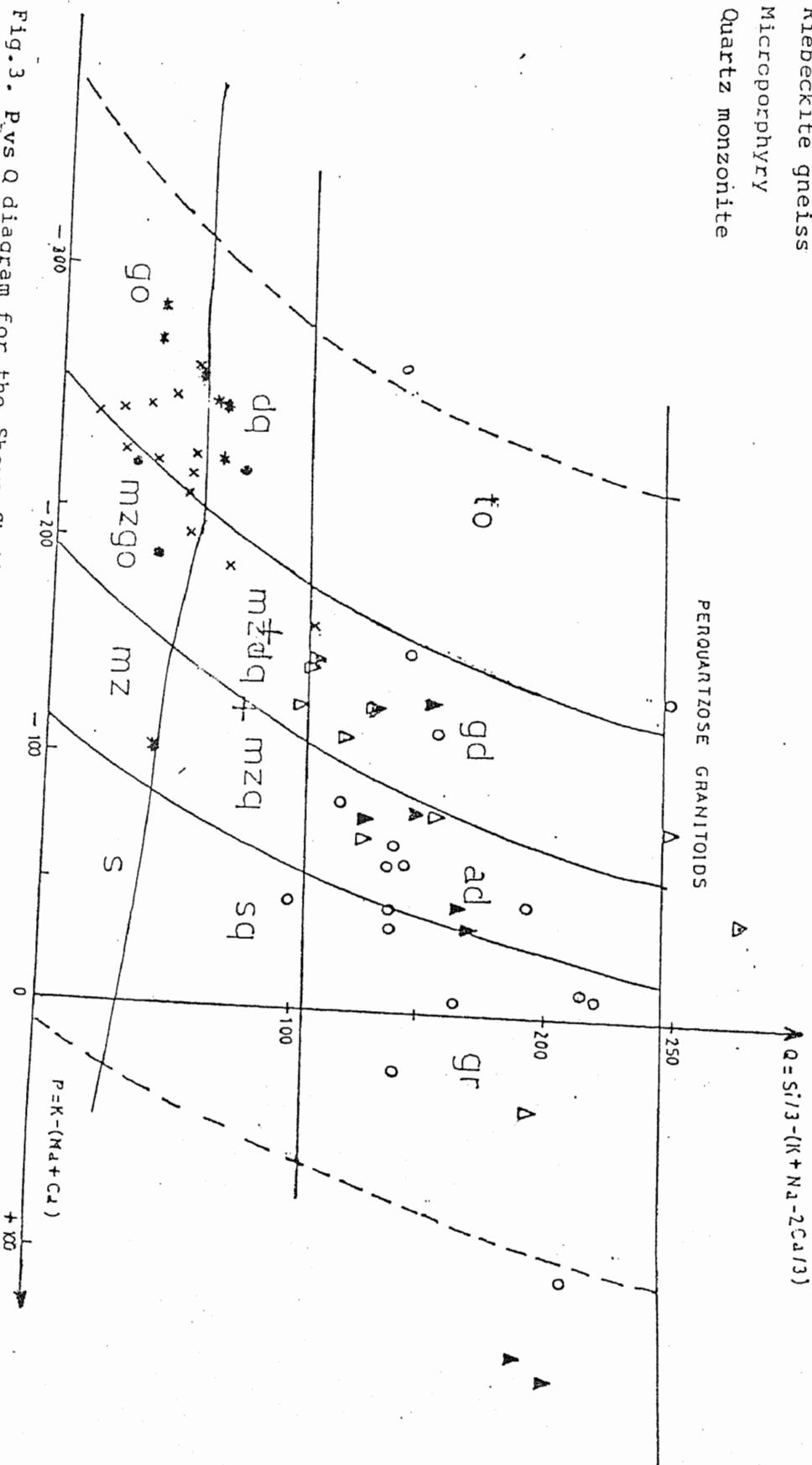


Fig.3. P vs Q diagram for the Shewa Shahbazgarhi complex with division into various fields after Debon and Lefort (1983).

to= Tonalite; gd= Granodiorite; ad= Adamellite; gr= granite; dq= quartz diorite;
mzdq= Quartz monzodiorite; mzoq= Quartz monzonite; sq= quartz syenite; go= Gabbro;
mzo= Monzodiorite; mz= Monzonite; s= Syenite.

and solidification index (S.I.), while the acidic rocks are presented on plots of (S.I.) and differentiation index (D.I.).

Major Element

Basic rocks: Variation in major elements against FeO^*/MgO is shown in Fig. 5. SiO_2 shows a good positive trend while MgO and CaO show a linear negative trend. TiO_2 , MnO , Na_2O , Al_2O_3 , K_2O and FeO^* (total iron calculated as FeO) show scatter. The positive correlation of SiO_2 vs. FeO^*/MgO indicates that SiO_2 is enriching in liquid during fractionation. The same relation is also shown against S.I. (Fig.6). The decrease of MgO with increasing FeO^*/MgO indicates the probable fractionation of mafic minerals, i.e. olivine and clinopyroxene, which is also evident from the positive correlation of MgO vs. S.I. (Fig.6). The negative relation of CaO vs. FeO^*/MgO presumably indicate clinopyroxene or plagioclase fractionation. P_2O_5 shows a good positive trend with exception of four analyses, indicate that there has little or no apatite fractionation during fractional crystallization. The gap on FeO^*/MgO plot is due to the lack of samples.

The positive correlation of CaO with S.I. indicates presumably clinopyroxene fractionation. Fe_2O_3 and FeO show scatter which is probably related to oxidation.

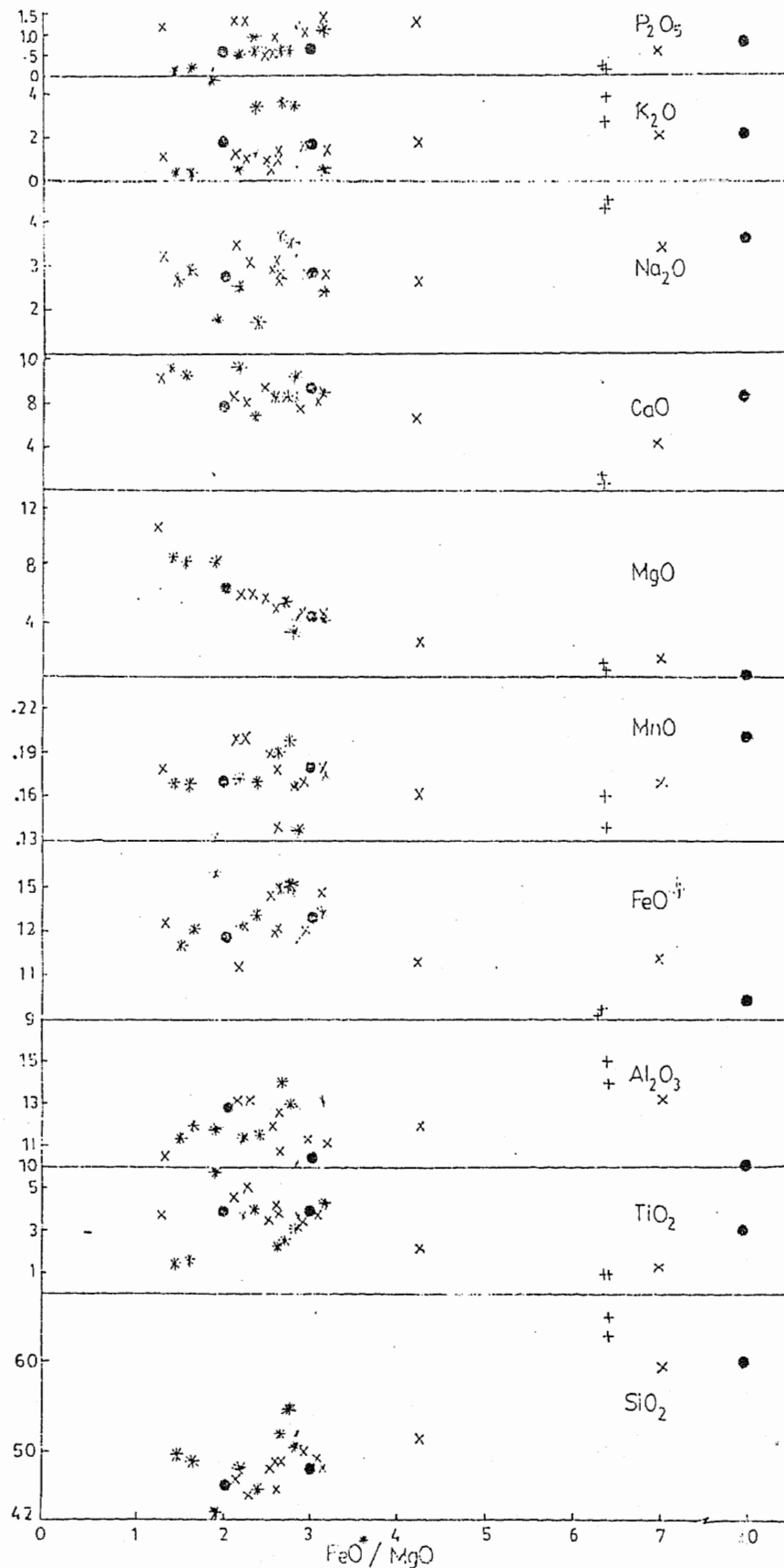


Fig.5. Plot of various oxides against FeO^*/MgO ratio for the basic rocks of Shewa Shahbazgarhi complex. Symbols as in Fig.3.
 FeO^* : Total iron calculated as FeO .

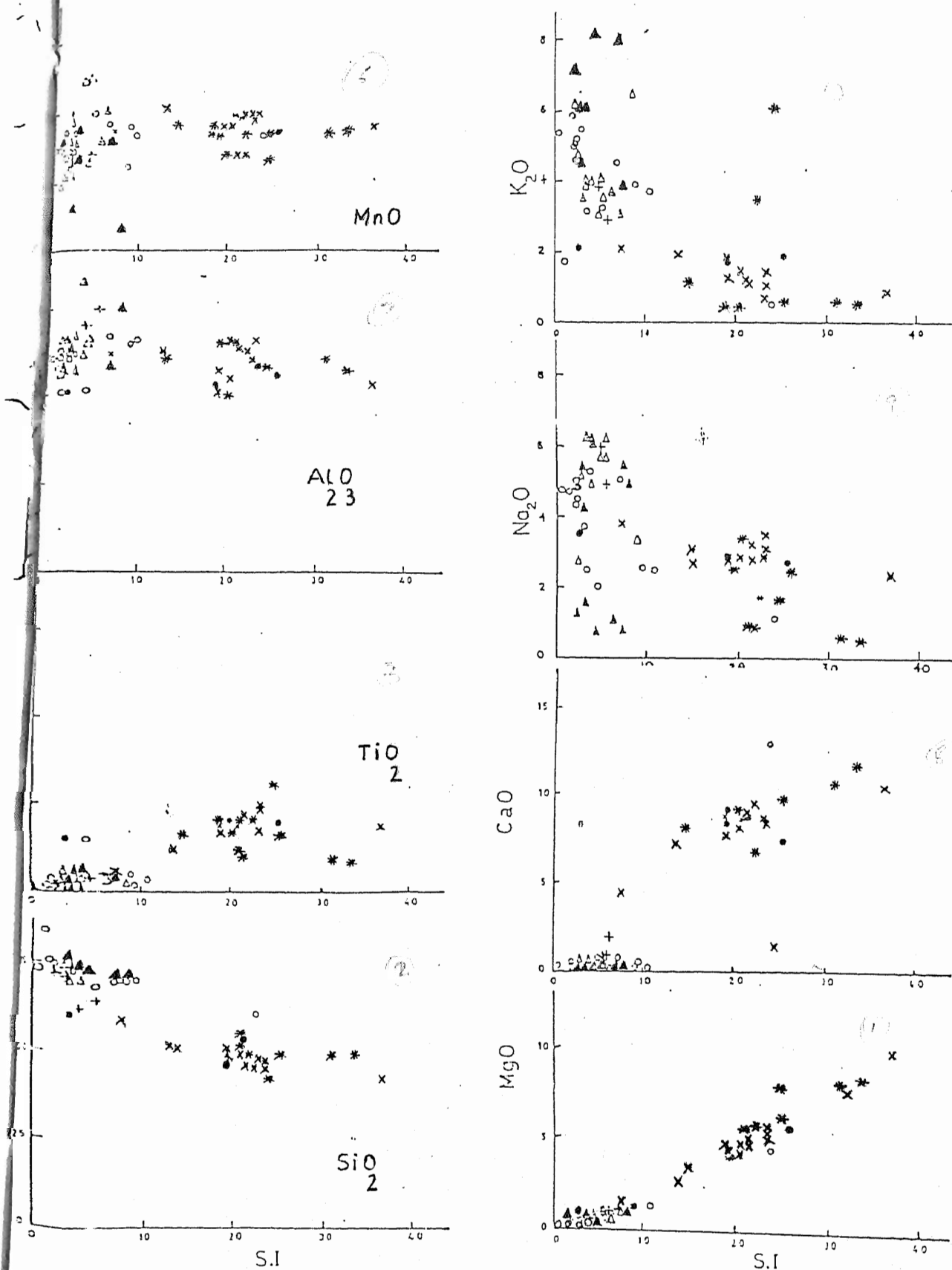


Fig. 6.. Plot of various oxide against solidification index for the basic and acidic rocks of the Shewa-Shahbazgarhi Complex.

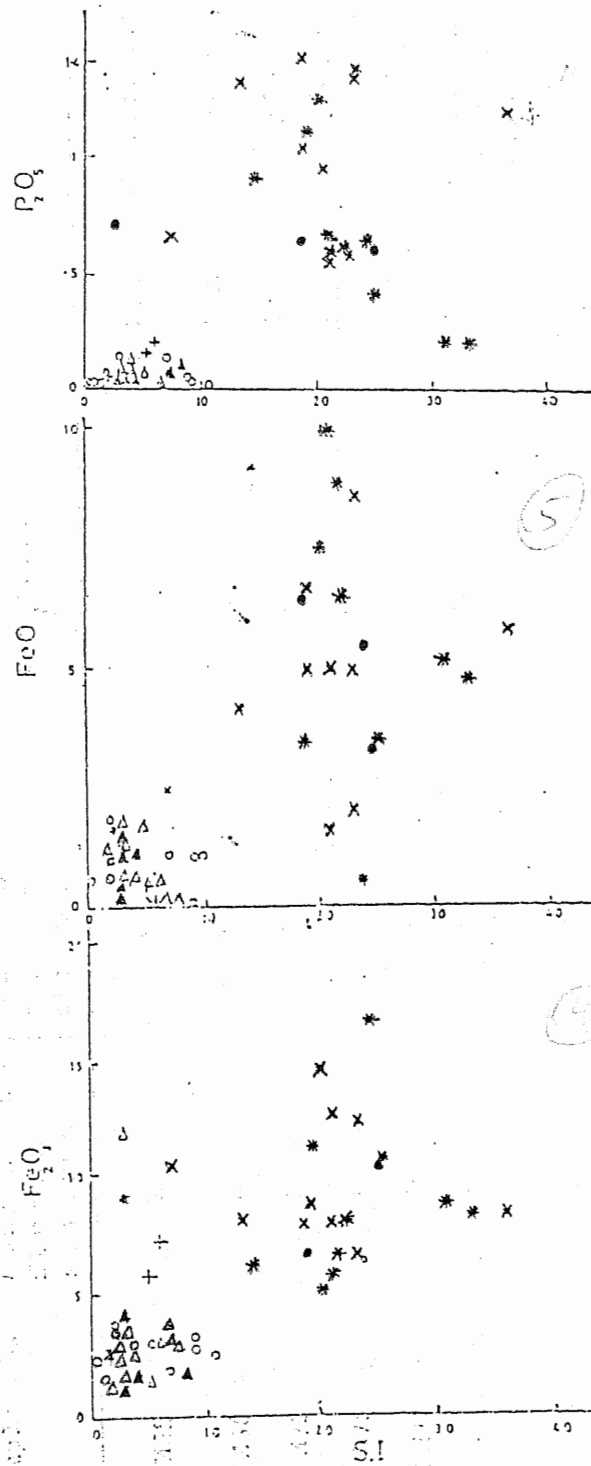


Fig. 6. (Continued)

Na_2O vs. S.I. shows scatter while a negative trend for K_2O indicates the enrichment of K_2O in the residual liquid. TiO_2 and Al_2O_3 show scatter. Negative trend for P_2O_5 reflects that there has been no apatite fractionation.

Analyses of
Acidic rocks: /the acidic rocks were plotted against S.I. (Fig.6) for comparison with the basic rocks to show whether they are comagmatic or not. On major elements against S.I. diagram (Fig.6) MgO and Al_2O_3 show good positive trends. SiO_2 shows negative trend. Na_2O , K_2O , FeO , Fe_2O_3 , MnO and TiO_2 show scatter.

The negative correlation of SiO_2 shows its enrichment in the residual liquid. In major elements vs. D.I. (Fig.7), majority of the elements except SiO_2 , CaO and K_2O show scatter. SiO_2 and K_2O show positive trend while CaO shows negative trend which is consistent with the previous interpretation against S.I.

Trace Elements

Basic rocks: Majority of the basic rocks show a continuous variation trend, a negative correlation on Cr, Co and Ni vs FeO^*/MgO (Fig.8) and positive correlation on Cr, Co and Ni

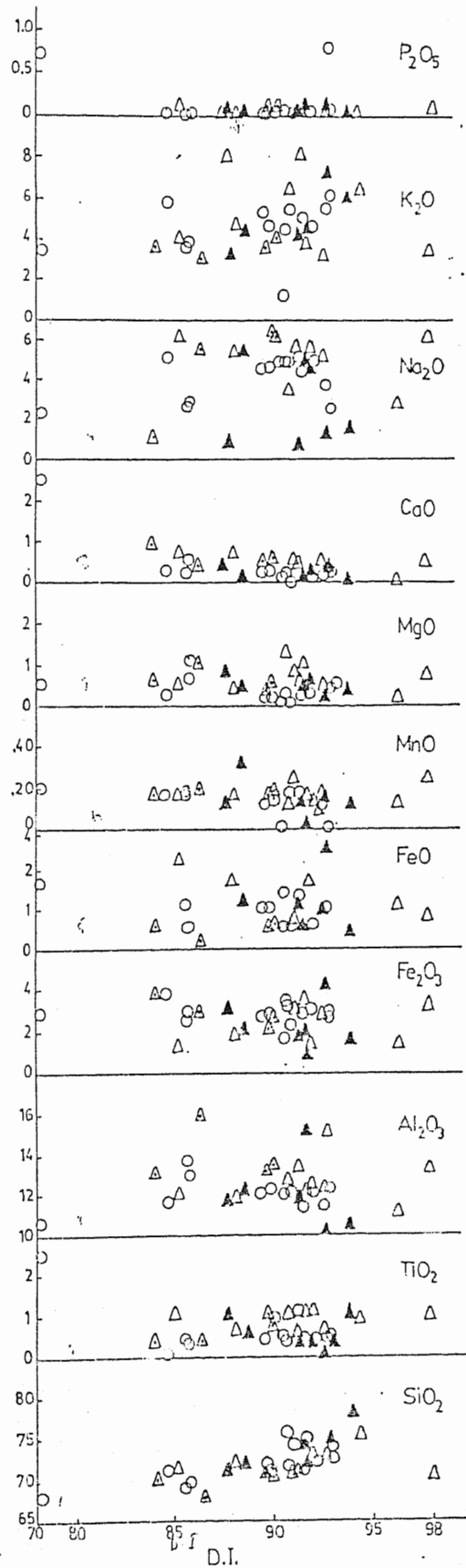


Fig.7. Plot of various oxides against Differentiation index for the acidic rocks of Shewa-Shahbazgarhi complex

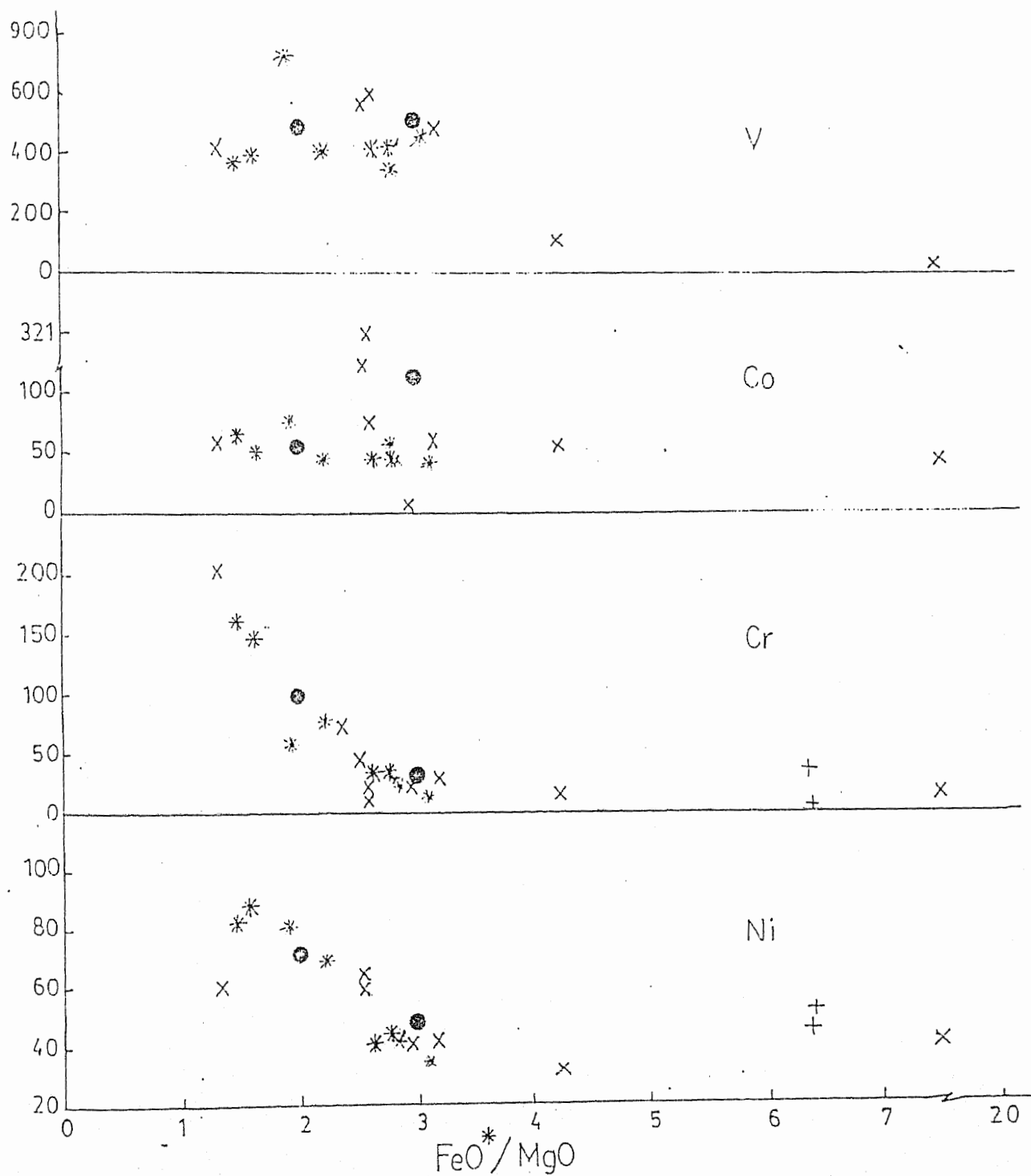


Fig.8. Various trace element against FeO^*/MgO for the basic rocks of the Shewa-Shahbazgarhi Complex.

Key as in Fig.6.

vs. MgO (Fig.9) indicate fractionation of mafic phases, i.e. olivine and clinopyroxene (see major element). The three odd analyses with high Co content are probably over estimated.

The negative Sr vs. CaO (Fig.10) relation indicates clinopyroxene fractionation. Rb vs. K_2O (Fig.11) shows positive correlation but is probably fortuitous because of the extreme alteration of the rocks (see element stability).

Acidic rocks: Ni, Cr and Co vs. MgO (Fig.9) for the acidic rocks show scatter. Similar relation is also shown for Ni and Cr against D.I. (Fig.12). On Co vs. D.I. the porphyritic granites are plotting separate from the other acidic rocks and show a strong increase in Co with increase in D.I. The other varieties are constant with increasing D.I. (Fig.11) Sr shows scatter both against Ca (Fig.10) and D.I. (Fig.12). K/Rb vs K_2O is also scattered indicating alteration.

Ni, Cr and Co vs. MgO plot along different trend for acidic and basic rocks (Fig.9). This does not support a comagmatic origin for the two suites.

Element Stability and Alteration

Majority of major and mobile trace elements indicate the effect of alteration. This is exemplified by the scatter in the plots of TiO_2 , FeO, Fe_2O_3 , K_2O , Na_2O , Al_2O_3 and CaO

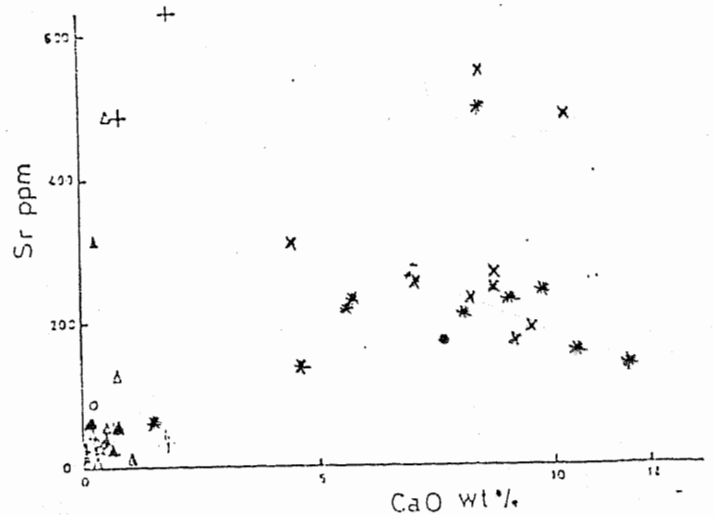
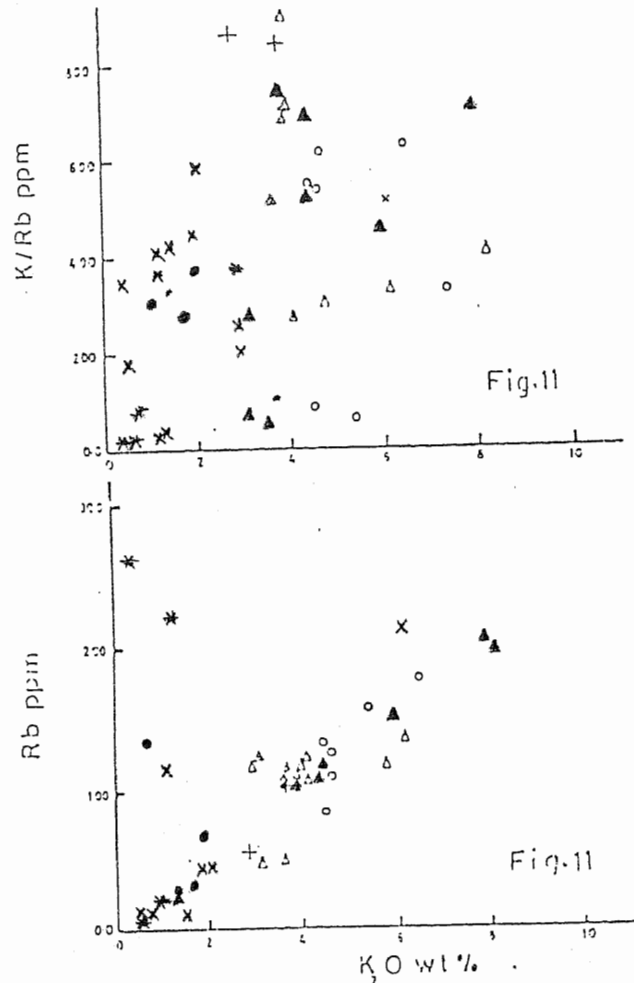
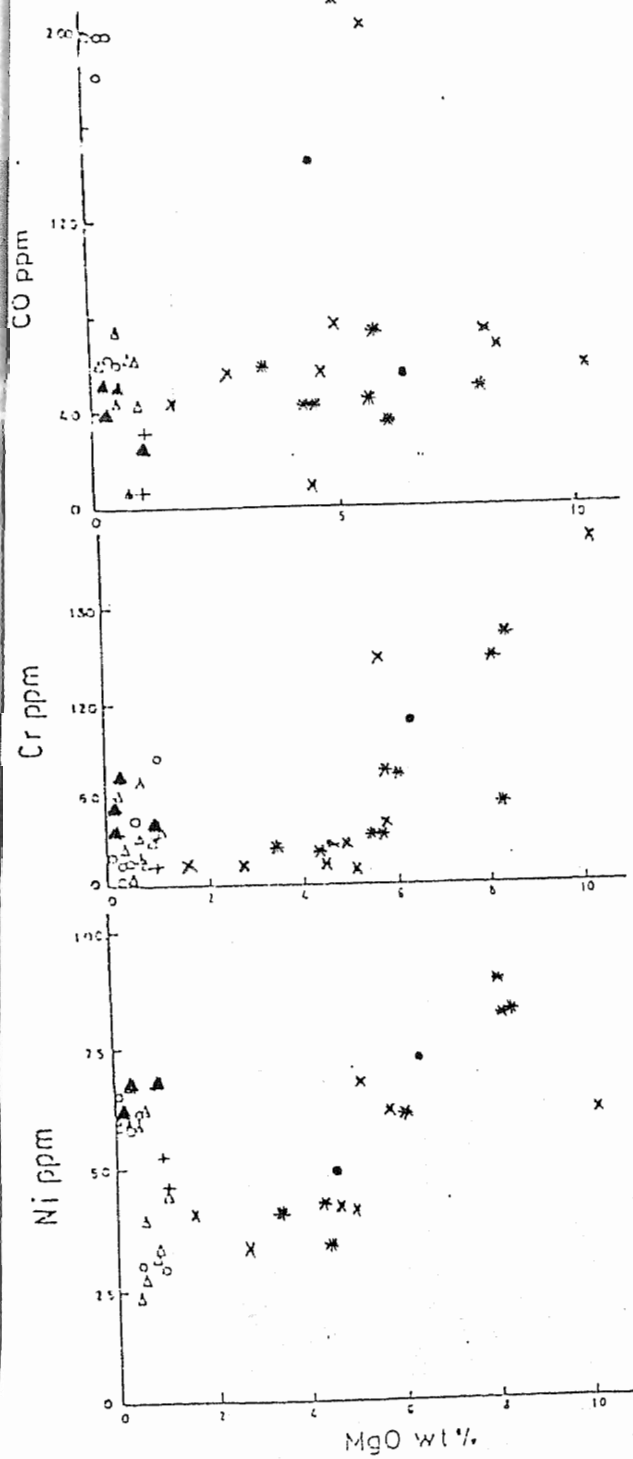


Fig. 9, 10 Various trace element against various oxide for the basic and acidic rocks of Shewa-Shahbazgarhi Complex. Symbols as in Fig. 3.

Fig. 10

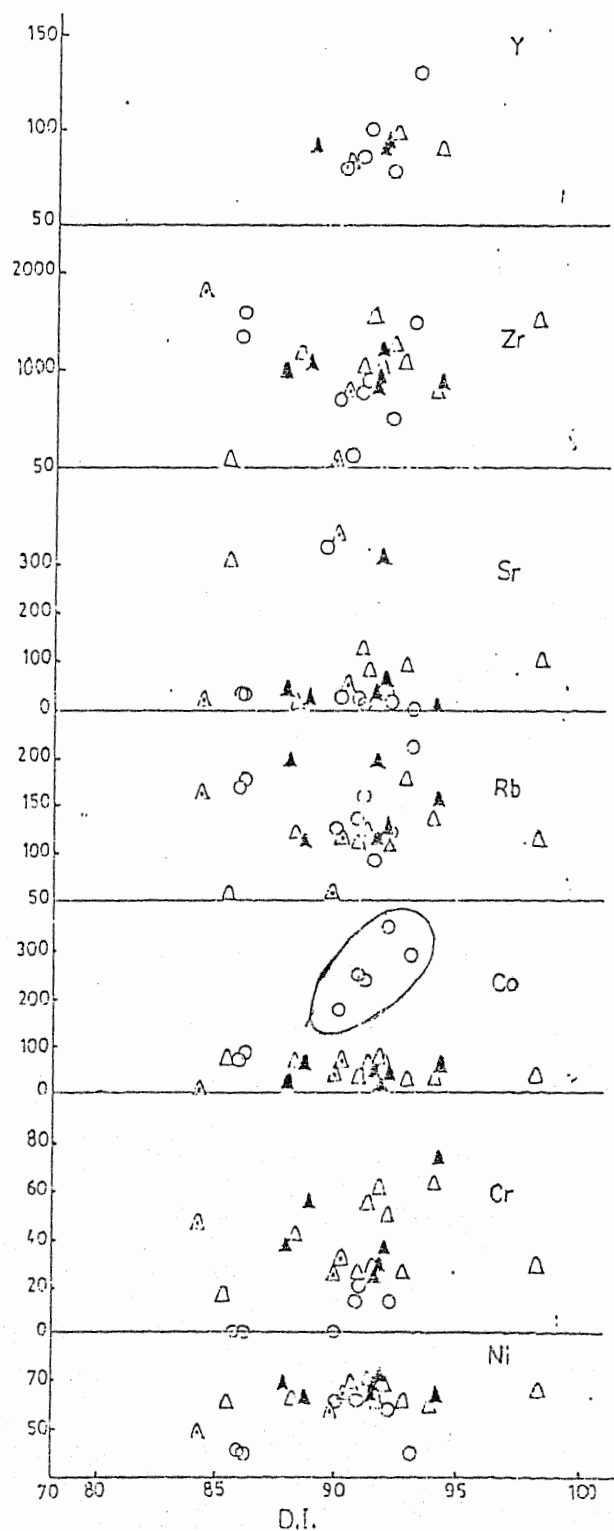
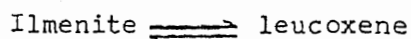
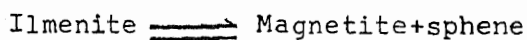


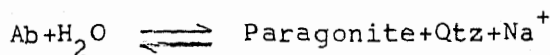
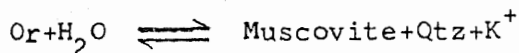
Fig.12. Plot of various trace elements against differentiation index for the acidic rocks of Shewa Shahbazgarhi complex.

against FeO^*/MgO , S.I. and also D.I. (Fig. 5,6 and 7 respectively) in the case of acidic rocks. The scatter in TiO_2 may probably be related to the formation of leucoxene during the alteration of ilmenite in the metagabbro and meta-dolerite (see section 3).



The scatter in $\text{FeO}/\text{Fe}_2\text{O}_3$ is due to oxidation. Introduction of potash is indicated by the development of biotite after amphibole (see section 3, metagabbro). The alteration of plagioclase and clinopyroxene to secondary minerals affects the CaO content of the rock.

$\text{Plagioclase (An} > 50) \rightleftharpoons \text{Oligoclase (An} \approx 15) + \text{epidote} + \text{Qtz}$
~~quartz~~ Excessive Na_2O is probably caused by addition of alkalis. The scatter in the major elements of the acidic rocks is due to the fact that these rocks are highly mylonitized and cataclasized. Some removal of alkalies may be indicated by the break down of alkali feldspar and subsequent development of muscovite and is reflected by the presence of normative corundum.



Trace elements vs. Zr (Fig.13) show that Zr, Y, Nb and Ce are stable. Rb, Ba and Sr are mobilized to varying extent.

Magmatic Affinity

A number of diagrams for magmatic affinity were plotted but only two of the plots are/ presented here. Many of the diagrams were discarded because many of the major and trace elements are strongly affected by alteration.

Basic rocks: On Nb/Y vs. SiO_2 (Fig.14a) plot of Floy and Winchester (1975) majority of the analyses are plotting in the field of subalkaline basalt while three occur in the alkali basalt field and one in the phonolite field. The quartz monzonites are plotting in the field of trachyte.

Acidic rocks: On alkalinity ratio variation diagram after Wright (1969, Fig.14b) the acidic rocks are plotting in the alkaline and peralkaline (+strongly alkaline) fields. Three of the analyses plot in the calc-alkaline field, probably due to the loss of alkalies during mylonitization.

In Nb and Y vs. Zr (Fig.13), the acidic rocks can be compared with alkaline rocks investigated by Bowden (1974) by from Nigeria and/Kempe (1973) from Warsak and Shahbazgarhi on such diagram. The present rocks also show high content of Zr (above 500 ppm) and lie in the peralkaline field.

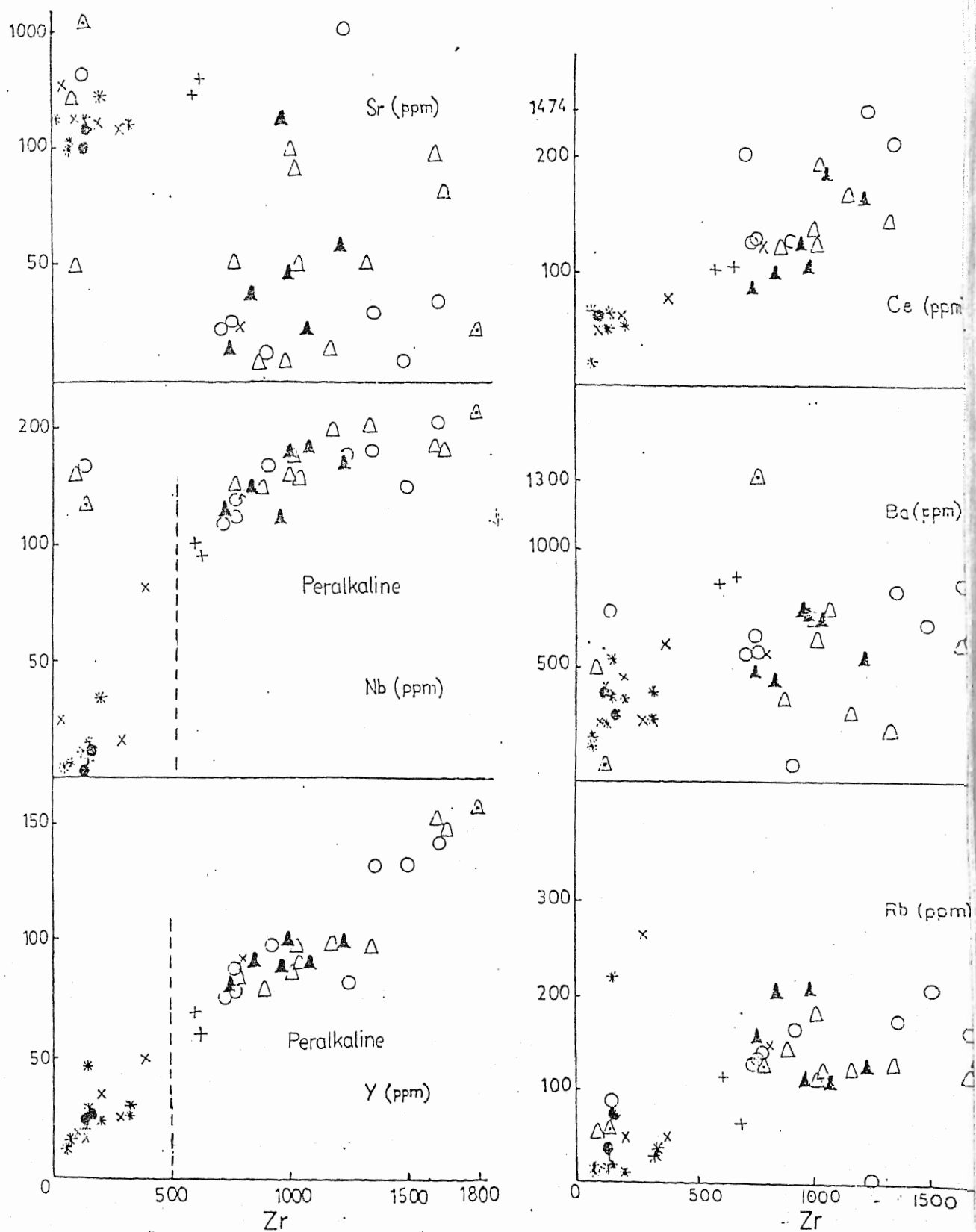


Fig.13. Various trace elements against Zr for the basic and acidic rocks of the Shewa Shahbazgarhi complex. Symbols as in Fig.3.

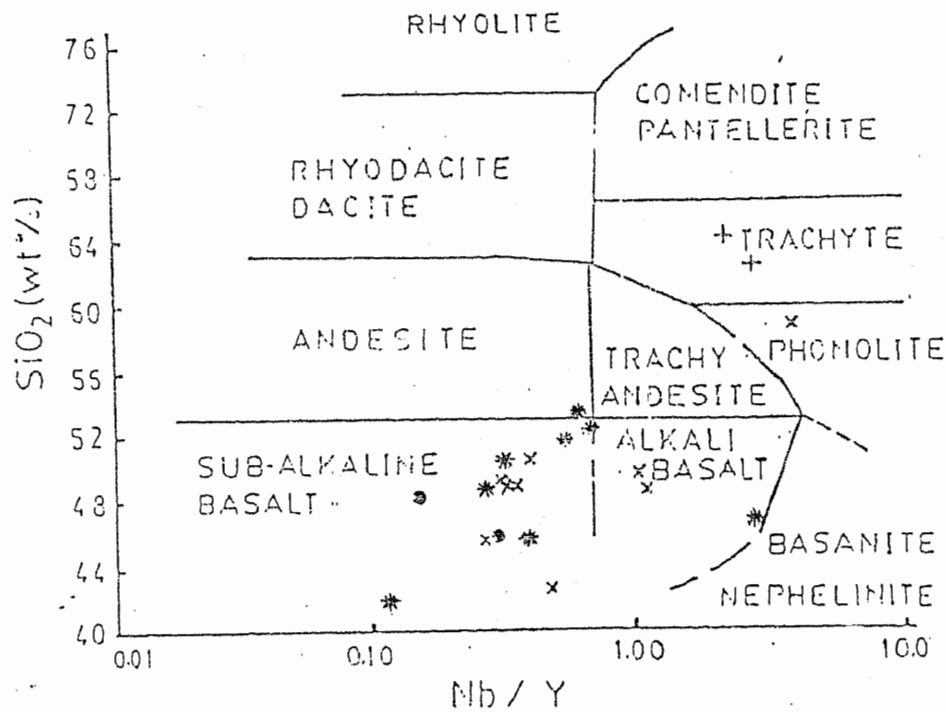


Fig. 14a. SiO_2 -Nb/Y plot of Floyd and Winchester (1975) for the basic rocks of Shewa-Shahbazgarhi complex. Showing the delimited fields for common volcanics rocks. The Shewa-Shahbazgarhi rocks plot in the subalkaline basalt and alkali basalt field.

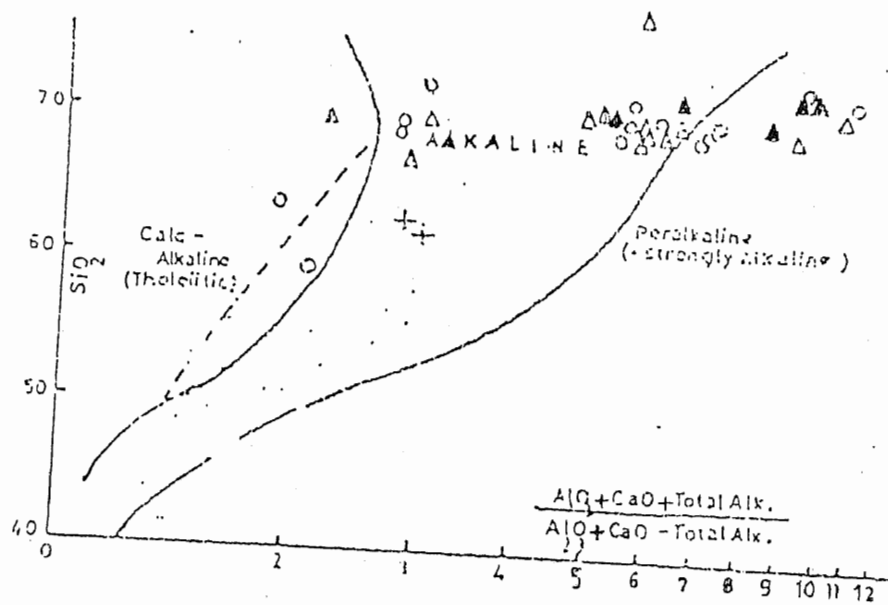


Fig.14 b Alkalinity ratio variation diagram for Shewa Shahbazgarhi complex. Field after Nockold (1954) and Wright (1969).

Non-comagmatic Nature of Acidic and Basic Rocks

The non-comagmatic nature of acidic and basic rocks can be supported by the facts that the basic rocks are sub-alkaline (infact tholeiitic in character) while the acidic rocks are alkaline to peralkaline. There^{is} also a big difference in the range of SiO_2 content between the two types and the lack of intermediate rock compositions (except two possible hybrids). On Ni, Cr and Co vs. MgO, the basic and the acidic rocks follow different trends (Fig.9). On SiO_2 vs. Zr plot (Fig.15), comagmatic rocks should show a good linear trend. In the case of Shewa Shahbazgarhi this is not so; the basic rocks have a positive correlation for the two elements whilst the acidic rocks vary vertically.

The range of FeO^*/MgO ratios for the acidic rocks is quite high and shows their different character. The basic rocks are clearly intrusive into the acidic rocks which show that the basic rocks are formed later. All the above criteria suggest that the basic and the acidic rocks are not comagmatic but are the products of two different types of magma.

Tectonic Environments

The tectonic features of the Shewa-Shahbazgarhi complex are explained, using various discriminant diagrams as follow:

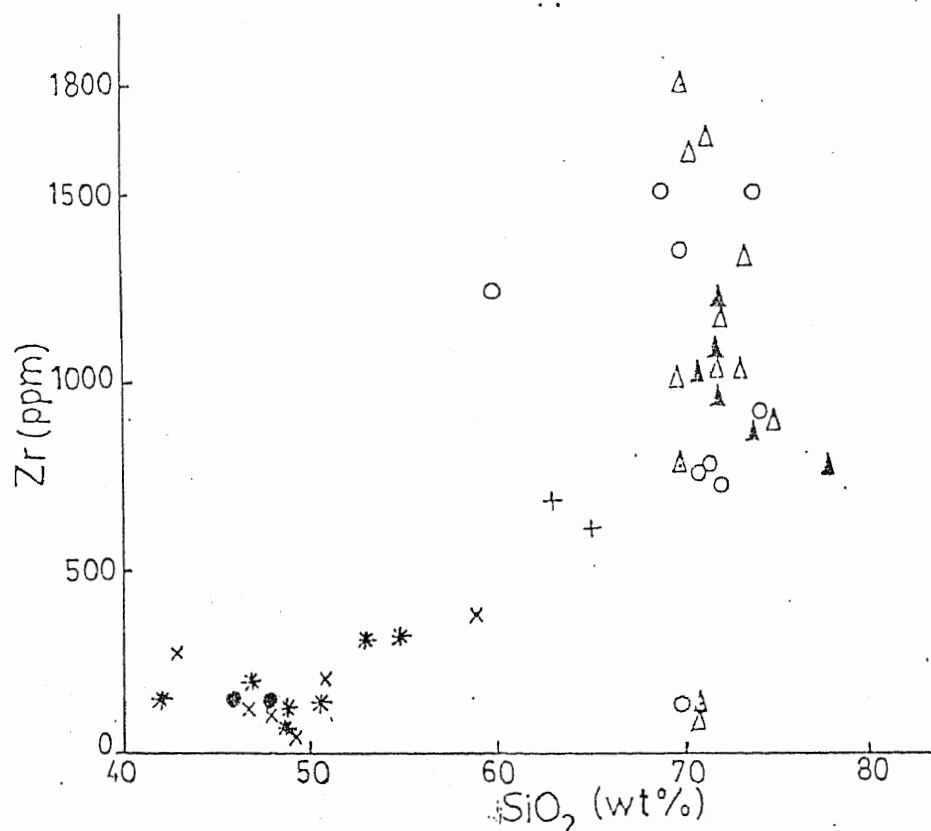


Fig.15. Zr vs SiO₂ plot for the basic and acidic rocks of the Shewa-Shahbazgarhi complex.

Basic rocks: On Cr-Y plot of Pearce (1982, Fig.16) majority of the analyses plot in the field of "within plate basalt" (WPB) but few also plot as "volcanic arc basalt" (VAB). Two of the analyses (e.g. SHM113 and SN12) plot outside the fields shown in Fig.16 because of their high Y contents.

On Ti vs. Zr diagram (Fig.17) of Winchester and Floyd (1977) majority of the analyses are plotting in the field of within plate lavas, but three of the analyses plot outside the arc and WPB fields.

The data was also plotted on several other diagrams of Pearce and Cann (1973) and Floyd and Winchester (1975, 1977) suggesting continental type of environment. The diagrams are not presented here.

Acidic rocks: The acidic rocks are also plotted on Ti-Zr diagram (Fig.17) which except three analyses are confined to the field of within plate lavas. Two of the three compositions plot in the field of arc lavas and one occurs in the overlapping field of mid-ocean ridge basalt.

Ta

Nb, Y and SiO_2 and Nb vs. Y plot of Pearce et al. (1984) are presented in Fig.18 and Fig.19 respectively. Also shown are the fields of within plate granite (WPG), volcanic arc granite (VAG), collisional granite (COLG), orogenic granite (ORG) and syn-collisional granite (Syn-COLG). On Ta, Nb and Y

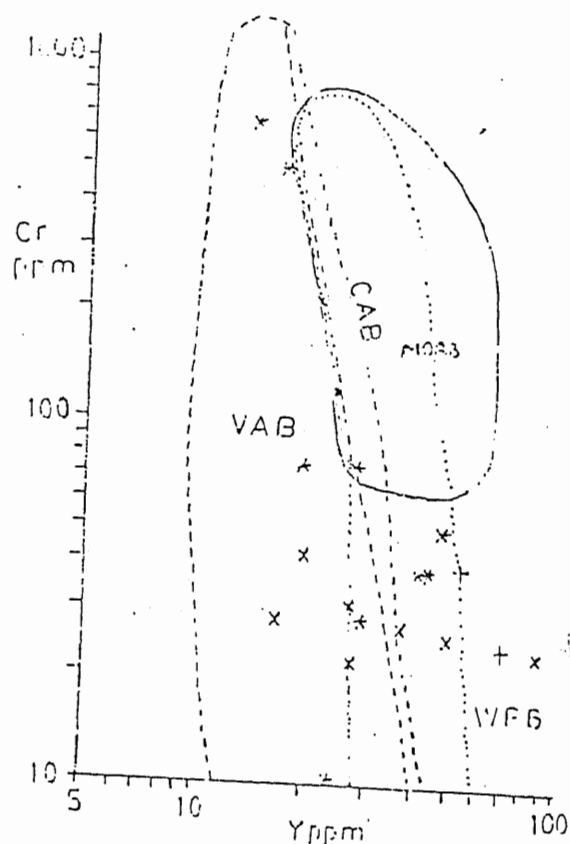


Fig. 16. Cr-Y plot for the basic rocks of Shewa-Shahbazgarhi complex. Fields volcanic arc basalt (VAB), continent alkali basalt (CAB), ocean ridge (MORB) and within plate basalt (WPB) after Pearce (1982).

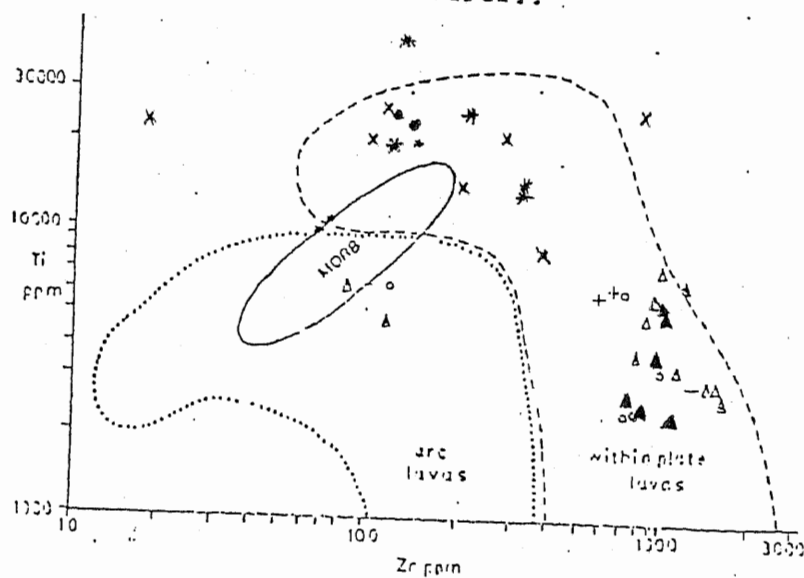


Fig. 17. Ti-Zr plot of the basic and acidic rocks Shewa-Shahbazgarhi complex. Fields are arc lavas, within plate lavas and mid ocean basalt (MORB) after Winchester and Floyd (1977).

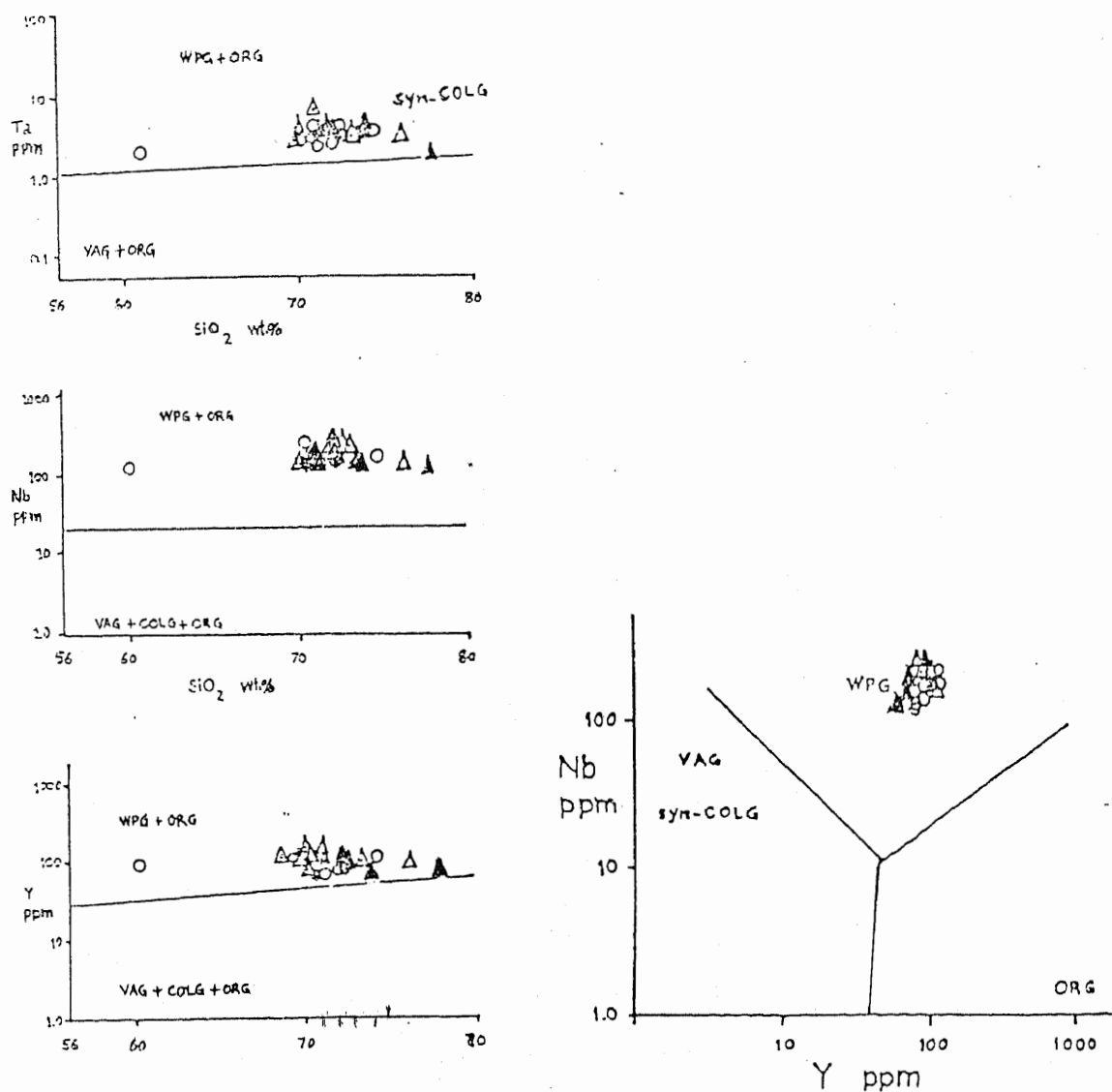


Fig.18,19. Y- SiO_2 , Nb- SiO_2 , Ta- SiO_2 and Nb-Y plots for the acidic rocks of Shewa Shahbazgarhi complex. Fields within plate granite (WPG) and syn-collisional granite (Syn-COLG) after Pearce et al., 1984.

vs. SiO_2 diagrams the acidic rocks plot in the field of within plate granites (WPG) plus orogenic granites (ORG) whereas on Nb vs. Y plot they are confined to WPG field.

Treatment of the data on the above discriminant diagrams suggests "within plate" type of environment for Shewa-Shahbagarhi complex. In table 12 average analyses of within plate granites from different places are given for comparison.

Fractional Crystallization

Since all oxides in the chemical analyses have been influenced to some extent by the alteration of the rocks, study of the fractionation of the basic magma with the help of oxide-oxide plots is of doubtful reliability. To avoid this, Pearce type diagrams are used in which each element concentration is divided by the concentration of an element not participating in the process under investigation (Pearce, 1968, 1970), with Zr as the divisor element.

The plots of Ca/Zr and Al/Zr vs. Si/Zr (Fig.20) have well defined slopes which are satisfied by fractionation of about 45% plagioclase, 35% clinopyroxene and 20% olivine. This mineral association is in agreement with the slope defined by $(\text{Fe}+\text{Mg/Zr})$ vs. Si/Zr plot (Fig.20).

TABLE 12 . COMPARISON OF SHEWA SHAHBAZGARHI GRANITE WITH WITHIN
PLATE GRANITE FROM OTHER PARTS OF THE WORLD.

	1	2	3	4	5	6	7	8	9
SiO ₂	73.16	70.41	76.02	73.26	71.61	73.52	72.19	70.04	71.75
TiO ₂	0.26	0.31	0.29	0.33	0.19	0.53	0.65	0.65	0.85
Al ₂ O ₃	12.28	13.01	12.60	12.65	11.68	12.00	12.19	14.43	12.57
Fe ₂ O ₃	2.72	3.79	1.95	3.73	4.48	2.26	3.06	2.92	2.75
MnO	0.20	0.05	0.02	0.08	0.14	0.15	0.14	0.62	0.18
MgO	0.10	0.12	0.08	0.08	0.17	0.58	0.47	0.17	0.69
CaO	0.23	1.34	0.06	1.07	0.13	0.27	0.86	0.46	0.49
Na ₂ O	6.14	2.90	4.07	4.05	5.50	2.72	4.07	4.72	5.34
K ₂ O	4.58	5.46	4.40	4.47	4.68	6.08	4.57	3.60	4.15
P ₂ O ₅	0.04	0.06	ND	0.03	ND	0.06	0.15	0.04	0.08
Ig.loss	ND	1.74	0.76	0.08	0.08	0.83	-	-	0.39
TOTAL	99.72	99.19	99.25	99.73	98.77	99.00	98.35	98.01	99.24
Rb	251	127	97	187	94	150	130	132	119
Sr	6	40	75	59	1	41	26	39	126
Ba	80	195	545	970	53	616	584	648	486
Zr	827	509	258	520	1089	1033	984	916	1127
Y	55	84	57	103	92	98	114	125	108
Nb	226	56	24	21	168	163	166	198	179
Th	3	18	906	18.03	24	ND	ND	ND	ND
Ta	15	30	1.54	2.11	16	2.60	3	2.66	3
Hf	21	15.50	7.40	14.86	42	ND	ND	ND	ND
La	72	196.90	39.40	53.40	90.06	ND	ND	ND	ND
Ce	139	404.00	96.40	119.40	274.40	129.60	285.66	ND	147.16
Nd	NA	182.40	38.60	58.00	122.20	ND	ND	ND	ND
Sm	9.80	29.2	7.70	14.20	17.20	ND	ND	ND	ND
Eu	1.38	1.84	1.06	2.36	2.09	ND	ND	ND	ND
Gd	NA	NA	NA	14.96	NA	ND	ND	ND	ND
Tb	1.30	3.16	1.21	2.36	3.98	ND	ND	ND	ND
Yb	4.30	7.33	4.00	10.18	16.50	ND	ND	ND	ND
Ni	NA	NA	NA	NA	NA	62.00	50.00	51.25	55.25

1. Oslo Rift (Neumann et al., 1977 and Khalil et al., 1978); 2. Saboloka (Hariss et al., 1983); 3. Skeargaard (Pearce et al., 1984); 4. Mull (Walsh et al., 1979); 5. Ascension Island (Fisk et al., in press).

6, 7, 8, 9. Shewa Shahbazgarhi complex.

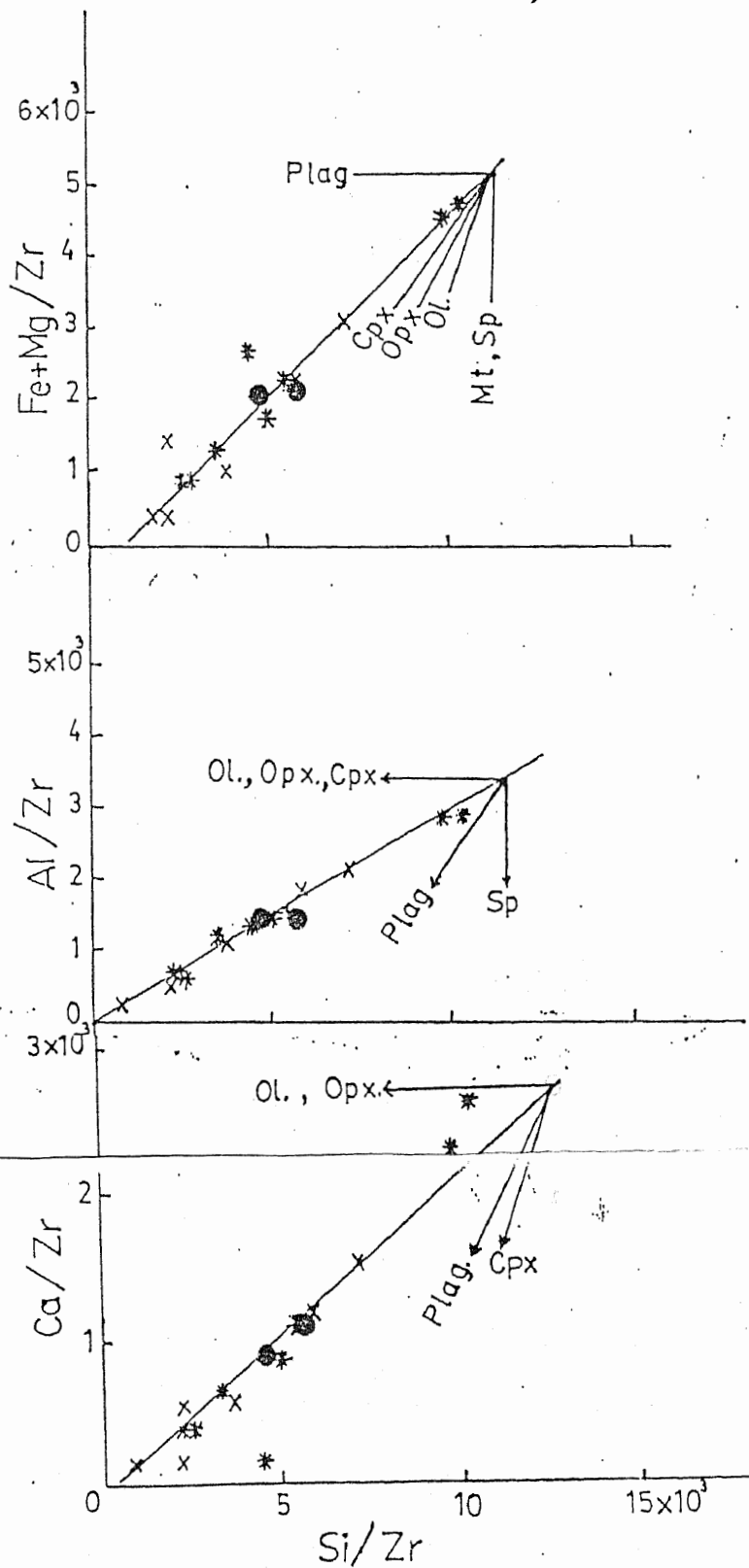


Fig.20. Pearce diagrams to illustrate the fractionation of the Shewa Shahbazgarhi complex, with the slopes of the lines with best fit. The arrows indicate the direction in which the removal of the certain minerals would move the composition of the system.

To confirm plagioclase and clinopyroxene fractionation in basic rocks CMAS plots (Cox et al., 1979) are presented in Figs.21 and 22 respectively. The acidic rocks are also presented on these diagrams, as their major and trace element plots against D.I. do not show any relation due to strong alteration.

A dominant clinopyroxene fractionation in the meta-dolerite and metagabbro is shown by the compositional plots of these rocks lying on a trend which is subparallel to Cpx-Ky join in a projection from quartz into En-Ky-Wol plane (Fig.21). The occurrence of the acidic rock types closer to the position of feldspar indicate the dominant control of plagioclase on the liquidus during fractionation. Similar conclusion can be drawn from the plots of both basic and acidic rocks in a projection from Ky into plag-En-Qtz plane (Fig.22) in which (a) occurrence of the basic rocks composition closer to the Cpx position indicates a dominant clinopyroxene fractionation at early stages and (b) the bend in the general fractionation trend near the plagioclase apex indicates the appearance of plagioclase at later stages. In addition the occurrence of the acidic rocks compositions on a trend parallel to the plag-Qtz join the same projection indicates prominent plagioclase fractionation in these rocks and the enrichment of SiO_2 in the residual liquid.

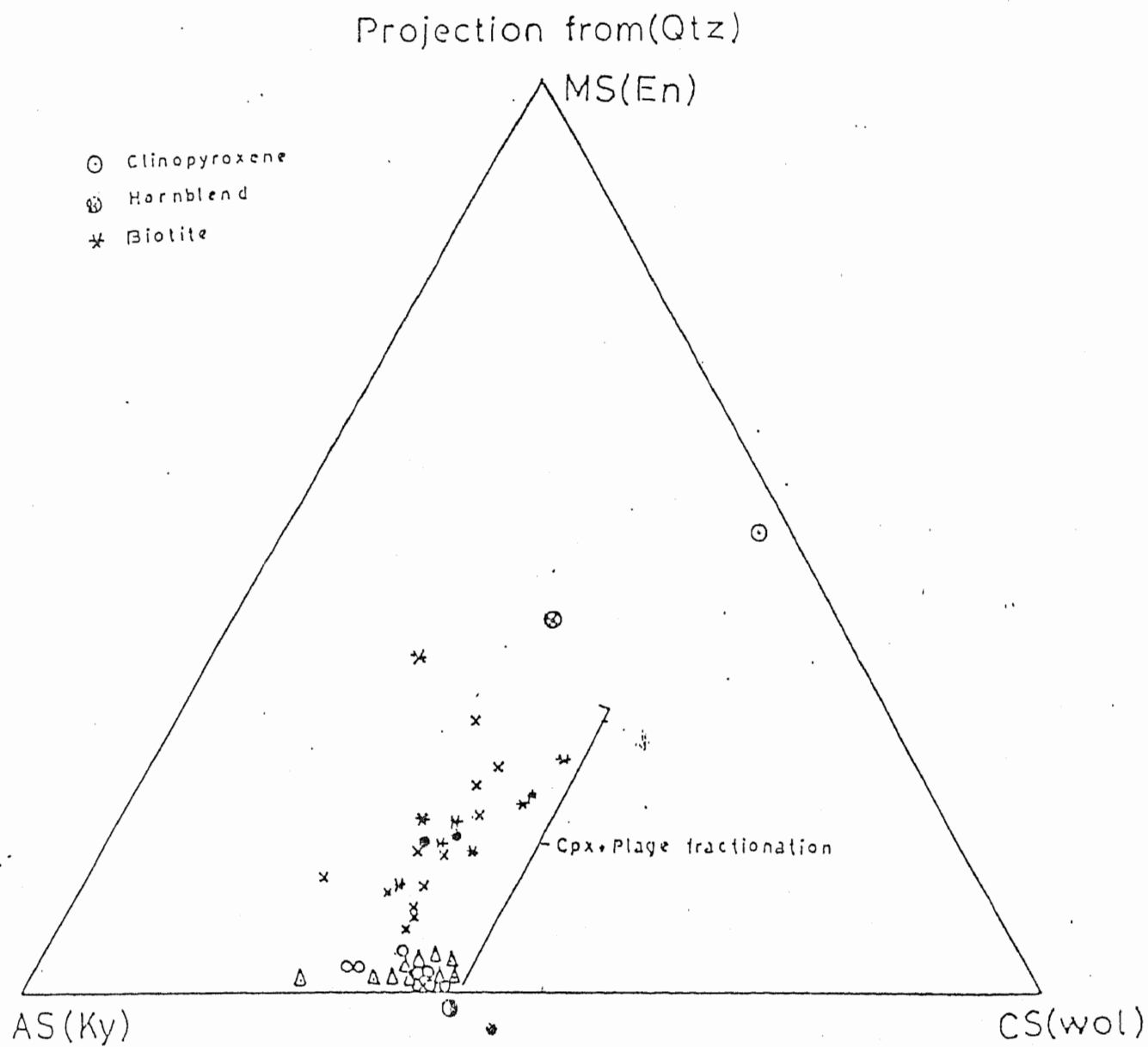


Fig.21. Projection from quartz into En-Ky-Wol plane for the Shewa Shahbazgarhi rocks.

Projection from (Ky)

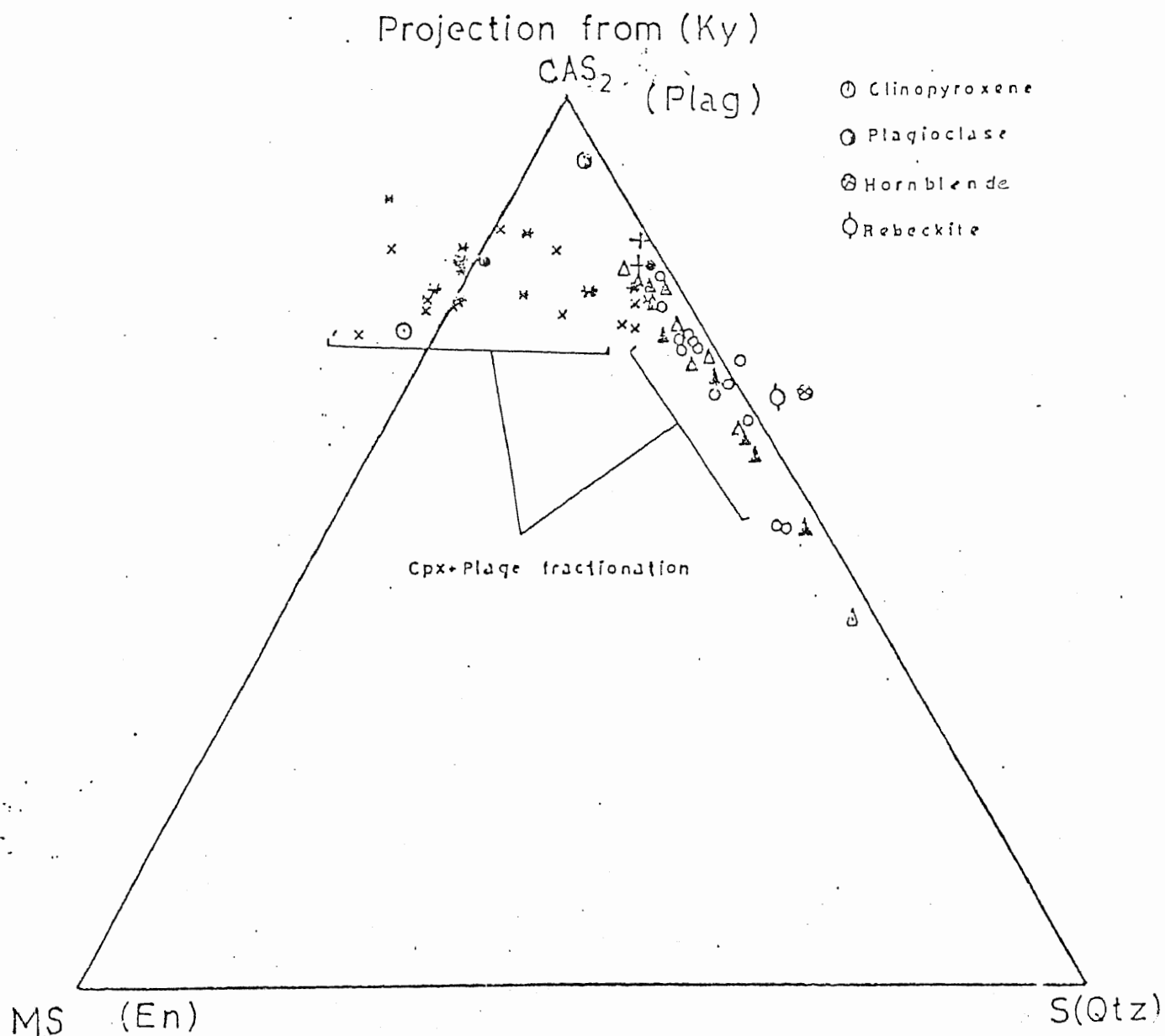


Fig.22. Projection from Ky into plag-En-Qtz plane the Shewa-Shahbazgarhi rocks.

MINERAL CHEMISTRY

Alkali amphiboles, reported by several workers^{e.g.}/Martin et al. (1962), Kempe (1973) and Bakhtiar and Waleed (1980) from the complex, are referred to optically as riebeckite. The present study confirms that the composition of these amphibole is that of riebeckite. The acidic rocks containing alkali amphibole are aegirine riebeckite porphyry, riebeckite gneiss and, locally, porphyritic granite.

Amphibole analyses were made on two samples from riebeckite gneiss of Machai section. The dominant minerals of these samples are perthesized orthoclase, orthoclase, quartz and biotite with alkali amphibole showing parallel alignment. Spene, epidote, Ore and sillimanite occur as accessory. The alkali amphibole occurs as thin elongated, tabular crystals and is generally associated with biotite. Its pleochroism is from light green to deep blue.

Chemical analysis were made using the computer-automated Jeol electron microprobe JCSA-733. Analyses are given in table 15. Total iron calculated as Fe_2O_3 was converted to FeO and the analyses were recalculated to 100%. The ions are calculated on anhydrous basis (23 oxygen) and FeO substitution to Fe^{+3} and Fe^{+2} was made by computer programme assuring that the sum of cations in T+C site equal 13 (Leake, 1978).

TABLE 15 MICROPROBE ANALYSES OF ALKALI AMPHIBOLES FROM SHEWA-SHAHBAZGARHI COMPLEX.

Sample No.	SHM44				SHM45				
	RE1	RE2	RE3	RE4	RE5	RE6	RE7	RE8	RE9
SiO ₂	50.802	51.61	51.09	48.13	51.29	49.91	50.89	50.19	49.83
TiO ₂	0.294	0.28	0.20	0.33	0.13	0.15	0.16	0.21	0.16
Al ₂ O ₃	1.689	1.91	2.02	1.70	1.67	1.73	1.69	1.71	1.71
Fe ₂ O ₃	29.153	28.20	28.67	32.74	28.93	28.48	29.42	27.48	28.85
MnO	2.068	1.95	2.34	2.13	2.42	2.02	1.81	1.73	1.83
MgO	3.920	3.48	3.55	3.05	3.85	3.80	3.61	3.92	3.41
CaO	2.018	2.98	2.96	2.38	1.73	1.62	1.75	1.84	1.87
Na ₂ O	5.165	5.39	5.10	5.08	5.58	5.93	5.79	5.60	5.48
K ₂ O	0.540	0.95	0.92	0.90	0.48	0.41	0.57	0.59	0.60
P ₂ O ₅	0.000	0.08	0.10	0.03	0.00	0.00	0.00	0.00	0.00
Cr ₂ O ₃	0.000	0.00	0.00	0.00	0.00	0.00	0.00	0.00	0.00
NiO	0.000	0.00	0.00	0.00	0.00	0.00	0.00	0.00	0.00
CoO	0.000	0.12	0.02	0.00	0.00	0.00	0.00	0.00	0.00
Total	95.711	96.99	96.97	106.47	96.12	94.09	95.70	93.27	93.77

ATOMIC PROPORTION ON THE BASIS OF 23 OXYGEN ATOM

Si	8.00	8.17	8.06	7.69	8.04	7.96	8.06	7.97	8.07
Ti	0.03	0.03	0.02	0.04	0.01	0.03	0.02	0.02	0.02
Al	0.31	0.36	0.37	0.32	0.31	0.32	0.32	0.32	0.33
Fe ⁺³	1.23	0.17	0.66	1.63	1.20	1.14	1.03	1.13	0.89
Fe ⁺²	2.23	3.19	2.74	2.30	2.21	2.36	2.48	2.39	2.63
Mn	0.27	0.26	0.31	0.29	0.32	0.27	0.24	0.23	0.25
Mg	0.92	0.82	0.83	0.73	0.90	0.90	0.85	0.93	0.82
Ca	0.35	0.51	0.50	0.41	0.29	0.28	0.30	0.31	0.36
Na	1.58	1.82	1.56	1.57	1.69	1.83	1.78	1.82	1.76
K	0.11	0.19	0.19	0.18	0.10	0.10	0.11	0.12	0.12
P	0.00	0.01	0.01	0.00	0.00	0.01	0.00	0.00	0.00
Ni	0.00	0.00	0.00	0.00	0.00	0.00	0.00	0.00	0.00
Cr	0.00	0.00	0.00	0.00	0.00	0.00	0.00	0.00	0.00
Al ⁴	0.00	0.00	0.00	0.31	0.00	0.04	0.00	0.03	0.00
Al ⁶	0.31	0.36	0.37	0.01	0.31	0.29	0.32	0.29	0.33

On $100 \text{ Fe}^{+2}/(\text{Fe}^{+2} + \text{Mg} + \text{Mn})$ vs. $100 \text{ Fe}^{+3}/(\text{Fe}^{+3} + \text{Al}^6 + \text{Ti})$ diagram (Fig.24) Miyashiro and Banno (1958) majority of the analyses plot in the riebeckite field while two analyses plot in the crossite field.

On Ca vs (Na+K) diagram of Thompson, 1976 (Fig.25) majority of the Shewa-Shahbazgarhi amphibole are plotting close to riebeckite but with some ferrorichterite substitution. Other natural alkali amphiboles from other parts of the world are also represented from Thompson diagrams for comparison.

The low values of Al^4 from 0-0.04 with exception of one analysis ($\text{Al}^4 = .31$) is also suggestive of a riebeckite composition.

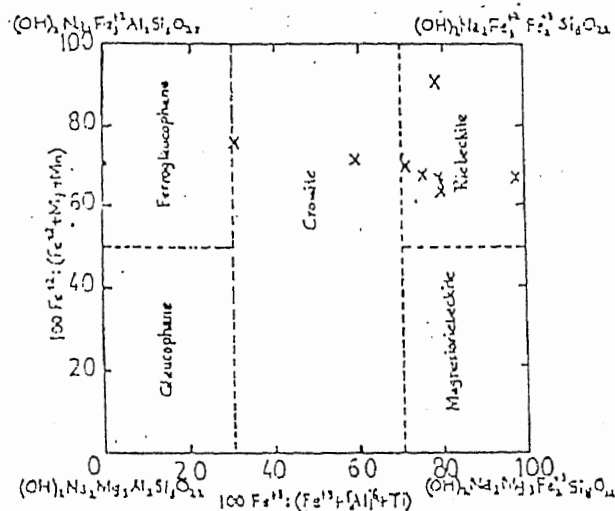


Fig. 23. The variation in chemical composition, expressed as $100 \text{ Fe}^{3+} / (\text{Fe}^{3+} + \text{Al}^{6+} + \text{Ti})$ ratios and nomenclature of the glaucophane-crossite-riebeckite amphiboles. (Deer et al., 1962).

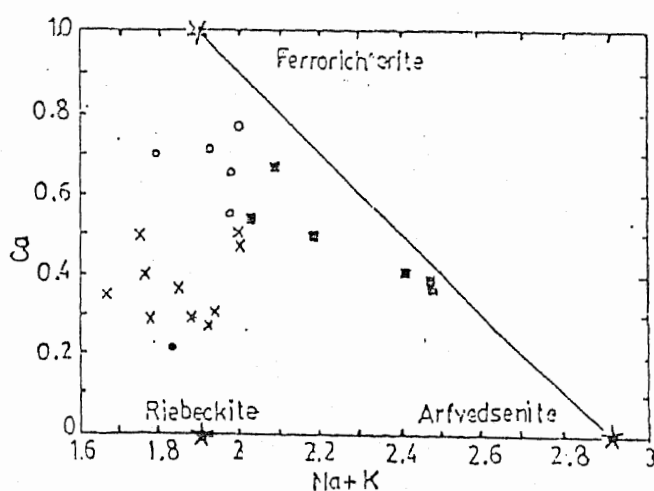


Fig. 24. CAVS (Na+K) plot for the alkali amphibole of the Shewa Shahbazgarhi complex and comparable Fe-rich and Al-poor examples. Key to analyses.

x = Shewa Shahbazgarhi complex.

o = Golden Horn batholith, Washington USA (Stull, 1973).

■ = Maolna Gainmhich epigranite (Thompson, 1976).

* = Fe-amphibole end members.

• = Southern porphyritic epigranite, Maolna Gainmhich (Thompson, 1976).

CHAPTER - 5

SUMMARY AND CONCLUSIONS

Petrography: . On the basis of petrography and field relationship, rocks of the Shewa-Shahbazgarhi complex can be divided into two major groups: (1) basic rocks and (2) acidic rocks.

The basic rocks are represented by metagabbros and, metadolerite. The presence of fractured and corroded grains of amphibole, plagioclase and quartz, and wavy extinction displayed by these minerals show that these rocks have remained under stresses.

At least two stages of metamorphism are predicted from the petrography of metagabbro and metadolerite (a) an amphibolite facies metamorphism indicated by the development of amphibole at the expense of plagioclase and magnetite and also from pyroxene in the metadolerite, and (b) a retrogressive epidote amphibolite facies metamorphism shown by the development of dark brown biotite, and epidote at the expense of amphibole, and the development of chlorite after biotite. Garnet is absent which can be attributed either to a low pressure type metamorphism or a lower Fe^{+2}/Mg ratio of the rocks (see Miyashiro, 1973, p. 259).

The changes noted above may involve cataclasis or metasomatism because many of the new products can not be formed without the presence of considerable amount of fluids (Harker, 1932, p. 175-176).

The acidic rocks include microporphyry, porphyritic granite, riebeckite gneiss and aegirine riebeckite porphyry. All of the rock units, except the medium grained variety of the porphyritic granite, are highly foliated or gneissosed and show augen structure. The presence of fluxion structure, mortar texture, broken and elongated grains of quartz and feldspar, the laminated groundmass and the evidence of recrystallization indicate that these rocks have suffered intense cataclasization and/or mylonitization (see Harker, 1932 p. 165-172, Higgins, 1971). In addition, the following microstructure have also been observed:

i. Deformation structures: These include andulose extinction and deformation bands displayed by quartz and feldspar.

ii. Recovery structure: This is represented by the broken aggregate known as polygonization.

iii. Recrystallization: This includes the formation of the new mineral grains which are mostly lying around the margin and along the fractures in the quartz and feldspar crystals.

The microstructures displayed by quartz and feldspar porphyroclasts suggest ductile deformation (see Bell and Ethridge, 1973, Ethridge and Wilkie, 1979).

Cataclasism and/or mylonitization has resulted in the formation of some new minerals. Biotite has formed after k-feldspar in association with magnetite. Epidote has developed after plagioclase, and aegirine in the aegirine riebeckite porphyry. Riebeckite has formed at the expense of biotite and feldspar in association with magnetite. Sillimanite has developed after k-feldspar in the riebeckite gneiss and aegirine riebeckite porphyry. This may probably be related to the diffusion of alkalis out of the feldspars along the boundaries during alteration, the excess Al_2O_3 left during the process having been precipitation as sillimanite.

Following Reed (1964) and Higgins (1971) classification of the cataclastic rocks, the texture varieties of the present acidic rocks can be classified as:

Structureless cataclasite: The medium grained variety of the porphyritic granite belongs to this group. Such rock type displays coherent appearance and a mortar texture without foliation or preferred orientation. This texture is characterized by the presence of porphyroclasts set in a matrix of finely crushed material.

Mylonites: The microporphyry, coarse and fine-grained variety of the porphyritic granite, riebeckite gneiss and aegirine riebeckite porphyry belong to this group. Such rocks

represent coherent features showing flow structure (foliation) of cataclastic origin (see Lapworth, 1885, Water and Campbell, 1935). The terms protomylonite, mylonite and ultramylonite are used to represent the three subclasses of mylonites in order of increasing degree of cataclasis respectively. (see Table 11). Most of the rocks belonging to each of three classes of mylonites show some minor recrystallization which commonly produces green schist facies minerals such as quartz, chlorite, epidote and calcite.

Cataclasite rocks: The fine grained variety of the porphyritic granite belongs to this group. Such rock types are apparently subjected to a considerable extent of recrystallization. They usually show flow structures.

Pseudotachylite: Some of the microporphyries belong to this group. Such rock types are highly grinded in a mylonite zone and become submicroscopic in grain size and look dark between cross polars even if they are not true glasses. A detailed classification based on the grain size and porphyroclast ground-mass ratio of Higgins is presented in table 11.

Chemistry and Petrogenesis: The chemical data of the Shewa-Shahbazgarhi complex was treated on various types of diagrams. Trace elements plotted against different variables (Ni, Cr and Co vs MgO Fig.11) and Zr vs SiO_2 (Fig,15) show that the

basic and the acidic rocks are not comagmatic but are the result of crystallization of two different of magmas. The affinity diagrams (Nb/Y vs SiO_2 for the basic rocks and SiO_2 vs $\text{Al}_2\text{O}_3 + \text{CaO} + \text{total alk.}/\text{Al}_2\text{O}_3 + \text{CaO} - \text{total alk.}$ for the acidic rocks), suggest a subalkaline magma for the basic rocks and alkaline to peralkaline magma for the acidic rocks.

The tectonic environment of the Shewa-Shahbazgarhi complex deduced from various discriminant diagrams (Cr , vs Y , Ti , vs Zr for basic rocks and Nb , Y and Ta vs SiO_2 and Nb vs Y for the acidic rocks) are suggestive of "within plate" origin and are related to continental rifting (Pearce, 1982).

Rocks with more or less similar character have been found at Warsak about 100 km west of the area under study (Kempe, 1973). Also the Ambela granite and Koga syenite have been considered as the members of the same alkaline province (Kempe and Jan, 1970, 1980). A K/Ar age of 41 m.y. has been suggested for the Warsak alkaline granites and 50 m.y. for the Koga syenite (Kempe, 1973). The Warsak granites are metamorphosed at least upto upper green schist facies. If the Shewa-Shahbazgarhi rocks are contemporaneous with these latter types, then they may be as old as Warsak granites. However, Permian ages have now been suggested for the Shewa-Shahbazgarhi rocks and Warsak granites by Kempe and Ihsanullah Mian (Personal Commn. through M.Q. Jan).

In the light of the tectonic history of the region, the development of the acidic rocks (alkaline to peralkaline) of the Shewa-Shahbazgarhi rocks may be explained as follow:

According to the model suggested by Bailey (1974) the large scale generation of alkaline felsic magmas takes place by partial melting in the lower crust accompanied by volatiles fluxing from the mantle. The influx of these volatiles is due to rift-related release of pressure (Bailey, 1964). This is supported by the pattern shown by the major and trace elements of the Shewa-Shahbazgarhi rocks normalized against ORG values of Pearce et al., 1984. The pattern of the Shewa-Shahbazgarhi rocks is more or less similar to that of the Sabaloka complex Sudan, which is described as crust dominated (Fig.25, Pearce et al., 1984). The production of the acidic rocks by fractional crystallization of alkali basalt magma is not considered feasible due to the absence of large bodies of alk. basic rocks. The few basic rocks present are the rift related continental flood basalt type (Cox, 1980).

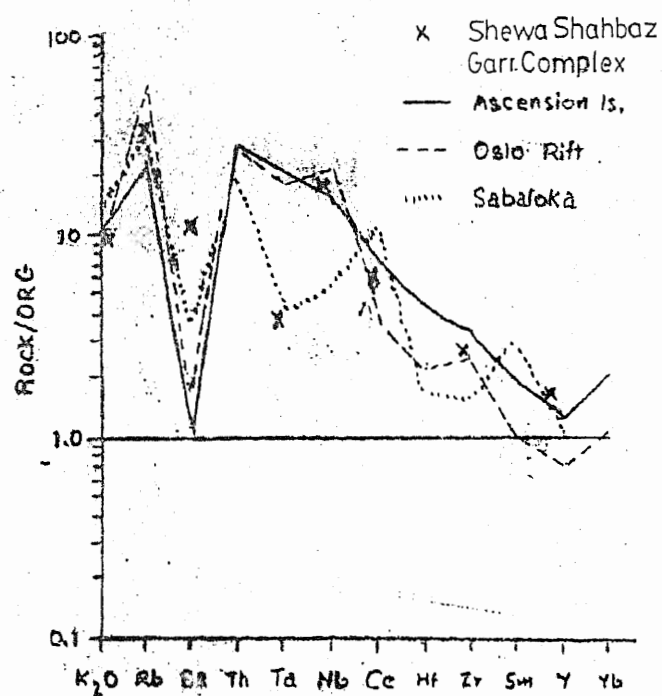


Fig.25. ORG normalized against K_2O , Rb, Ba, Th, Ta, Nb, Ce, Hf, Zr, Sm, Y, Yb, plot for Shewa Shahbazgarhi rocks after Pearce (1984).

REFERENCES

- Ahmed, S and Ahmad, Z., 1974. Petrochemistry of the Ambela granites, southern Swat Distt. Pakistan., Pak. J. Sci-Res. 26, 63-69.
- Andrews-Speed, C.P. & Brookfield, M.E., 1982. Middle Paleozoic to Cenozoic geology and tectonic evolution of northwestern Himalaya., Tectonophysics, vol.82.
- Bailey, D.K., 1964. Crustal warping- a possible tectonic control of alkaline magmatism. J. Geophys. Res., 69, 1103-11.
- , 1974. Origin of alkaline magmas as a result of anatexis. In the alkaline rocks (ed. H. Sorenson), John Willey and Sons.
- Bakhtiar and Waleed, A.K., 1980. Geology of the Shewa-Shahbazgarhi formation, Dist. Mardan, N.W.F.P. Pakistan, Unpub. M.Sc. Thesis, Univ. of Peshawar.
- Bell, T.H. & Etheridge, M.A., 1973. Microstructure of mylonites and their descriptive terminology. Lithos. 6.
- Bowden, P. & Turner, D.C., 1974. Peralkaline and associated ring-complexes in the Nigeria-Niger Province, West Africa, the alkaline rocks (ed. H. Sorenson), John Willey & Sons.
- Calkins, J.A., Offield, T.W., Abdullah, S.K.M. and Ali, T., 1975. Geology of the southern Himalaya in Hazara, Pakistan and adjacent areas, U.S.G.S. Professional Paper 716-C, Washington.
- Chaudhry, M.N. and Shakoor, A., 1968. Geology and Petrology of feldspathoidal syenites and associated rocks of the Koga area, Chamla valley, Swat, west Pakistan. Geol. Bull. Punjab Univ. No.7.
- , Ashraf, M., Hussain, S.S. and Iqbal, M., 1976. Geology and petrology of Malakand and a part of Dir (Toposheet 38 N/4). Geol. Bull. Punj. Univ. v.12.
- , and Shams, F.A., 1984. Petrology of the Shewa porphyries of the Peshawar plain alkaline igneous province, NW Himalayas, Pakistan. In: "Granites of the Himalaya, Karakoram and Hindukush" Shams, F.A. (ed), Punj. Univ.

- Coulson, A.L., 1936. A soda granite suite in the north west Frontier Province. *Proc. Nat. Inst. Sci. Ind.* 2, No.3.
- Coward, M.P., Jan, M.Q., Rex, D., Tarney, J., Thirlwall, M. & Windley, B.F., 1982. Geotectonic frame work Himalaya of N. Pakistan. *Jour. Geol. Soc. London*, 139.
- Cox, K.G., Bell, J.D., and Pankhurst, R.J., 1979. Interpretation of Igneous rocks. G. Allen and Unwin Ltd. London.
- _____, 1980. A model for flood basalt volcanism. *J. Petrology* 21, 629-50.
- Debon, F. and Le Fort, P., 1982. A chemical-mineralogical classification of common plutonic rocks and associations. *Trans. R. Soc. Edinb. Earth Sciences*, 73, 135-49.
- Desio, A., 1964. Tectonic relationship between the Karakoram Pamir and Hindukush. Report XXLL Sess. India Intern. Geol. Congr. New Dehli. v.11.
- Etheridge, M.A. and Wilkie, J.C., 1979. Grain size reduction, grain boundary sliding and the flow strength of mylonites. *Tectonophysics*, v.58.
- Fisk, M.R., Upton, G.C.J., & White, W.M., in press. Chemistry of Reunion Island volcanic rocks and minerals: 1. The nature of the mantle and fractionation processes.
- Floyed, P.A. & Winchester, J.A., 1975. Magma type and tectonic setting discrimination using immobile elements. *Earth Planet. Sci. Letters*. 27.
- Harker, A., 1932. Metamorphism: a study of the transformations of Rock-masses Methuen and Co. Ltd. London.
- Higgins, W.M., 1971. Cataclastic Rocks. U.S.G.S. Prof. papers, No.687.
- Jan, M.Q. & Asif, M., 1983. Geochemistry of tonalites and (Quartz) diorites of the Kohistan Ladakh (Trans Himalayan) granite belt in Swat, NW Pakistan. In "(Granite of Himalaya, Karakoram and Hindukush" (F.A. Shams ed.), Inst. Geol. Punjab Univ. Lahore, Pakistan.
- Jan, M.Q., & Howie, R.A., 1981. The mineralogy and geochemistry of the metamorphosed basic and ultrabasic rocks of Jijal complex, Kohistan, NW Pakistan. *Jour. Petrology*, 22.
- Kempe, D.R.C., 1973. The petrology of the Warsak alkaline granites and their relationship to other alkaline rocks of the region. *Geol. Mag.* 110.

- _____, 1983. Alkaline granites, syenites and associated rocks of the Peshawar plain alkaline igneous province, NW Pakistan. In "Granites of Himalayas, Karakoram and Hindukush" (Ed. F.A. Shams) Inst. Geol. Punjab Univ.
- _____, Jan, M.Q., 1970. An alkaline igneous province in the North West Frontier Province, West Pakistan. Geol. Mag. 107.
- _____, _____, 1980. The Peshawar plain alkaline igneous province, NW Pakistan, Geol. Bull. Univ. Peshawar (Spec. Issue), 13.
- Khalil, S.E., Neef, J.A., & Brunfelt, A.O., 1978. Trace element abundances of the Holter Kollen pluton complex, Oslo area Norway. Chem. Geol. 22, 121-55.
- Klootwijk, C., Sharma, M.L., Gergan, J., Tirkey, B., Shah, S.K. & Agarwal, V., 1979. The extent of greater India, II. Paleomagnetic data from the Ladakh intrusives at Kargil north-western Himalayas. Earth Planet. Sci. Letters 44.
- Lapworth, C., 1885. The Highland controversy in British geology; its causes, course and consequences: Nature, v.32.
- Leake, B.F., 1978. Nomenclature of Amphiboles. Mineral. Mag. v.42.
- Martin, N.R., Siddiqui, S.F.A., and King, B.H., 1962. A geological reconnaissance of the region between the lower Swat and the Indus rivers of Pakistan. Geol. Bull. Punjab Univ. No.2.
- Miyashiro, A., 1973. Metamorphism and metamorphic belts. George Allen. London.
- _____, and Banno, S., 1958. Nature of glaucophanitic metamorphism. Amer. Jour. Sci. 256.
- Neumann, E.R., Brunfelt, A.O., & Finstad, K.G., 1977. Rare earth elements in some igneous rocks in the Oslo rift, Norway. Lithos. 10, 311-19.
- Nockolds, S.R., 1954. Average chemical composition of some igneous rocks. Bull. Geol. Soc. Amer., v.65.
- Noor Jehan, 1985. Geology of a part of the Shewa Shahbazgarhi complex, District Mardan, NWFP, Pakistan. Unpub. M.Sc. Thesis, Univ. of Peshawar.
- Pearce, J.A., 1982. Trace element characteristics of lavas from destructive plate boundaries. In "Andesites" (R-S. Thorpe, ed.), John Willey & Sons, Chichester.
- _____, & Cann, J.R., 1973. Tectonic setting of basic volcanic rocks determined using trace element analyses. Earth Planet. Sci. Letters. 19.

- _____, Harris, N.B.W. and Tindle, A.G., 1984. Trace Element Discrimination Diagrams for the Tectonic Interpretation of Granitic Rocks. *Jour. Petrology*, v. 25, Part 4.
- Pearce, T.H., 1968. A contribution to the theory of variation diagrams. *Ibid.* 19.
- _____, 1970. Chemical variations in the Palisade Sill. *Jour. Petrology*, 11.
- Powell, C. McA., 1979. A speculative tectonic history of Pakistan and surroundings: some constraints from the Indian Ocean. In "Geodynamics of Pakistan" (A. Farah and DeJong eds.) G.S.P. Quetta.
- _____, and Conaghan, P.J., 1973. Plate tectonics and the Himalayas. *Earth Planet. Sci. Letters*, 20.
- Rafique, M., Ahmad, I., Shah, T., 1983. Major faults lineaments of the surroundings of the Peshawar plain. *Geol. Bull. Univ. Peshawar.*, v.17.
- _____, Shah, T., Rehman, M. and Ihsan, M., 1984. Petrochemistry of the rocks from Babaji area, a part of the Ambela granitic complex, Buner, Northern Pakistan. *Geol. Bull. Univ. Peshawar.* vol.17, 31-42.
- Reed, J.J., 1964. Mylonites, cataclasites, and associated rocks along the Alpine fault, south Island, New Zealand. *N.Z.J. Geol. Geophys.* 7.
- Siddiqui, S.F.A., 1965. Alkaline rocks in Swat-Chamla. *Geol. Bull. Punjab Univ.* v.5.
- _____, 1967. Notes on the discovery of Carbonatite rocks in the Chamla area, Swat State, West Pakistan. *Geol. Bull. Punjab Univ.* v.6.
- Streckieson, A., 1967. Classification and nomenclature of igneous rocks, *Naues Jahrb. Mineral. Abh.*, 107, 144-214.
- Tahirkheli, R.A.K., & Jan, M.Q. (eds), 1979. The geology of Kohistan, Karakoram Himalaya, northern Pakistan. *Geol. Bull. Univ. Peshawar. Spec. Issue*, 11.
- Thompson, R.N., 1976. Alkali amphiboles in the Eocene high-level granites of Skye, Scotland. *Mineral. Mag.* vol.40.
- Thornton, C.P. and Tuttle, O.F., 1960. Chemistry of igneous rocks, 1, Differentiation index. *Amer. Jour. Sci.* 258.

- Walsh, J.N., Beckinsale, R.D., Skelhorn, R.R., & Thorpe, R.S., 1979. Geochemistry and petrogenesis of Tertiary granitic rocks from the island of Mull, Northwest Scotland. *Contr. Miner. Petrol.* 71, 99-116.
- Waters, A.C. and Campbell, C.D., 1935. Mylonites from the San Andreas fault zone. *Amer. Jour. Sci.*, 5th Ser. v. 29.
- Wilson, N.D., 1955. A new method for the determination of ferrous iron in rocks and minerals. *Bull. Geol. Survey, G.B.* 9, 56.
- Winchester, J.A. & Floyd, P.A., 1977. Geochemical Discrimination of the different magma series and their differentiation products using immobile elements. *Chem. Geol.* v. 20.
- Wright, J.B., 1960. A simple alkalinity ratio and its application to questions of non-orogenic granite genesis. *Geol. Mag.*, 106, 370-384.